Dissertation

submitted to the

Combined Faculties for the Natural Sciences and for Mathematics

of the Ruperto-Carola University of Heidelberg, Germany

for the degree of

Doctor of Natural Sciences

Presented by

Diplom-Biologist Florian Freudenberg

Born in Twistringen

Oral examination: 29.06.2009   12:00

The role of hippocampal GluA1-containing AMPA receptors in learning and memory

Referees: Prof. Dr. P. H. Seeburg

                     Prof. Dr. H. Monyer

Erklärung gemäß § 8 (3) b) und c) der Promotionsordnung:

Ich erkläre hiermit, dass ich die vorgelegte Dissertation selbst verfasst und mich dabei keiner anderen als der von mir ausdrücklich bezeichneten Quellen und Hilfen bedient habe. Des Weiteren erkläre ich, dass ich an keiner anderen Stelle ein Prüfungsverfahren beantragt bzw. die Dissertation in dieser oder anderer Form bereits anderweitig als Prüfungsarbeit verwendet oder einer anderen Fakultät als Dissertation vorgelegt habe.

Heidelberg, 30. April 2009

Für Stephanie

Table of Contents

Summary

The hippocampus (HPC), a brain area important for spatial learning and memory, requires concerted excitatory synaptic transmission via intrinsic and extrinsic connections. This transmission is mainly mediated by AMPA receptors. AMPA receptor subunit GluA1 knock-out ($GluA1^{-/-}$) mice show distinct HPC-dependent behavioral phenotypes. These mutant mice are hyperactive, have no spatial working memory (SWM) and are impaired in the expression of experience-dependent behavioral despair. However, since $GluA1^{-/-}$ mice are globally lacking GluA1, the specific contribution of the HPC to these behaviors has not been investigated. I therefore examined the role of GluA1 in HPC by stereotaxically injecting recombinant adeno-associated viruses (rAAVs) to alter the GluA1 content of infected neurons. I employed two approaches. In the first approach, to elucidate the contribution of hippocampal GluA1-containing AMPA to different behaviors, $GluA1^{-/-}$ mice were injected with a GluA1-expressing rAAV in HPC, thereby reintroducing GluA1 into this area (*knock-in approach*). In the second approach, to detect behaviors requiring hippocampal GluA1-containing AMPA receptors in HPC, mice with floxed GluA1 alleles ($GluA1^{2lox/2lox}$ mice) were stereotaxically injected with an rAAV expressing Cre-recombinase, thereby deleting GluA1 from this area (*knock-out approach*). After virus injection, the mice were tested in open field, rewarded alternation on the T-maze, and Porsolt forced swim test (FST). The results show that hyperactivity was abolished in mice from the *knock-in approach*, indicating that lack of GluA1 in HPC induces hyperactivity. *Knock-in approach* mice still had impaired SWM, while *knock-out approach* mice only had a partially impaired SWM, suggesting that hippocampal GluA1-containing AMPA receptors are necessary but not sufficient for intact SWM. *Knock-out approach* mice showed no experience-dependent changes in immobility in the FST, suggesting that hippocampal GluA1-containing AMPA receptors are required for the expression of learned behavioral despair in the FST. Overall, my thesis work dissected behaviors strictly dependent on hippocampal GluA1-containing AMPA receptors. Interestingly, and in contrast to what was hypothesized so far, SWM was not solely dependent on the HPC. Thus, this study further improves our understanding on the expression of HPC-dependent behaviors.

Zusammenfassung

Der Hippokampus (HPC), ein wichtiges Gehirngebiet für räumliches Lernen, benötigt konzertierte erregende synaptische Übertragung mittels intrinsischer und extrinsischer Verbindungen. Diese synaptische Übertragung wird hauptsächlich durch AMPA-Rezeptoren gewährleistet. Mäuse in denen die AMPA-Rezeptoruntereinheit GluA1 fehlt (*GluA1⁻ᐟ⁻*) zeigen bestimmte HPC-abhängige Verhaltensweisen. *GluA1⁻ᐟ⁻* Mäuse sind hyperaktiv, haben kein räumliches Arbeitsgedächtnis und zeigen gestörtes *behavioral despair*. Da diesen Mäusen GluA1 global fehlt, konnte der spezifische Einfluss des HPC an diesen Verhaltensänderungen noch nicht untersucht werden. Aus diesem Grund untersuchte ich die Rolle von GluA1 im HPC indem ich rekombinante Adeno-assoziierte Viren (rAAVs) stereotaktisch in den HPC injizierte, um den GluA1-Gehalt der infizierten Neurone zu verändern. Dazu nutze ich zwei Ansätze. Im ersten Ansatz, um die Rolle von GluA1 im HPC zu untersuchen, wurden *GluA1⁻ᐟ⁻* Mäuse mit einem GluA1-expremierenden rAAV injiziert, wodurch GluA1-haltige AMPA-Rezeptoren in dieses Gehirnareal zurückgebracht wurden (*knock-in* Ansatz). Im zweiten Ansatz, um Verhaltensänderungen zu erkennen die GluA1 im HPC benötigen, wurden Mäuse mit gefloxten GluA1-Allelen stereotaktisch mit einem Cre-Rekombinase expremierenden rAAV im HPC injiziert, wodurch GluA1 aus diesem Areal herausgenommen wurde (*knock-out* Ansatz). Nach der Virusinjektion wurden die Mäuse im Offenfeld, belohnter Alternierung im T-maze und dem Porsolt Schwimmtest getestet. Die Ergebnisse zeigen, dass in den *knock-in* Ansatz Mäusen die Hyperaktivität aufgehoben wurde, was darauf hinweist, dass fehlendes GluA1 im Hippokampus Hyperaktivität verursacht. *Knock-in* Ansatz Mäuse hatten noch immer ein fehlendes räumliches Arbeitsgedächtnis, während *knock-out* Ansatz Mäuse ein teilweise verschlechtertes räumliches Arbeitsgedächtnis hatten. Diese Ergebnisse wiesen darauf hin, dass GluA1 im HPC notwendig, jedoch nicht ausreichend für ein intaktes räumliches Arbeitsgedächtnis ist. *Knock-out* Ansatz Mäuse zeigten keine erfahrungsabhängigen Immobilitätsänderungen im Porsolt Schwimmtest, was darauf hinweist, dass GluA1 im HPC notwendig für *behavioral despair* im Porsolt Schwimmtest ist. Zusammengenommen untersuchte ich in meiner Arbeit Verhaltens-weisen, die ausschließlich von GluA1 im HPC abhängig sind. Interessanterweise und im Gegensatz zu dem, was bisher angenommen wurde, ist räumliches Arbeitsgedächtnis nicht allein vom HPC abhängig. Daher hilft diese Studie unsere Kenntnisse über HPC-abhängige Verhaltensweisen zu verbessern.

1 Introduction

1.1 Hippocampus (HPC)

Scoville and Milner's patient H.M. suffered from severe epilepsy with minor and major seizures from the age of 10. Despite strong anticonvulsant medication, the epileptic seizures worsened. To alleviate seizures, a medial temporal lobe resection was carried out at the age of 27. After surgery H.M., at first glance, seemed like a normal person, since his intelligence, personality, understanding and reasoning were unchanged. However, bilateral removal of the medial temporal lobes (including large parts of the hippocampal formation) led to a complete inability to form new memories. For example, he never knew the correct date and did not remember people he met shortly before or the food he had just eaten. Additionally, H.M. suffered from partial retrograde amnesia. While his remote memory was unimpaired, recent memory (up to three years before the operation) was partially or completely lost (Scoville & Milner, 1957; Squire, 2009). Interestingly, the described memory deficits only affected declarative (*e.g.* facts and episodes) and not procedural (*e.g.* skills) memories. For example, when H.M. was asked to trace the contours of a star through a mirror, he learned this task with high accuracy within a few trials, although he never remembered having done this task before (Milner, 1962). Until he deceased at the age of 82 on December 2, 2008, H.M. became one of the best known and most studied patients in neuroscience (Squire, 2009).

After Scoville and Milner (1957) described their findings about H.M. and other patients with similar phenotypes, the interest on memory formation in the medial temporal lobe increased significantly. Further studies delineated a major role of the hippocampal formation for declarative memories. Hippocampal lesions in both, monkeys and rodents, further increased knowledge about the role of this brain area in learning and memory (Squire & Zola-Morgan, 1991; Neves et al., 2008; Squire, 2009). The interest in hippocampal learning and memory increased with the finding of long-term potentiation (LTP) by Bliss and Lømo (1973), a putative physiological correlate of learning and memory, which was first described for the HPC. The finding of hippocampal place fields by O'Keefe and Dostrovsky (1971) and spatial memory impairments after hippocampal lesions in rats (Hughes, 1965; Stevens & Cowey, 1973; Sinnamon et al., 1978) increased the focus of spatial processing within the

HPC. Today, the importance of the hippocampal formation in spatial and non-spatial learning and memory is widely accepted (Neves et al., 2008).

1.1.1 Anatomy of the hippocampal formation

The HPC is a complex but highly organized structure in the mammalian brain. The word 'hippocampus' (Greek for "sea horse") was chosen, because of the similarity of this brain structure in humans to the sea horse (Amaral & Lavenex, 2007).

The term HPC describes an area, which is composed of three subfields CA1, CA2 and CA3 (CA=cornu ammonis (Latin for "Ammon's horn")). The hippocampal formation comprises four regions, namely the HPC, dentate gyrus (DG), subicular complex (consisting of the subiculum, presubiculum and parasubiculum) and entorhinal cortex (Figure 1a). The subicular complex and entorhinal cortex are often referred to as the parahippocampal region (Amaral & Witter, 1989). Most of these areas were identified and named by Santiago Ramón y Cajal (Ramón y Cajal, 1893) and his student Raphael Lorente de Nó (Lorente de Nó, 1933; Lorente de Nó, 1934).

In rodents the hippocampal formation looks like an elongated, banana-shaped structure. It extends from the midline close to the septal nuclei (septal pole/dorsal HPC) over and behind the thalamus into the beginning temporal lobe (temporal pole/ventral HPC) (Figure 1a).

The areas of the hippocampal formation are, almost exclusively, unidirectionally connected. The entorhinal cortex projects to the DG via a fiber bundle called the perforant pathway. The mossy fibers of the DG granule cells in turn project to pyramidal neurons of the CA3 subfield. The so-called Schaffer collaterals are connecting CA3 with CA1 pyramidal neurons. The CA1 neurons project back to the entorhinal cortex. This loop-like connection is often referred to as the trisynaptic circuit (Amaral & Witter, 1989; Amaral & Lavenex, 2007) (Figure 1b).

a

b
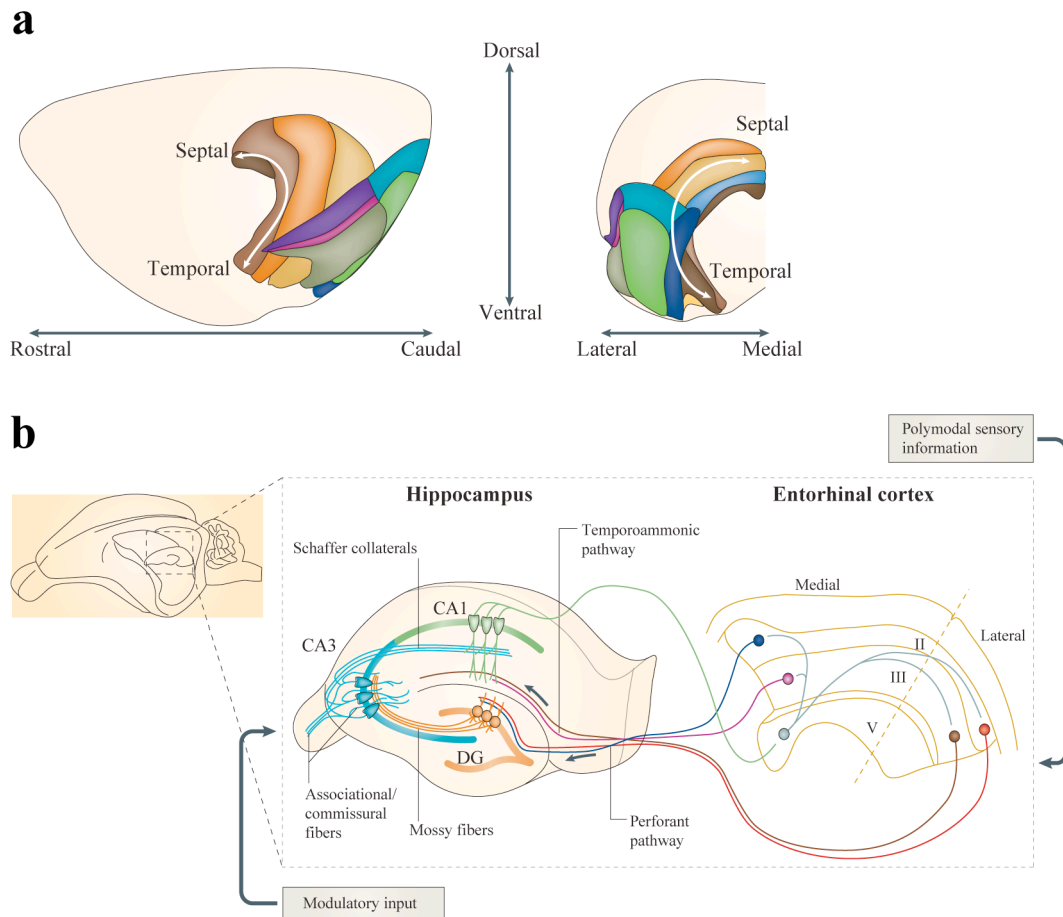
Figure 1: (**a**) Position of the hippocampal formation in the rat brain (consisting of DG (dark brown), CA3 (medium brown), CA2 (not indicated), CA1 (orange), subiculum (yellow), presubiculum (medium blue), parasubiculum (dark blue), the lateral (dark green) and medial (light green) entorhinal cortex). Moreover the perirhinal cortex is shown (pink and purple). For a detailed description see text (adapted from van Strien et al., 2009). (**b**) Basic anatomy of the HPC and its connections with the entorhinal cortex. For a detailed description see text (adapted from Neves et al., 2008).

1.1.2 Cell types and intrinsic connections

1.1.2.1 DG

The DG comprises three layers, the granule cell layer, the molecular layer, and the polymorphic cell layer. The granule cell layer is the principal cell layer of the DG. It contains the granule cells, which are the only principal neurons within the DG. They mainly give rise to excitatory projections to pyramidal neurons of CA3 via the so-called mossy fibers. However, mossy fibers also terminate on interneurons of the granule cell layer and mossy cells of the polymorphic cell layer (Amaral & Lavenex, 2007).

The polymorphic cell layer contains a large variety of neurons the most common of which are the excitatory mossy cells. They project to the dendrites of granule cells and interneurons of the DG. Therefore, mossy cells provide both feedforward excitatory (directly) and inhibitory (via interneurons) control of DG granule cells. The mossy cells cannot be defined as projection neurons, since their axons are confined to the DG, however they also do not follow the common pattern of interneurons, since they are excitatory (Amaral & Lavenex, 2007).

The molecular layer surrounds the granule cell layer and mainly contains dendrites from neurons of the granule and polymorphic cell layers and axons from the entorhinal cortex and other projection areas (Amaral & Lavenex, 2007).

1.1.2.2 HPC (CA1, CA2 and CA3)

As mentioned above the HPC comprises three subfields, CA1, CA2 and CA3. In all subfields the pyramidal cell layer contains the principal neurons of the HPC, the pyramidal neurons. The pyramidal cell layer is surrounded by the stratum oriens, which contains the basal dendrites of the pyramidal neurons. The pyramidal cell layer itself surrounds the stratum radiatum, which contains the apical dendrites of the pyramidal neurons. The stratum radiatum surrounds the so-called stratum lacunosum-moleculare, which contains the apical tufts of the apical dendrites (Amaral & Lavenex, 2007) (Figure 2).

The CA3 (but not CA2) is the only subfield of the HPC that receives input from granule cells of the DG via the mossy fibers. These fibers give rise to presynaptic terminals called mossy fiber expansions that make synaptic contacts with CA3 neurons (Amaral & Dent, 1981). Each mossy fiber makes approximately 15 expansions (*i.e.* one granule cell projects approximately to 15 CA3 neurons). One CA3 pyramidal neurons receives input from about 72 granule cells. The site of termination, which is located between the pyramidal cell layer and stratum radiatum of CA3, is called the stratum lucidum. CA3 cells do not project back to the molecular layer of the DG except for a few neurons from the most temporal part of the HPC. Additionally, some CA2 and CA3 neurons project to the polymorphic layer of the DG (Amaral & Lavenex, 2007) (Figure 1&2).

CA3 and CA2 pyramidal neurons are strongly innervated by their own axons and axons of the contralateral CA3 and CA2. This connection is referred to as the associational connection. Additionally, CA2 and, more so, CA3 pyramidal neurons project to CA1 neurons via the Schaffer collaterals. These collaterals terminate on the

apical and basal dendrites of CA1 pyramidal neurons. The axonal projection of a single CA3 neuron can make as many as 60,000 synaptic connections. However, a single CA3 pyramidal neuron only makes up to 10 synaptic contacts with an individual CA1 pyramidal neuron (Li et al. 1994; Ishizuka et al., 1995; Amaral & Lavenex, 2007) (Figure 1&2).

CA1 neurons have no associational connection. However, some of these cells project to interneurons within the CA1, thereby giving inhibitory feedback. CA1 neurons project to the adjacent subiculum and the entorhinal cortex (Amaral & Lavenex, 2007).
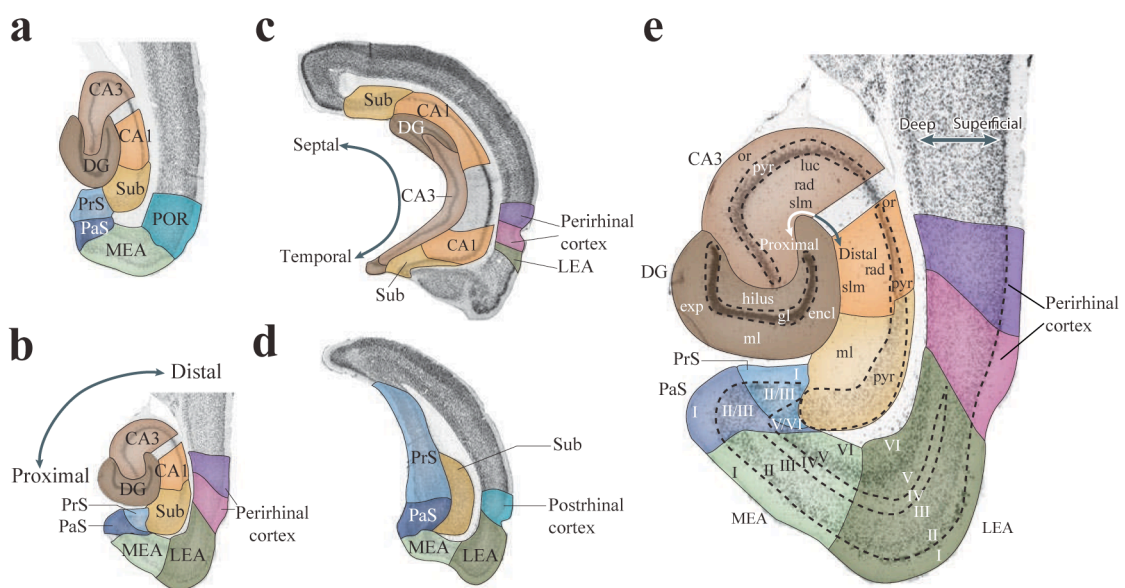
Figure 2: Representations of the hippocampal formation in the rat brain. Horizontal (**a, b**) and coronal sections of the rat hippocampal formation are shown. In (**e**) an enlarged representation of the horizontal section from (**b**) is shown. The hippocampal subfields are color-coded in all images (DG (dark brown), CA3 (medium brown), CA2 (not indicated), CA1 (orange), subiculum (Sub, yellow), presubiculum (PrS, medium blue), parasubiculum (PaS, dark blue), the lateral (LEA, dark green) and medial (MEA, light green) entorhinal cortex, perirhinal cortex (pink and purple) and postrhinal cortex (blue-green)). The Roman numerals indicate cortical layers (Abbreviations: gl = granule cell layer, luc = stratum lucidum, ml = molecular layer, or = stratum oriens, pyr = pyramidal cell layer, rad = stratum radiatum, slm = stratum lacunosum-moleculare) (adapted from van Strien et al., 2009).

1.1.2.3 Interneurons of the hippocampus

Interneurons, which can be essentially found in all layers of the DG and HPC, play an important role in the proper physiological functioning of the hippocampal

formation. One interneuron can make more than 10,000 inhibitory synaptic contacts with principal neurons. Thereby, interneurons have strong inhibitory control over the excitability of granule and pyramidal neurons. The most important interneurons found in the DG and HPC will be presented in the following section.

The most intensively studied type of interneuron is the pyramidal basket cell, which is found in the principal cell layers of the DG and HPC. Pyramidal basket cells form inhibitory synapses with the cell bodies of principal neurons in a 'basket'-like fashion. A single pyramidal basket cell makes about 10,000 synapses on 1,000 or more principal neurons. In turn, dendrites of the pyramidal basket cells receive at least 2,000 excitatory inputs, mostly from principal neurons (Freund & Buzsáki, 1996).

A second prominent type of interneuron is the chandelier or axo-axonic cell. This type of interneuron is located in the molecular layer of the DG and the pyramidal cell layer of the HPC. A single chandelier cell synapses on the axon-initial segments of about 1,200 principal neurons and the axon initial segment of each principal neuron receives input from 4 to 10 different chandelier cells (Freund & Buzsáki, 1996).

The bistratified cells are located close to the pyramidal cell layer. Their axons reach into stratum oriens and stratum radiatum, where they generate up to 16,000 synaptic contacts. Their dendrites reach into all strata except stratum lacunosum-moleculare. In CA3 they most likely receive input from associational fibers (feedback inhibition), while in CA1 they receive input from Schaffer collaterals (feedforward inhibition) (Freund & Buzsáki, 1996; Tukker et al., 2007).

Additionally, there are several other kinds of interneurons in the HPC and DG, most of which project to the dendrites of principal neurons (Freund & Buzsáki, 1996).

1.1.3 Extrinsic connections

1.1.3.1 Intrahippocampal connections

The entorhinal cortex plays a critical role in hippocampal processing. Sensory information mainly enters and, when processed, leaves the hippocampal formation via this area (Amaral & Lavenex, 2007).

Layer II (but also layers V and VI) of the entorhinal cortex provide the main projection to the DG via the perforant pathway. The perforant pathway fibers terminate in the molecular layer of the DG (Steward & Scoville, 1976). The same entorhinal collaterals that project to the DG also project to the stratum lacunosum-

moleculare of CA3 and CA2. A different projection, mainly from layer III, terminates in the stratum lacunosum-moleculare of CA1 (Witter & Moser, 2006). Projections from layer II and III of the entorhinal cortex terminate in the molecular layer of the subiculum (Köhler, 1985). Layers III and V of the entorhinal cortex receive projections from the pyramidal neurons of CA1 and the subiculum. However, there are no projections to the entorhinal cortex from CA2/3 or DG (Naber et al., 2001). Layer III of the entorhinal cortex receives a strong projection from the presubiculum, and layer II is innervated by the parasubiculum (Amaral & Lavenex, 2007).

Pre- and parasubiculum also provide a minor projection to the molecular layer of the DG. In addition, the presubiculum weakly innervates CA1, CA2 and CA3. Subiculum, presubiculum and parasubiculum are all interconnected (Köhler, 1985).

1.1.3.2 Neocortex

The medial prefrontal cortex (PFC) projects to the presubiculum and receives input from pyramidal neurons in the transition from dorsal to ventral HPC. The orbitofrontal cortex receives a prominent projection from the subiculum and the entorhinal cortex. The entorhinal cortex projects back to the orbitofrontal cortex. The prelimbic and infralimbic cortices are reciprocally connected with the entorhinal cortex. The prelimbic cortex projects to the presubiculum, and the prelimbic and infralimbic cortices receive a projection from the subiculum (Verwer et al., 1997).

Additionally, the hippocampal formation is connected with the piriform cortex, the olfactory bulb, the anterior olfactory nucleus, the anterior cingulated cortex, agranular insular cortex and the occipital visual cortex. Furthermore there are connections with the temporal, parietal, retrosplenial, postrhinal and perirhinal cortices. Most of the connections of the hippocampal formation with neocortical areas are provided by the entorhinal cortex (Insausti et al., 1997; Verwer et al., 1997; Amaral & Lavenex, 2007).

1.1.3.3 Amygdala

The basal nucleus of the amygdala projects to the CA1/subiculum border region, where it preferentially innervates the molecular layer of the subiculum and the stratum lacunosum-moleculare of CA1. The basal nucleus of the amygdala receives a return projection from pyramidal neurons of this region (Pikkarainen et al., 1999; Pitkänen et al., 2000). The entorhinal cortex receives a substantial input from the amygdaloid complex, mainly from the lateral and basal nuclei and sends a feedback projection, mainly to the basal nucleus (Amaral & Lavenex, 2007).

1.1.3.4 Subcortical structures

The septal nuclei provide substantial projections to the hippocampal formation. They innervate by cholinergic synapses granule cells and neurons in the polymorphic layer of the DG and pyramidal neurons of CA1, CA3 and the subiculum. Furthermore, the pre- and parasubiculum, and the entorhinal cortex receive cholinergic inputs from the septal nuclei. Principal neurons from CA1, CA3, the subiculum and the entorhinal cortex project back to the septal nuclei. Additionally, there are γ-amino butyric acid (GABA)-ergic projections from the septal nuclei that terminate on GABAergic interneurons of the DG (Amaral & Lavenex, 2007).

The striatum, in particular the nucleus accumbens and the olfactory tubercle, receives projections from the subiculum and entorhinal cortex. The ventral subiculum also strongly innervates the bed nucleus of the stria terminalis and moderately the ventral part of the claustrum or endopiriform nucleus (Amaral & Lavenex, 2007).

1.1.3.5 Thalamus and Hypothalamus

Thalamic areas that are connected with the hippocampal formation include the anterior thalamic complex, the nucleus reuniens, interanteromedialis, gelatinosus and centralis medialis. Furthermore, the rhomboid, paraventricular and parataenial nuclei. Hypothamalic connections include the mammilary, supramammilary, premammilary and tuberomammilary nuclei and the ventromedial nucleus (Maglóczky et al., 1994; Kiss et al., 2000; Amaral & Lavenex, 2007).

1.1.3.6 Brain stem

The pontine locus coeruleus innervates the hippocampal formation with noradrenergic fibers. These mostly terminate in the DG, the CA3, the presubiculum, and the entorhinal cortex. The ventral tegmental area makes dopaminergic projections to the entorhinal cortex and the DG. Serotonergic input to the hippocampal formation comes from the raphe nuclei. Axons from this area project to the DG, CA3, the presubiculum and entorhinal cortex (Amaral & Lavenex, 2007).

1.1.4 Hippocampal physiology

Long-lasting changes in the strength of synaptic transmission were first postulated by Donald O. Hebb to be the physiological basis for learning and memory (Hebb, 1949). So far, the best correlate for these changes in synaptic plasticity is LTP, which was discovered in the rabbit HPC by Bliss and Lømo (1973). Excitatory postsynaptic

potentials of DG granule cells were shown to increase after tetanic stimulation of the perforant pathway fibers (Bliss and Lømo, 1973). In later studies this increase in potentials was also shown for mossy fiber projections from DG to CA3 (Alger & Teyler, 1976) and for the Schaffer collateral input from CA3 to CA1 (Schwartzkroin & Wester, 1975; Alger & Teyler, 1976). In fact, CA3 to CA1 LTP became the most commonly studied form of LTP. Notably, also other brain areas including the amygdala were shown to produce robust LTP after tetanic stimulation (Racine et al., 1975).

The molecular mechanisms that lead to LTP are mostly resolved. Essentially, Ca^{2+}-influx through N-methyl-D-aspartate (NMDA) receptors leads, via a second messenger cascade, to enhanced incorporation of α-amino-3-hydroxy-5-methyl-4-isoxazolepropionic acid (AMPA) receptors to the activated synapse and therefore to an increased response of this synapse to glutamate (Collingridge et al., 1983; Lynch et al., 1983; Lynch & Baudry, 1984; Malinow & Malenka, 2002). The role of AMPA receptors in LTP will be described in more detail later.

Since the induction of LTP is unphysiologic, its role in storage and retrieval of memories has long been disputed, and still is. However, several recent studies showed that learning induced LTP in the HPC *in vivo* and the reversal of this LTP abolished the acquired memory traces, indicating that LTP in fact contributes to learning and memory processes (Gruart et al., 2006; Pastalkova et al., 2006; Whitlock et al., 2006).

Important correlates of spatial processing in the hippocampal formation are the so-called place cells and grid cells. The place cells are pyramidal neurons of the HPC and granule cells of the DG that fire selectively, when an animal is in a certain location, regardless from which direction the animal approaches this location. Place cells were first described in the rat by O'Keefe and Dostrovsky (O'Keefe & Dostrovsky, 1971; O'Keefe, 1976). Later, place cells were also found in mice (McHugh et al., 1996; Rotenberg et al., 1996), monkeys (Ono et al., 1991) and humans (Ekstrom et al., 2003).

Grid cells, which were found by the Mosers and co-workers (Fyhn et al., 2004; Hafting et al., 2005), can be found in the superficial layer of the medial entorhinal cortex. They were first discovered in the rat, but recently shown to be also present in mice (Fyhn et al., 2008). These neurons fire, similar to place cells, specifically when an animal is in a certain location. However, unlike place cells, they fire in several places of a spatial location in a regular fashion, thereby forming a grid-like field. It is

very likely that input from grid cells to the HPC tunes the formation of place cells (Fyhn et al., 2008; Moser et al., 2008).

Place and grid cells seem to play an important role in the formation of spatial memories. How these neurons are able to encode memories, however, has not been resolved yet (Moser et al., 2008).

1.2 Ionotropic glutamate receptors (iGluRs)

iGluRs, the main mediators of excitatory neurotransmission in the vertebrates' central nervous system, are ligand-gated ion channels (Dingledine et al., 1999). According to their selective agonists iGluRs can be subdivided into three major classes: (1) NMDA receptors, (2) AMPA receptors, and (3) Kainate receptors (Dingledine et al., 1999; Mayer & Armstrong, 2004).

NMDA receptors form assemblies consisting of two GluN1 (also known as NR1) subunits and two GluN2 (NR2) subunits, of which four exist, termed GluN2A to GluN2D (NR2A to NR2D). The AMPA receptors are assembled from the four subunits GluA1 to GluA4 (GluR-A to GluR-D or GluR1 to GluR4). Kainate receptors are assembled from the five subunits GluK1 to GluK5 (GluR5, GluR6, GluR7, KA1 and KA2). Additionally, there are two known orphan receptors, termed GluD1 and GluD2 (δ1 and δ2) (Mayer & Armstrong, 2004, Collingridge et al., 2009).

The NMDA and AMPA receptors are the best-studied iGluRs in hippocampal physiology. While NMDA receptors are responsible for the slow, relatively long lasting (50 times longer then AMPA receptors) postsynaptic currents, AMPA receptors mediate the fast component of postsynaptic currents (Seeburg et al., 2001).

All iGluRs share a common subunit topology. Every subunit has an amino-terminal domain (ATD), three transmembrane-spanning domains (termed M1, M3, and M4), a channel-pore forming domain (termed M2), and a carboxy-terminal domain (CTD) (Figure 3a,b) (Mayer & Armstrong, 2004).

The ATD is partially responsible for the correct channel assembly. Two subunits build a dimer through interaction via their ATDs. Two of these dimers then form a tetrameric channel via their transmembrane domains (Mayer & Armstrong, 2004; Stern-Bach, 2004). Additionally, a part of the ATD (termed S1 region) together with the extracellular domain between M3 and M4 (termed S2 region) form the ligand binding domain of iGluRs. The S1 and S2 region fold in a clam shell like structure

with two domains termed D1 (which is composed of S1 and the carboxy-terminal part of S2) and D2 (the amino-terminal part of S2). Glutamate (or glycine in the case of the GluN1 subunit) binds first to D1. Subsequently, D2 rotates towards D1 to close the clam shell. This rotation leads to a conformational change, which allows the channel to conduct ions (Mayer & Armstrong, 2004; Stern-Bach, 2004).

iGluRs essentially can adopt three different conducting states, that is resting, active and desensitized. During the resting state, the agonist binding site is spared and the channel is closed (*i.e.* no ions are conducted). Upon glutamate binding, iGluRs transform into the active state by opening the channel (*i.e.* the channel is free for ion-conductance). After the activation iGluRs convert into the desensitized state, which is closure of the channel with agonist in the binding site. The time iGluRs need to change their conformation from active to desensitized state depends on the type of iGluR (AMPA receptors desensitize faster than NMDA receptors) and on the subunit composition (*e.g.* GluN2A-containing NMDA receptors desensitize faster than those containing GluN2B) (Figure 3c) (Mayer & Armstrong, 2004).

A highly conserved element within the M2 domain of each iGluR subunit is the pore loop, which is forming the channel pore. The pore loop enters the membrane from the intracellular side and then kinks and exits the membrane again to the intracellular side. The region where the pore loop kinks is critical for Ca^{2+}-permeability and the Mg^{2+}-block in NMDA receptors and for the control of Ca^{2+}- and Na^+-conductances in AMPA receptors. In the case of the NMDA receptor pores, an asparagine residue, while in the case of AMPA receptors, a glutamine and, in the GluA2 subunit, arginine residue are the critical determinants for channel pore function (Seeburg et al., 2001).

The CTD of iGluRs varies subunit-specifically in length. This domain is mainly responsible for the interaction of iGluRs with other proteins, for instance post-synaptic density (PSD) proteins (Mayer & Armstrong, 2004; Elias & Nicoll, 2007).
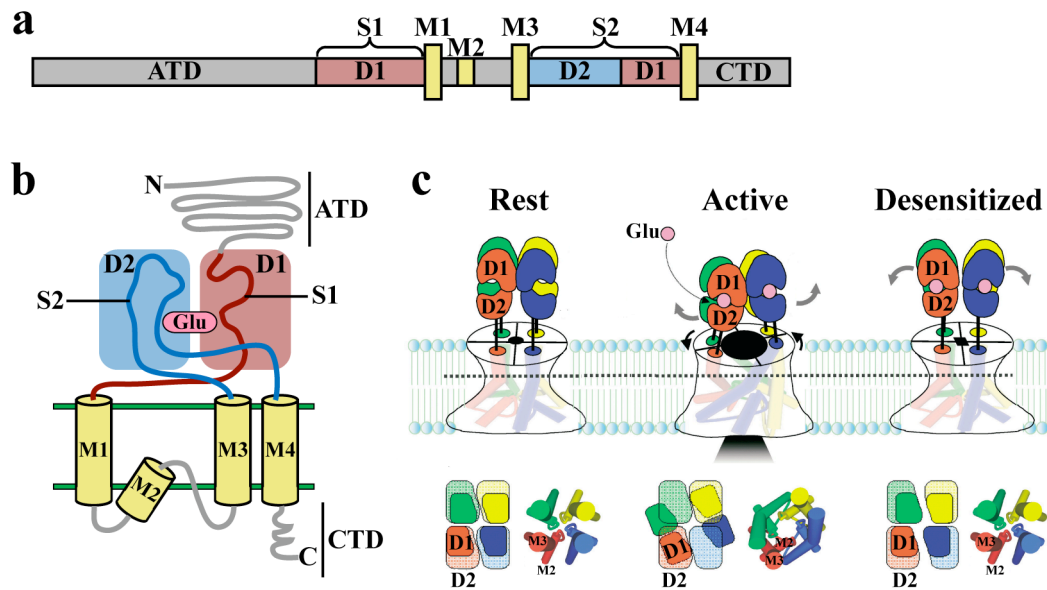
Figure 3: Schemes of the structure and function of iGluRs. (**a**) Single subunit domain organization. The glutamate binding domains are shown in red (D1) and blue (D2), (trans)membrane domains are illustrated in yellow and all other domains, including ATD and CTD are shown in grey. (**b**) Domain organization of an iGluR using the same color-coding as in (**a**). Additionally, a bound glutamate (Glu) is shown in pink. (**c**) Subunit orientation during different conductive states. The top images show side views and the bottom images top views of the subunit assemblies (adapted from Stern-Bach, 2004).

1.2.1 AMPA receptors

Among the iGluRs AMPA receptors are the main mediators of fast excitatory neurotransmission with rapid onset, offset and desensitization kinetics. They are mainly responsible for the enhanced synaptic strength after potentiation. The most abundant channel assemblies in adult principal neurons of the HPC are GluA1/A2 and GluA2/A3. However, GluA1 can also form homomeric channels (Sprengel, 2006; Shepherd & Huganir, 2007). The GluA4 subunit is mainly expressed in hippocampal interneurons and projection neurons of the juvenile HPC (Jensen et al., 2003; Fuchs et al., 2007).

All four AMPA receptor subunits can undergo alternative splicing events. One alternative splicing event affects the "flip/flop" module close to the S2-region. Early in development AMPA receptor subunits containing the "flip" module are most prominent. However, with increasing age "flip" containing subunits are replaced by subunits containing the "flop" module. AMPA receptors that contain "flip" subunits desensitize slower than those with "flop" subunits (Figure 4a) (Sprengel, 2006).

Another alternative splicing event affects the CTD-length of the GluA2 and GluA4 subunits. While the GluA1 subunit only contains a long CTD and the GluA3 subunit only exists with a short CTD, the GluA2 and GluA4 subunits can be alternatively spliced, carrying either a short or long CTD (for GluA2, the short form is most abundant, while for GluA4 the long form is more common). The differences in the CTD lead to pronounced differences in protein interaction and phosphorylation of the different subunits (Figure 4a,b) (Shepherd & Huganir, 2007).

Another modification found for AMPA receptors is RNA editing. One RNA editing event affects the channel pore forming domain of the GluA2 subunit. In AMPA receptors the critical amino acid for channel conductance is usually a glutamine. However, almost all mRNAs of the GluA2-subunit are edited to code for an arginine at this site (Q/R-editing). Q/R-editing leads to a strong reduction in Ca^{2+}-conductance and blocks rectification of AMPA receptors at positive potentials. Moreover, it blocks the transport of homomeric GluA2 subunits from the endoplasmatic reticulum (ER) to the plasma membrane (Figure 4a) (Seeburg et al., 2001; Sprengel, 2006; Shepherd & Huganir, 2007).

There is an additional RNA editing site before the flip/flop sequence of the GluA2, GluA3 and GluA4 subunits. In this position a codon that usually encodes an arginine is edited to code for a glycine (R/G-editing). However, R/G-editing is less efficient than Q/R-editing, since only 80-90 % of the GluA2 and GluA3 and about 50 % of the GluA4 mRNA are edited at the R/G-editing site. AMPA receptors that include subunits with a glycine at the R/G-editing site show faster recovery from desensitization (Figure 4a) (Sprengel, 2006; Shepherd & Huganir, 2007).
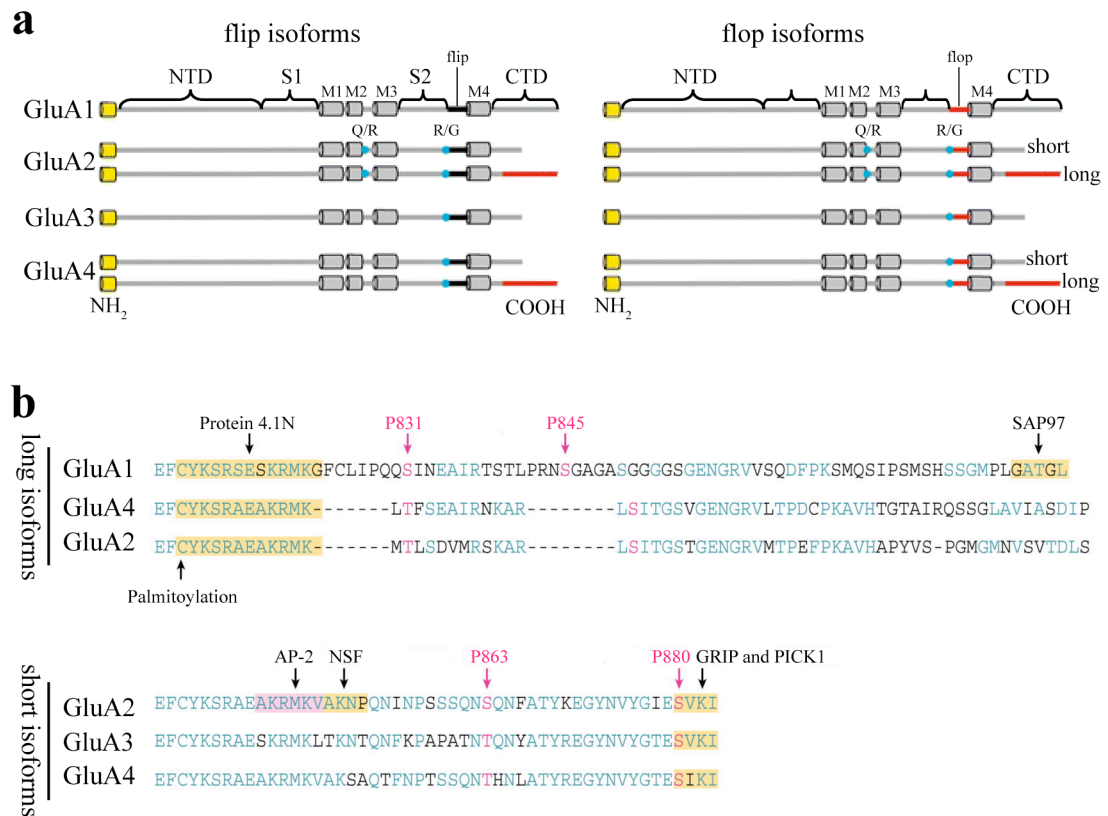
Figure 4: AMPA receptor subunit isoforms. (**a**) Flip (left; illustrated in black) and flop (right; illustrated in red) isoforms are schematically shown for each AMPA receptor subunit. Short and long CTDs are represented where applicable. Q/R- and R/G-editing sites are illustrated in blue (adapted from Sprengel, 2006). (**b**) Long and short isoforms of all AMPA receptor subunits are shown. The different CTDs determine binding partners and phosphorylation sites which are highlighted (adapted from Shepherd & Huganir, 2007).

AMPA receptors contribute to synaptic plasticity in a specific way. The induction of LTP leads to insertion of AMPA receptors into synapses and, vice versa, long-term depression (LTD) leads to endocytosis of AMPA receptors (Malinow & Malenka, 2002). This activity-dependent insertion/removal apparently requires GluA1-containing AMPA receptors (*i.e.* GluA1/A2 assemblies). However, maintenance of AMPA receptors in synapses is independent of GluA1, but requires GluA2-containing AMPA receptors (*i.e.* GluA2/A3 assemblies) (Shi et al., 2001; Malinow & Malenka, 2002). These subunit-specific rules seem to be mostly dependent on the CTD of the subunits, suggesting that C-terminal interaction with scaffolding proteins and/or phosphorylation are required for these properties (Shi et al., 2001).

The prototypical class of synaptic scaffolding proteins are the membrane associated guanylate kinases (MAGUKs) that consist of four members: PSD protein

of 95 kDa (PSD-95), PSD protein of 93 kDa (PSD-93), synapse-associated protein (SAP)-97 and SAP-102. All MAGUKs share a common domain structure with three amino-terminal PSD-95/Discs large/zona occludens-1 (PDZ) domains, an Src-homology 3 (SH3) domain and a carboxy-terminal catalytically inactive guanylate kinase domain (Elias & Nicoll, 2007).

The MAGUKs bind to the CTD of GluN2 subunits and thereby most likely localize NMDA receptors to the synapse. However, only one MAGUK, SAP-97, is known to directly bind to the CTD of GluA1, and this interaction was shown to be necessary for clustering GluA1 containing AMPA receptors to synapses. Although, none of the other MAGUKs is known to directly bind to AMPA receptors, overexpression of PSD-95 led to an increase of AMPA receptor responses. Vice versa, downregulation of PSD-93 or PSD-95 induced a strong reduction in AMPA receptor-mediated transmission (Elias et al., 2006; Elias & Nicoll, 2007). Therefore an intermediary protein is required that binds to both AMPA receptors and MAGUKs. This property is provided by the transmembrane AMPA receptor regulatory proteins (TARPs) (Nicoll et al., 2006).

There are four canonical TARPs named γ-2 (or stargazin), γ-3, γ-4 and γ-8 (Nicoll et al., 2006). These TARPs bind to AMPA receptors, probably via the transmembrane domains. TARPs fulfill complex roles in AMPA receptor function. They are required for proper ER-maturation of AMPA receptor subunits. They translocate AMPA receptors to the cell surface and are required for AMPA receptor transport to synapses by binding to MAGUKs. Additionally, TARPs directly influence AMPA receptor function. They increase AMPA receptors affinity for glutamate, enhance single-channel conductance and slow the rate of deactivation and desensitization (Nicoll et al., 2006).

More recently also γ-5 and γ-7 were shown to function as TARPs (Kato et al., 2007; Kato et al., 2008; Soto et al., 2009). γ-7, which is mainly expressed in the cerebellum, fulfills similar functions to the canonical TARPs with respect to AMPA receptor trafficking and kinetics (Kato et al., 2007). However, γ-5 seems to control AMPA receptor function differently. γ-5 does not influence AMPA receptor surface trafficking, and in great contrast to the canonical TARPs, lowers agonist affinity and accelerates deactivation and desensitization of AMPA receptors. However, like the

canonical TARPs, γ-5 increases single channel conductance (Kato et al., 2008; Soto et al., 2009).

Very recently, two members of the cornichon family of transmembrane proteins were shown to associate with AMPA receptors. Similar to TARPs, these proteins increase surface expression and slow the rate of deactivation and desensitization of AMPA receptors (Schwenk et al., 2009).

In addition to binding to TARPs, phosphorylation of AMPA receptors is required for changes in synaptic plasticity. The most important phosphorylation sites affecting synaptic plasticity are the serine residues 831 and 845 of the GluA1 subunit. Phosphorylation of these residues is required for LTP, and dephosphorylation of these residues induces LTD, and endocytosis of AMPA receptors. Additionally, several phosphorylation sites on the GluA2 subunit have been characterized. Phosphorylation and dephosphorylation of these residues differentially modulates binding of interacting proteins but also seems to be directly involved in synaptic plasticity. For the GluA3 and GluA4 subunits, phosphorylation sites have been found which mostly resemble those of GluA1 (for GluA4) and GluA2 (for GluA3) (Figure 4b) (Lee, 2006). Interestingly, also TARPs and MAGUKs can be phosphorylated. Phosphorylation of TARPs (Nicoll et al., 2006) and SAP-97 (Lee, 2006) were shown to be required for synaptic plasticity.

1.3 GluA1 knock-out (*GluA1$^{-/-}$*) mice

As mentioned above and suggested by the subunit-specific rules (Shi et al., 2001) the AMPA receptor subunit GluA1 is critical in the induction of synaptic plasticity in hippocampal neurons. So far, the most studied model to investigate the function of GluA1-containing AMPA receptors *in vivo* is the *GluA1$^{-/-}$* mouse. Besides a smaller size during the first postnatal weeks and a slightly reduced weight of males, these mice are largely inconspicuous in appearance (Zamanillo et al., 1999; Bannerman et al., 2004). In hippocampal slice recordings, these mice show almost normal strength of excitatory synaptic transmission, mediated by the remaining GluA2/A3 heteromeric AMPA receptors, but deficits in tetanus-induced cellular and field LTP in hippocampal CA3 → CA1 connections (Zamanillo et al., 1999, Jensen et al., 2003). Interestingly, after theta burst pairing in HPC, *GluA1$^{-/-}$* mice only show deficits during early phase potentiation, while late phase potentiation remains intact (Hoffman et al.,

2002). Moreover, when measuring spike timing-dependent plasticity, *GluA1*$^{-/-}$ mice show wild type (WT)-like potentiation (unpublished data), clearly suggesting GluA1-independent modes of potentiation. These electrophysiological changes might in part be attributed to lower protein levels of other AMPA receptor subunits since at least one report (Jensen et al., 2003) found that the amounts of the GluA2 and GluA4 subunits, the main partners of GluA1 in HPC, are reduced in *GluA1*$^{-/-}$ mice. However, these reductions in GluA2 and GluA4 are most likely due to a shorter half-life of these subunits in the un-assembled form (Jensen et al., 2003). A better explanation for the change of electrophysiological properties in *GluA1*$^{-/-}$ mice is the lack of extrasynaptic AMPA receptors, which are required for the induction of synaptic plasticity (Andrásfalvy et al, 2003). This view is also supported by the fact that in immunostainings of *GluA1*$^{-/-}$ mice the GluA2 subunit is most prominent in the somata, where it is most likely trapped in the ER, while the residual dendritic GluA2 is located in synapses (Zamanillo et al., 1999, Jensen et al., 2003). In fact, the GluA2 subunit was even slightly enriched in hippocampal synapses of *GluA1*$^{-/-}$ mice, perhaps explaining the intact synaptic transmission (Jensen et al., 2003). Another report (Chourbaji et al., 2008) showed that *GluA1*$^{-/-}$ mice express increased levels of the principal NMDA receptor subunit GluN1 and glutamate in HPC. This might be a compensatory mechanism for the reduction in AMPA receptor signaling and might give additional explanations for the unchanged basal transmission in these mice (Chourbaji et al., 2008).

Interestingly, the deficits in LTP can be partially rescued upon transgenic reintroduction of a green fluorescent protein (GFP)-tagged GluA1 subunit in principal neurons of the forebrain. In fact, already about 10 % of endogenous GluA1 levels are sufficient to induce a cellular and field LTP with a strength of about 50 % of that found in WT mice (Mack et al, 2001).

Besides these electrophysiological and biochemical phenotypes, *GluA1*$^{-/-}$ mice show very distinct behavioral phenotypes. These phenotypes are mostly related to hippocampal learning and memory, but also other systems are affected.

1.3.1 Behavioral changes in *GluA1*^{-/-} mice

1.3.1.1 Locomotor activity

Rodents exposed to a novel environment show enhanced locomotor and exploratory behavior. Locomotor activity is commonly measured in the open field.

GluA1^{-/-} mice show hyperactivity when exposed to an open field (Bannerman et al., 2004; Wiedholz et al., 2007). This hyperactivity is not rescued by expression of a GFP-tagged GluA1 subunit in principal forebrain neurons (Marx, 2007; Freudenberg et al., 2009).

It has clearly been shown that lesions of the complete HPC induce hyperactivity in rats (Teitelbaum & Milner, 1963; Good & Honey, 1997; Bannerman et al., 1999; Bannerman et al., 2002). Lesions that are confined to the dorsal HPC also induce hyperactivity, however not as pronounced as in complete HPC lesioned rats (Bannerman et al., 2002). In contrast, rats with lesions of the ventral HPC only show hyperactivity after being exposed to stressors (*e.g.* mild foot-shocks, swim stress in the Morris water maze) (Richmond et al., 1999; Bannerman et al., 2002; Bannerman et al., 2003). Locomotor activity is commonly associated with dopamine release in the nucleus accumbens (Sharp et al., 1987). Interestingly, complete HPC lesioned rats show increased hyperactivity upon amphetamine challenge (Whishaw & Mittleman, 1991; Bannerman et al., 1999). Therefore it is likely that the lack of projections to the nucleus accumbens from the hippocampal formation leads to the hyperactivity observed in HPC lesioned rats. Interestingly, *GluA1*^{-/-} mice were shown to have a retarded dopamine-clearance in the striatum (Wiedholz et al., 2007), which might be the cause for the hyperactivity.

1.3.1.2 General cognitive abilities

Charles Spearman was the first to describe that different cognitive abilities have an underlying cognitive trait that contributes to these abilities. Spearman described this as general cognitive abilities (*g* factor). The *g* factor was supposed to represent what diverse cognitive abilities have in common. In other words, difficulties in one cognitive task are most likely predictive of difficulties in a different cognitive task, which can be described by the *g* factor (Spearman, 1904). The *g* factor was generally described for humans and suspected to account for about 40 % of the total variance of cognitive tests in a given group. However, it is suggested that the *g* factor is also existent in mice (Plomin, 2001). To prove this, Galsworthy et al. (2005) developed a

behavioral test battery for general cognitive abilities and found that the g factor in mice accounts for 20 to 40 % of the variance within groups (*i.e.* the likelihood was between 20 and 40 % that a mouse that performed badly in one test also showed weak performance in a different test). One test that was strongly predictive for the g factor was the puzzle box paradigm that was developed specifically for this study (Galsworthy et al., 2005). In this test, mice have to escape from an anxiogenic start compartment to a more pleasant goal compartment through barriers of different features (*i.e.* a door barrier, an underpass, a sawdust-filled underpass and a plug-covered underpass). Reductions in the escape latency, particularly when using the sawdust-filled and plug-covered underpass, where mice have to develop a strategy to make the underpass accessible, are predictive of a low g factor (Galsworthy et al., 2005).

In a pilot study from our laboratory $GluA1^{-/-}$ mice were tested in the puzzle box paradigm. In this study $GluA1^{-/-}$ mice were strongly impaired in shuttling to the goal compartment when using the underpass, the sawdust-filled underpass and the plug-covered underpass. This impairment cannot be attributed to lower levels of anxiety in these mice, since they normally shuttled to the dark goal compartment when using the door barrier. Additionally, when mice were retested after an inter-trial interval (ITI) of 24 hours, the impairment was not found anymore, meaning that they were only impaired when first being confronted with the task and when retested after an ITI of 1 min (unpublished data).

1.3.1.3 Spatial working memory (SWM)

Rodents exposed to a T-maze have a natural tendency to alternate. In the T-maze, they tend to explore the previously unvisited arm. Successful performance in this task requires intact SWM. This refers to the fact that the rodents have to remember the information about specific spatial locations and to process that information over a short period of time. In contrast, spatial reference memory (SRM) is needed to remember information about a spatial location over a long time period (*e.g.* remembering the fixed location of a food reward in a radial maze) (Deacon & Rawlins, 2006).

The first and most striking behavioral phenotype described for $GluA1^{-/-}$ mice is a complete loss of SWM (tested *e.g.* with spontaneous and rewarded alternation on the T-maze and novel arm exploration on the Y-maze) (Reisel et al., 2002; Bannerman et al., 2004; Sanderson et al., 2007; Sanderson et al., 2009) while SRM (tested *e.g.* on

the Morris water maze and the Y-maze) stays intact (Zamanillo et al., 1999; Reisel et al., 2002). This dissociation cannot be explained by differences of cognitive demands in the apparatus that is used, since SRM can be induced on the same Y-maze were SWM is impaired (Reisel et al., 2002). On a 3/6-arm radial maze SRM is intact while, within the same trial, SWM is impaired (Schmitt et al., 2003). The SWM-deficit cannot be attributed to disturbed proactive interference (*i.e.* disturbing influences from previous trials), since SWM is already impaired after a single exposure (Sanderson et al., 2007). This SWM deficit is partially rescued by forebrain-specific expression of a GFP-tagged GluA1 subunit in both rewarded alternation on the T-maze and the SWM component of the 3/6-arm radial maze (Schmitt et al., 2005), showing that as little as about 10 % of endogenous GluA1 levels in principal neurons of the forebrain are sufficient to partially reinstate SWM.

Sanderson et al. (2009) give an alternative explanation for these deficits in that they do not underlie defective SWM but rather a disturbed short-term habituation.

Several lesion studies showed that the HPC is of great importance for learning and memory (Hughes, 1965; Stevens & Cowey, 1973; Sinnamon et al., 1978). Already very early a differentiation was found between dorsal and ventral HPC in that the dorsal HPC is more strongly involved in spatial memory formation than the ventral HPC. However, a clear functional differentiation for SRM was first shown by Moser et al. (1993; 1995) and later confirmed (additionally for SWM) by Bannerman et al., (1999; 2002; 2003) and others (Hock & Bunsey, 1998). These studies clearly demonstrated that the dorsal but not ventral HPC is required for the formation of SRM and SWM. Interestingly, input to the HPC from the entorhinal cortex seems to be required for the formation of SRM and SWM as well, since lesions of this area lead to equal impairments in tests for SRM and SWM (Ramirez & Stein, 1984; Good & Honey, 1997; Bannerman et al., 2001; Steffenach et al., 2005).

Additionally, the medial PFC seems to be partially required for the formation of SWM but not for SRM, since lesions of this area in rats lead to variable deficits in SWM that are usually only transiently found (van Haaren et al., 1985; Shaw & Aggleton, 1993; Schwabe et al., 2003; Mogensen et al., 2007). This suggests a more general involvement of the medial PFC in SWM that can be compensated by other brain areas like the HPC and/or entorhinal cortex.

1.3.1.4 Pavlovian fear conditioning

Animals tend to associate usually non-salient stimuli (*e.g.* environment, light, tone) with an unpleasant event (*e.g.* foot-shock), if both are temporally and spatially connected. Rodents that are subsequently exposed to such stimuli will show a conditioned fear response. The most obvious conditioned fear response is the arrest of any movement other than necessary for breathing, the so-called freezing (Fanselow, 1984).

Most commonly, rodents are tested for Pavlovian fear conditioning by subjecting them to one or more foot-shocks that are preceded by a tone. Subsequently, they are tested for 'cued' (presentation of the tone in a different context) and/or 'contextual' (exposure to the environment where the foot-shock was delivered) fear conditioning. Usually, rodents will react with an increased rate of freezing (or lower activity) when they are confronted with these stimuli.

GluA1$^{-/-}$ mice were tested for Pavlovian fear conditioning in three different studies. Two of these studies showed reduced fear behavior already during the acquisition phase (Bosch, 2008; Humeau et al., 2007) while the other (Feyder et al., 2007) does not show results from that phase. However, when testing for 'cued' or 'contextual fear', only two of these studies (Feyder et al., 2007; Humeau et al., 2007) showed that *GluA1$^{-/-}$* mice have reduced fear-elicited behaviors while the other (Bosch, 2008) showed normal expression of 'cued' and 'contextual fear' behavior in these mice.

The most important brain area for intact expression of fear-elicited behaviors is the amygdala. Lesions of the amygdala induce strong impairment in the acquisition of fear and the expression of 'cued' and 'contextual fear' (Fendt & Fanselow, 1999; Phelps & LeDoux, 2005). However, also the HPC is strongly involved in conditioned fear. Lesions of the dorsal HPC induce deficits in 'contextual' but not 'cued fear' conditioning if lesions are done after the acquisition. Lesions before acquisition elicit a less pronounced impairment in 'contextual fear' conditioning (Hock & Bunsey, 1998; Richmond et al., 1999; Fendt & Fanselow, 1999; Anagnostaras et al., 2001; Kjelstrup et al., 2003). The ventral HPC in contrast seems to have a more general role in Pavlovian fear conditioning, since lesions of this area, akin to amygdala lesions, lead to a strong deficit in the acquisition of conditioned fear and the expression of 'cued' and 'contextual fear' (Richmond et al., 1999; Anagnostaras et al., 2001; Bannerman et al., 2003; Kjelstrup et al., 2003). If this is due to the strong connectivity between ventral HPC and amygdala or a distinct feature of learning in the ventral

HPC remains to be elucidated. Notably, ventral HPC lesioned rats show a reduction in general anxiety (Bannerman et al., 2002; Bannerman et al, 2003; Kjelstrup et al., 2003), which might lead to the reduction in conditioned fear.

1.7.1.5 Porsolt forced swim test (FST)

The FST is commonly used to find antidepressant compounds. This test comprises two sessions, 24 hr apart, of forced swimming in an enclosed chamber. Rodents placed repeatedly into the chamber learn the uncontrollable and unpredictable nature of the task and develop signs of behavioral despair. This can be measured by assessing the time until the rodent becomes immobile and the overall amount of immobility. A reduction in the latency to immobility and an increase in overall immobility after repeated testing, reflect learned behavioral despair (Porsolt et al., 1977; De Pablo et al., 1989; West, 1990).

An earlier study from our laboratory (Marx, 2007; Freudenberg et al., 2009) showed that $GluA1^{-/-}$ mice are impaired in the expression of behavioral despair after repeated testing. These mice show no reduction in latency to, and overall immobility on second day of testing. This lack of reduction in latency to immobility and overall immobility was rescued in $GluA1^{-/-}$ mice expressing a GFP-tagged GluA1 subunit in principal neurons of the forebrain. In contrast, $GluA1^{-/-}$ mice transgenically expressing a GFP-tagged GluA1-subunit with a mutation in the PDZ-interacting domain resemble the phenotype of $GluA1^{-/-}$ mice (Marx, 2007; Freudenberg et al., 2009).

The deficit in FST found for $GluA1^{-/-}$ mice implies impairment in learned despair. The importance of hippocampal learning in the FST has already been discussed (De Pablo et al., 1989; West, 1990). Several studies indicate that both dorsal and ventral HPC are critical in FST. Neonatal but not adult lesions of the ventral HPC were shown to reduce immobility on the second day of FST (Daenen et al., 2001). Additionally, high-speed voltage sensitive dye imaging showed activation of the DG after FST in acute brain slices of the rat ventral HPC (Airan et al., 2007), and substances reducing mobility in FST were shown to increase serotonin-levels in the ventral HPC (Hoshaw et al., 2008). Also the dorsal HPC is important for performance in the FST, since experience dependent expression of behavioral despair was blocked by inhibition of neuronal nitric oxide synthase (Joca & Guimarães, 2006) or (after pre-exposure to stress) NMDA receptors (Padovan & Guimarães, 2004) in the dorsal HPC.

1.4 Viral gene transfer

The use of transgenic and knock-out mice aided in finding the contribution of certain genes to specific behavioral phenotypes. Conditional mutagenesis, using tetracycline controlled gene expression and the Cre/loxP system further refined our knowledge about gene function at specific time points in development and in certain tissues. However, transgenic and knock-out techniques have certain drawbacks. First, the production of mutant mice is cumbersome and time consuming, particularly when congenic lines are desired. Second, spatial targeting is very hard to assess and usually needs compromises in region-specific expression (*e.g.* HPC specific expression is confined to pyramidal neurons in certain subfields). Third, mosaic or low levels of transgene expression might aggravate interpretation of behavioral results (Babinet, 2000; Hickman-Davis & Davis, 2006).

To circumvent these problems, the use of recombinant viruses as carriers of genetic information has accelerated during recent years. A virus that gained lots of interest in this respect is the recombinant adeno-associated virus (rAAV). Adeno-associated viruses (AAVs) belong to the family of parvoviruses, specifically the Dependovirus genus. AAVs are 18-25 nm in diameter and have a genome of 4.7 kb of single-stranded DNA that includes two open reading frames coding for replication and capsid proteins (named *Rep* and *Cap* respectively) (Coura & Nardi, 2007). The sequences for *Rep* and *Cap* are flanked by the only cis-acting elements of AAV, the inverted terminal repeats (ITRs). The ITRs are necessary for virus replication and packaging, but additionally supply enhancer/promoter activity (During et al., 2003; McCown, 2005; Coura & Nardi, 2007).

In rAAVs the *Rep* and *Cap* genes are replaced by transgenes. rAAV has several advantages compared to other viral vectors: (1) it is non pathogenic and induces none or only a low immune response, (2) it is relatively resistant to changes in temperature and pH, (3) it only rarely integrates into the host genome, (4) it has a broad tropism, (5) it gives high levels of expression over a long period of time, (6) rAAVs are relatively easy to purify and (7) the relatively small size of rAAVs permits broad diffusion and therefore infects large areas (like the HPC). The only obvious disadvantage of rAAVs is the limited genetic capacity, which cannot exceed 5 kb, including the promoter and regulatory elements (During et al., 2003; Coura & Nardi, 2007).

Several AAV serotypes were identified, the first of which was AAV-2. This serotype has a heparan sulfate proteoglycan (HSPG) binding site, which renders the virus to be readily purified via affinity chromatography with heparin columns. AAV-2 generally infects neurons. However, in the HPC only neurons in the DG are adequately infected by AAV-2 while CA1 and CA3 are only sparsely infected. AAV-1 in contrast shows high tropism for all types of neurons and gives stronger expression of the transgene. However, AAV-1 capsids have no HSPG binding site and are therefore not as easy to purify (Hauck et al., 2003; Burger et al., 2005). Hauck et al. (2003) produced a chimeric virus containing both AAV-1 and AAV-2 capsids. This virus combines the advantages of both serotypes. It is able to transduce a broad range of neurons and can be easily purified via heparin columns. In fact this chimera was already successfully used by us (Celikel et al., 2007; Freudenberg et al., 2009) and others (*e.g.* Klugmann et al., 2005), to transduce the HPC for subsequent behavioral testing.

1.5 Aim of the thesis

As mentioned above, *GluA1*$^{-/-}$ mice, globally lacking GluA1, show several distinct behavioral phenotypes. These include hyperactivity (Bannerman et al., 2004; Wiedholz et al., 2007), impaired SWM (Reisel et al., 2002; Bannerman et al., 2004; Sanderson et al., 2007; Sanderson et al., 2009), deficits in Pavlovian fear conditioning (Feyder et al., 2007; Humeau et al., 2007; Bosch, 2008) and deficient experience-dependent expression of behavioral despair (Marx, 2007; Freudenberg et al., 2009).

Results from lesion and pharmacological studies suggest a major contribution of the HPC to the behavioral phenotypes of *GluA1*$^{-/-}$ mice (*e.g.* Bannerman et al., 1999; Anagnostaras et al., 2001; Daenen et al., 2001; Padovan & Guimarães, 2004). However, there are several other brain areas that might be involved in mediating these behavioral phenotypes. For example the nucleus accumbens is critical for locomotor activity (Sharp et al., 1987), lesions of the entorhinal cortex lead to impaired SWM (Ramirez & Stein, 1984; Good & Honey, 1997; Bannerman et al., 2001; Steffenach et al., 2005), and lesions of the amygdala induce deficits in Pavlovian fear conditioning (Fendt & Fanselow, 1999; Phelps & LeDoux, 2005). Therefore, the aim of this thesis was to investigate the role of hippocampal GluA1-containing AMPA receptors in the mediation of the behavioral phenotypes found in *GluA1*$^{-/-}$ mice.

For this purpose two approaches were used. The first (*knock-in approac*h; *i.e.* expressing GluA1 specifically in HPC) was employed to find if hippocampal GluA1-containing AMPA receptors are sufficient to mediate the behaviors impaired in *GluA1$^{-/-}$* mice. The second (*knock-out approach; i.e.* deleting GluA1 specifically from HPC) was employed to see if hippocampal GluA1-containing AMPA receptors are required to maintain behaviors impaired in *GluA1$^{-/-}$* mice. To achieve this, I made use of viral gene transfer by rAAVs. For the *knock-in approach*, *GluA1$^{-/-}$* mice were injected stereotaxically into dorsal HPC with an rAAV expressing GluA1, leading to GluA1-expression restricted to the HPC. For the *knock-out approach*, mice with 'floxed' GluA1 alleles (*GluA1$^{2lox/2lox}$* mice), were stereotaxically injected into the HPC with a Cre-recombinase expressing virus, thereby ultimately deleting GluA1 from HPC. After rAAV injection, mice from *the knock-in* and *knock-out approach* were tested in behavioral tasks for the phenotypes impaired in *GluA1$^{-/-}$* mice.

The results obtained in this study show that hyperactivity of *GluA1$^{-/-}$* mice is due to the lack of GluA1 in HPC. Surprisingly, SWM is not exclusively dependent on GluA1 in HPC. Additionally, Pavlovian fear conditioning seems to be independent from GluA1, while experience-dependent expression of behavioral despair in fact is critically dependent on hippocampal GluA1-containing AMPA receptors.

2 Materials and Methods

2.1 Mice

For the experiments reported, adult C57BL/6J (Charles River, Sulzfeld, Germany) and different transgenic mouse lines backcrossed to C57BL/6J (Max Planck Institute for Medical Research, Heidelberg, Germany) were used in accordance with the National Institutes of Health Guide for Care and Use of Laboratory Animals and animal welfare guidelines of the Max Planck Society and were registered in the Regierungspräsidien Karlsruhe and Tübingen. Mice were kept on a 12-hour light/dark cycle (lights on at 7 a.m.) and had *ad libitum* access to food and water at all times except during behavioral testing (unless otherwise specified). All behavioral experiments were performed during the light phase and after >30 min acclimation to the testing room.

Mice lacking one (*GluA1$^{+/-}$*) or both (*GluA1$^{-/-}$*) AMPA receptor GluA1 alleles and mice with "floxed" GluA1 alleles (*i.e. GluA1$^{2lox/2lox}$*) were generated by Zamanillo et al., 1999.

For the experiments an overall number of 87 mice was used. Of these, 19 were WT (7 females, 12 males), 38 were *GluA1$^{-/-}$* (2 females, 36 males), 10 were *GluA1$^{+/-}$* mice (all males) and 20 were *GluA1$^{2lox/2lox}$* (all females).

2.2 Viruses

2.2.1 Viral vectors

The AAV construct pAAV CAG-HA.Cre was obtained from Dr. Matthias Klugmann (University of Mainz, Germany). This vector contains the cytomegalovirus enhancer/chicken beta actin promoter (CAG), driving expression of a hemaglutinin (HA)-tagged Cre-recombinase, followed by the woodchuck hepatitis virus posttranscriptional regulatory element (WPRE) and a bovine growth hormone poly-adenylation (bGH pA) sequence (Figure 5a).

For generation of rAAV-GluA1 (Q/R) expression vectors, myc-tagged *GluA1* cDNA was subcloned into an rAAV backbone containing the 480 bp human synapsin (hSynapsin) core promoter, the WPRE and the bGH pA sequence using artificially introduced EcoRI and SpeI sites (Figure 5b).

a

b
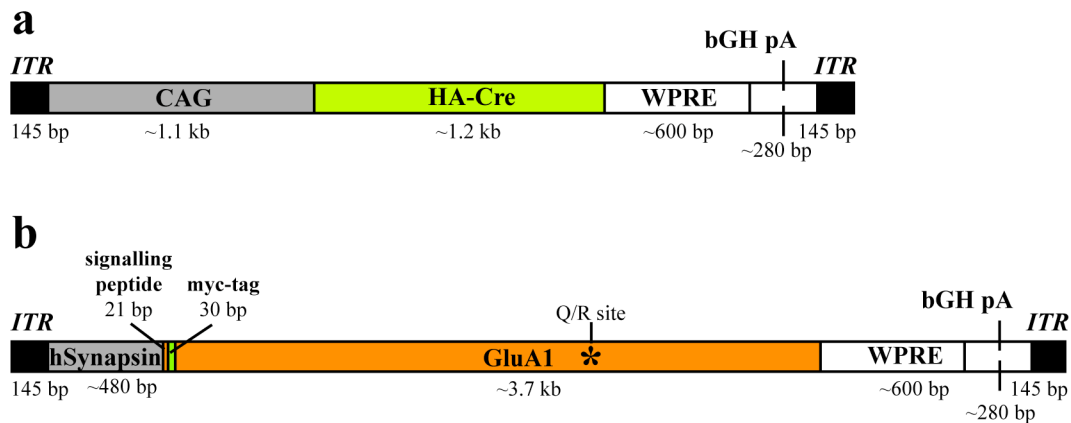
Figure 5: Schematic illustration of rAAV vectors. **(a)** HA-tagged Cre-recombinase is expressed under control of the CAG promoter. **(b)** Myc-tagged GluA1 is expressed under control of the hSynapsin promoter. Two versions of this viral vector were used, one coding for a glutamine (Q) and one for an arginine (R) at position 598, indicated by the asterisk.

2.2.2 Virus production

rAAV1/2 pseudo-typed virus (chimeric virions containing equal numbers of AAV serotype 1 and 2 capsid proteins with AAV2 ITRs; Hauck et al., 2003) was generated as described in During et al. (2003).

Shortly, ten plates (15 cm diameter) of human embryonic kidney 293 cells were transfected by standard calcium phosphate transfection. DNA mixtures for transfection contained the AAV expression plasmid (see 2.2.1; 12.5 µg/plate), the adenovirus helper plasmid pFdelta6 (25 µg/plate) and both the AAV1 and AAV2 helper plasmids (pH21 and pRV1 respectively; 6.25 µg/plate) (pFdelta6, pH21 and pRV1 were obtained from Dr. Matthias Klugmann (University of Mainz, Germany)).

48 hours after transfection cells were scraped in phosphate-buffered saline (PBS; pH 7.4) at room temperature (RT), centrifuged (10 min, 800 rpm, 4°C) and resuspended in 20 mM Tris 150 mM NaCl (pH 8.0, RT). Subsequently, cells were lyzed by two freeze-thawing cycles and incubated with sodium deoxycholate (0.5 % final concentration; Sigma-Aldrich, St. Louis, Missouri, USA) and Benzonase (35-50 U/ml final concentration; Sigma-Aldrich, St. Louis, Missouri, USA) at 37°C for 1 hour. After centrifugation (15 min, 3,000 x g, 4°C) the virus containing supernatant was loaded on a 1 ml HiTrap Heparin HP column (GE Healthcare, Chalfont St. Giles, Great Britain) and the virus was eluted under high-salt conditions (400-500 mM NaCl). Subsequently, the virus was concentrated and rebuffered with PBS in Amicon Ultra tubes (Millipore, Billerica, Massachusetts, USA) and sterile filtered through a

0.2 µm Acrodisc column (Pall Corporation, East Hills, New York, USA).

Purity and integrity of the virus preparation was monitored on a GelCode (Pierce Biotechnology, Rockford, Illinois, USA) stained sodium dodecyl sulfate (SDS)-protein gel. The genomic titers were determined by real-time polymerase chain reaction (PCR) using the ABI 7700 cycler (Applied Biosystems, Foster City, California, USA) with primers and probe designed to WPRE. The infectious titers were determined by serial dilutions on primary hippocampal cultures after counting infected neurons.

2.2.3 Primary hippocampal cultures

Primary hippocampal cultures were prepared from E18-19 Sprague-Dawley rat embryonic brains after dissociation with trypsin and plating on poly-L-lysine-coated 12-well chambers (Techno Plastic Products, Trasadingen, Switzerland) at a density of 50,000 cells per well. The neurons were plated in minimal essential medium containing Earle's salts and glutamine with 10 % fetal bovine serum, 0.45 % glucose, 1 mM sodium pyruvate, 25 µM glutamate, 100 U/ml penicillin and 100 µg/ml streptomycin. After 3-6 hours, the medium was replaced by neurobasal medium supplemented with B27, 0.5 mM glutamine, 100 U/ml penicillin and 100 µg/ml streptomycin. One week after plating the neurons, AraC was added at a final concentration of 3 µM. Half of the medium was exchanged once a week (all media and additives from Invitrogen, Carlsbad, California USA).

2.2.4 Virus injection

For stereotaxic rAAV delivery, mice (10-12 weeks of age) were anesthetized intraperitoneally with a mixture of ketamine hydrochloride (90 mg/kg)/xylazine (5 mg/kg) in PBS. The skin above the skull was shaved and afterwards numbed with 1 % lidocainhydrochlorid at least 5 min before incision.

The skull was exposed and a craniotomy was performed 2.1 mm anterior to bregma and 1.4 mm from the midline (dorsal HPC) or 2.65 mm anterior to bregma and 3.35 mm from the midline (ventral HPC) using a stereotaxic frame (David Kopf Instruments, Tujunga, California, USA). Levels of the anterior-posterior and medio-lateral plain were adjusted using an eLeVeLeR (Sigmann-Elektronik, Hüffenhardt, Germany) leveling device. A 33 gauge beveled needle fitted to a 10 µl syringe

containing the viral solution was inserted at a depth of 1.25 and 2 mm (dorsal HPC) or 3.3 mm (ventral HPC) relative to bregma and virus-containing solution was injected bilaterally at a speed of 100 nl/min (dorsal HPC: 2x1 µl; ventral HPC: 2 µl) by a microprocessor-controlled minipump (World Precision Instruments, Sarasota, Florida, USA). For injections of the complete HPC, coordinates for dorsal and ventral HPC were used in combination.

2.3 Immunohistochemistry

2.3.1 Fluorescent staining of primary hippocampal cultures

After three weeks in culture, neurons were fixed with 4 % paraformaldehyde (PFA; Sigma-Aldrich, St. Louis, Missouri, USA) and 0.12 M sucrose in PBS for 30 min, permeabilized with 0.2 % Triton X-100 for 5 min, blocked in 5 % normal goat serum (NGS), 0.05 % Triton X-100 in PBS for 1 hour, and incubated overnight (ON) at 4°C in primary antibody-containing solution (2 % NGS, 0.05 % Triton X-100 in PBS). After washing 3x10 min in PBS, cultures were incubated in secondary antibody-containing solution (2 % NGS, 0.05 % Triton X-100 in PBS) for 2 hours. After washing in 2 % NGS, 0.05 % Triton X-100 in PBS for 15 min and twice in PBS for 15 min, cover-slips were mounted on Superfrost glass slides (Menzel, Braunschweig, Germany) with Aqua/Poly-Mount (Polysciences, Warrington, Pennsylvania USA). All steps, except primary antibody incubation, were carried out at RT.

Primary antibodies and concentrations: mouse anti-myc (1:500; Santa Cruz Biotechnology, Santa Cruz, California, USA), rabbit anti-Cre (1:5,000; Covance, Princeton, New Jersey, USA).

Secondary antibodies and concentrations: Cy3-conjugated goat anti-rabbit IgG, Cy3-conjugated donkey anti-mouse IgG (1:200; both Jackson ImmunoResearch Laboratories Inc., West Grove, Pennsylvania, USA).

2.3.2 Fluorescent immunostaining of brain slices

Mice were transcardially perfused with Heparin-containing (5 U/ml) PBS followed by 4 % PFA (Sigma-Aldrich, St. Louis, Missouri, USA) in PBS. Free-floating vibratome brain sections (50 µm) were pre-incubated in 0.1 M glycine in PBS for 20 min and subsequently transferred to a solution containing 3 % bovine serum albumin (BSA), 5 % fish gelatine (both Sigma-Aldrich, St. Louis, Missouri, USA), 1 % Triton

X-100 in PBS for 1 hour. Brain slices were then transferred to antibody-containing solution (3 % BSA, 2.5 % fish gelatine, 0.5 % Triton X-100 in PBS) and incubated ON at 4°C. Afterwards, slices were washed 4x10 min in 0.1 M glycine in PBS, and incubated with fluorescently labeled secondary antibody in 3 % BSA, 2.5 % fish gelatine, 0.5 % Triton X-100 in PBS for 2 hours. After washing 4x10 min in 0.1 M glycine in PBS, the sections were mounted on Superfrost glass slides (Menzel, Braunschweig, Germany), dried and cover-slipped with Aqua/Poly-Mount (Polysciences, Warrington, Pennsylvania USA). All steps, except primary antibody incubation, were carried out at RT.

Primary antibodies and concentrations: mouse anti-NeuN (1:1,000; Millipore (Chemicon), Billerica, Massachusetts, USA), rabbit anti-Cre (1:5,000; Covance, Princeton, New Jersey, USA).

Secondary antibodies and concentrations: Cy3-conjugated donkey anti-mouse IgG (1:200; Jackson ImmunoResearch Laboratories Inc., West Grove, Pennsylvania, USA), Alexa Fluor® 488 goat anti-rabbit IgG (1:300; Invitrogen, Carlsbad, California USA)

2.3.3 Diaminobenzidine (DAB) immunohistochemistry of brain slices

Mice were transcardially perfused as described above. Free-floating vibratome brain sections (50 μm) were pre-incubated in 4 % NGS, 1 % BSA, 1 % H_2O_2 (all Sigma-Aldrich, St. Louis, Missouri, USA), 0.3 % Triton X-100 in PBS for 2 hours. Slices were then transferred into antibody-containing solution (1 % NGS, 1 % BSA, 0.3 % Triton X-100 in PBS) and incubated ON. Slices were then washed 4x10 min in PBS, and afterwards incubated with horseradish-peroxidase (HRP)-conjugated secondary antibody in 0.3 % BSA 0.1 % Triton X-100 in PBS for 1 hour. Subsequently, slices were washed 3x10 min in 0.3 % BSA, 0.1 % Triton X-100 in PBS and once for 10 min in PBS. Sections were then incubated in 0.5 mg/ml DAB, 0.01 % H_2O_2 for 5-8 min. Staining was stopped by washing 4x5 min in PBS. Afterwards, sections were mounted on Superfrost glass slides (Menzel, Braunschweig, Germany), dried and dehydrated by dipping in serially increasing ethanol concentrations (70/95/100 %). Slides were then incubated in xylene and subsequently mounted with Eukitt (Sigma-Aldrich, St. Louis, Missouri, USA). All steps were carried out at RT.

Primary antibodies and concentrations: rabbit anti-GluA1 (1:400), rabbit anti-GluA2 (1:200; both Millipore (Chemicon), Billerica, Massachusetts, USA).

Secondary antibody and concentration: HRP-conjugated goat anti-rabbit IgG (1:600; Vector Laboratories, Peterborough, UK).

2.3.4 Microscopy and image analysis

Fluorescently stained hippocampal cultures were imaged using a Zeiss microscope connected to a UV-lamp and a filter set fitted to Cy3-flourescence. The microscope was connected to a camera (Axiocam). Images were acquired and saved using the Axiovision software (all microscope equipment by Carl Zeiss AG, Oberkochen, Germany). For virus titer determination five images of each virus dilution were taken with a 20x magnifying objective and the number of infected neurons over all neurons (imaged with dark field) was calculated.

Detection of fluorescent neurons on stained coronal sections was conducted by confocal laser scanning microscopy with a Zeiss LSM5 microscope (Carl Zeiss AG, Oberkochen, Germany) with a 5x-magnifying objective.

Cre and NeuN co-localization was analyzed by a software written by Dr. Tansu Celikel (USC, Los Angeles, California, USA) running in MATLAB (MathWorks, Natick, Massachusetts, USA). All images containing Cre-positive neurons were analyzed. After normalization, the software located hippocampal areas. Within these areas, Cre- and NeuN-immunopositive neurons were quantified in pixels. After analysis each image was assigned as representing either dorsal, or ventral hippocampal areas. An average of Cre and NeuN positive pixels over all images was made for dorsal and ventral HPC.

For imaging of DAB-stained brain slices, bright field images were obtained with a Zeiss microscope (2.5x magnifying objective) connected to a camera (Axiocam). Images were acquired and saved using the Axiovision software (all microscope equipment by Carl Zeiss AG, Oberkochen, Germany).

2.4 Immunoblotting

2.4.1 Preparation of synaptoneurosomes

Two *GluA1*^{-/-} mice (females) were injected into the right hemisphere with the GluA1(Q)-expressing virus. Three weeks after injection, these mice together with two untreated WT mice (males) were sacrificed and HPCs were dissected.

Synaptoneurosomes were prepared as described in Whitlock et al. (2006). Briefly, after dissection, HPCs were split in to three equal pieces. The most septal (dorsal) pieces were homogenized in 0.5 ml ice-cold homogenization buffer (10 mM Hepes, 1.0 mM EDTA, 2.0 mM EGTA, 0.5 mM DTT) supplemented with Complete EDTA-free Protease inhibitor cocktail (1 tablet/50 ml; Roche Diagnostics AG, Risch, Switzerland). HPCs were homogenized in a glass/Teflon tissue homogenizer (900 rpm; 10 strokes), and homogenates were passed through a 100-μm-pore nylon-mesh filter (BD Biosciences, Franklin Lakes, New Jersey, USA) and then through a 5 μm pore-filter (Whatman (Schleicher & Schuell), Maidstone, Great Britain). Filtered homogenates were centrifuged at 3,600 x g for 10 min at 4°C. Resulting pellets were resuspended in 100 μL pre-heated (72°C) 1 % SDS (in homogenization buffer), incubated for 5 min at 72°C, and stored at −70°C.

2.4.2 Quantitative immunoblotting

Equal amounts of synaptoneurosome lysate, determined by Bradford assay (BioRad, Hercules, California, USA), were resolved on 8 % polyacrylamide gels, and blotted onto polyvinylidene fluoride membranes (GE Healthcare, Chalfont St. Giles, Great Britain). Membranes were blocked with 10 % non-fat dry milk in tris-buffered saline (TBS)-Tween 20 (0.1 %) for 1 hour and incubated in primary antibody (rabbit GluA1 1:1,000; Millipore (Chemicon), Billerica, Massachusetts, USA) containing solution (1 % non-fat dry milk in TBS-Tween 20). Blots were then washed 4x10 min in TBS-Tween 20 and placed in HRP-conjugated anti-rabbit secondary antibody (1:5,000; GE Healthcare, Chalfont St. Giles, Great Britain) containing solution (1 % non-fat dry milk in TBS-Tween 20). Blots were then washed 4x10 min in TBS-Tween 20, and incubated in ECL plus reagent (GE Healthcare, Chalfont St. Giles, Great Britain) for 5 min.

ECL plus treated blots were developed using autoradiographic ECL-hyperfilms (GE Healthcare, Chalfont St. Giles, Great Britain). Digital images, produced by densitometric scanning of autoradiographs were quantified using the Gel Analyzer tool in ImageJ (National Institutes of Health, USA).

2.5 Behavioral testing

2.5.1 Groups and tests assessed

For behavioral testing two different approaches were used. For the first approach (further referred to as '*knock-in approach*'), *GluA1$^{-/-}$* mice were injected with GluA1 expressing virus in dorsal or complete HPC. For the *knock-in approach* two cohorts of mice were injected and subsequently tested for behavior. In the first cohort *GluA1$^{-/-}$* mice were injected with GluA1(Q)- (dHPC A1(Q), N=8, all males) or GluA1(R)-expressing virus (dHPC GluA1(R), N=5, all males) in dorsal HPC. *GluA1$^{+/-}$* littermates (N=10, all males) were used as controls. For the second cohort *GluA1$^{-/-}$* mice were injected with the GluA1(Q)-expressing virus in complete HPC (cHPC A1(Q), N=12, all males). In this cohort uninjected *GluA1$^{-/-}$* and WT mice served as controls. In both cohorts behavioral testing started four weeks after virus injection.

In the second approach (further referred to as '*knock-out approach*'), *GluA1$^{2lox/2lox}$* mice were injected with Cre-expressing virus in dorsal (ΔdHPC, N=7, all females) or ventral (ΔvHPC, N=13, all females) HPC. WT controls were injected with a Cre-expressing virus in ventral HPC (WT-Cre, N=7, all females). For these groups, behavioral testing started twelve weeks after virus injection.

The behavioral tests performed can be classified into three groups: (1) Tests for activity and general cognitive abilities, (2) tests for SWM and (3) tests for emotionally motivated learning. The tests performed are illustrated in Table 1.

Table 1: Behavioral tests performed and their behavioral context. The numbers in the three right columns represent the actual order in which the tests were performed for each approach. In parentheses the number of days needed for each test is given.

Name of the test	Behavioral context	Knock-in approach 1st cohort	Knock-in approach 2nd cohort	Knock-out approach
Open field	*Locomotor activity*	4. (1 day)	1. (1 day)	Not tested
Puzzle box	*General cognitive abilities*	3. (4 days)	Not tested	Not tested
Rewarded alternation	*SWM*	1. (6 days)	2. (6 days)	2. (16 days)
Novel arm exploration	*SWM*	2. (1 day)	3. (1 day)	Not tested
Pavlovian fear conditioning	*Learned fear*	5. (3 days)	Not tested	3. (3 days)
Porsolt forced swim test	*Behavioral despair*	Not tested	Not tested	1. (2 days)

2.5.2 Tests for activity and general cognitive abilities

2.5.2.1 Locomotor activity in the open field

Open field exploration was studied in a black-painted wooden arena (60x60x30 cm) with a white ground. Each mouse was placed at a corner of the open field and allowed to explore for 5 min while motor activity was monitored using a video camera (COHU; Pieper GmbH, Schwerte, Germany) placed 200 cm above the open field registered sessions at 25 Hz with a spatial resolution of ~0.6 mm/pixel. Software written by Tansu Celikel (USC, Los Angeles, California, USA) running in MATLAB (MathWorks, Natick, Massachusetts, USA) acquired a copy of each frame on-line and located the mouse in the arena using center of mass calculation. Distance traveled and the amount of time mice spent in the center (the center 36x36 cm) of the open field, were calculated from these activity traces.

2.5.2.2 General cognitive abilities in the puzzle box

The puzzle box consisted of a transparent Plexiglas box (30 x 40 x 25(H) cm) divided into two compartments of equal size. The dark goal compartment was coated with black carton and covered with a lid. Inside this compartment a Plexiglas petri dish containing home-cage bedding was put. The open start compartment was coated

with white carton and brightly illuminated (~1,000 lux) with a neon lamp. A wall separated the two compartments. Mice were able to enter the dark compartment through different barriers (see below). The box was positioned on a table to allow direct observation of behavior by the experimenter.

Testing took place in a gently lit room. A trial started by placing a mouse into the start compartment with its head facing the back wall (opposite of the entrance). Trial duration was 3 min for the first seven trials and 4 min for the last three trials. Trials were separated by either a short (1 min) or long (24 hours) ITI (*i.e.* the time between two trials). At the end of each trial mice were kept in the dark goal compartment for approximately 20 sec and then returned to their home cage. The box was cleaned with water after testing.

The following barriers were used: (trial 1) Door barrier, (trial 2-4) open underpass, (trial 5-7) underpass filled with sawdust, (trial 8-10) underpass covered with a cardboard plug (2.9 g weight). Each barrier, except for the door barrier, was used three times. Between the first and second exposure to a barrier an ITI of 1 min was used. Between second and third exposure to a barrier an ITI of 24 hours was used (Figure 6).
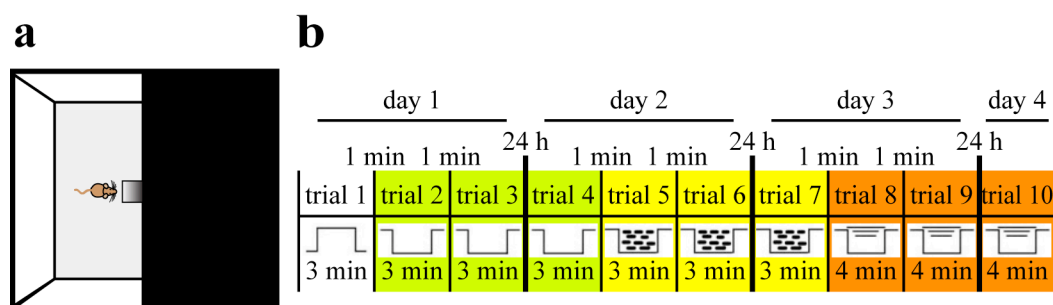
Figure 6: Schematic representation of the puzzle box paradigm. The mouse was put into the brightly lit white start compartment and had to shuttle to the dark goal compartment through barriers of different features. **(a)** These barriers were a door barrier (trial 1), an opened underpass (trial 2-4; highlighted in green), an underpass filled with sawdust (trial 5-7; highlighted in yellow) and an underpass covered with a cardboard plug (trial 8-10; highlighted in orange). These trials were separated by a 1 min or 24 hours ITI **(b)**.

2.5.3 Tests for spatial working memory

2.5.3.1 Rewarded alternation on the T-maze

Rewarded alternation was studied on a T-maze as described in Deacon & Rawlins (2006). In brief, every trial of the training included two runs, sample run and choice run. On each trial, the sample arm was assigned to one of the two target arms

randomly, and the mouse was directed to the sample arm where it was rewarded with 50 % diluted (in water) sweetened condensed milk. After the mouse drank the milk it was taken out of the maze and after approximately 5 sec the choice run was given, during which it was required to choose one of the two accessible goal arms. If the mouse chose the previously unvisited arm ("successful alternation"), it was rewarded.

Mice received eight trials per day (separated in two sessions) with a minimal retention interval (*i.e.* the interval between sample and choice run) of approximately 5 sec until groups reached asymptotic levels of performance. When a group other than the control group performed above chance level (50 %), mice were tested for eight sessions (four trials per session, two sessions per day) with different retention intervals (~5, 30, 60 and 120 sec) randomly distributed within each session to increase load of working memory.

The wooden T-maze was painted in black and elevated 150 cm from the ground. The start arm (47x10 cm) and the two identical goal arms (35x10 cm) were surrounded by a 10 cm high wall. A metal food well was located 3 cm from the end of each goal arm (Figure 7).
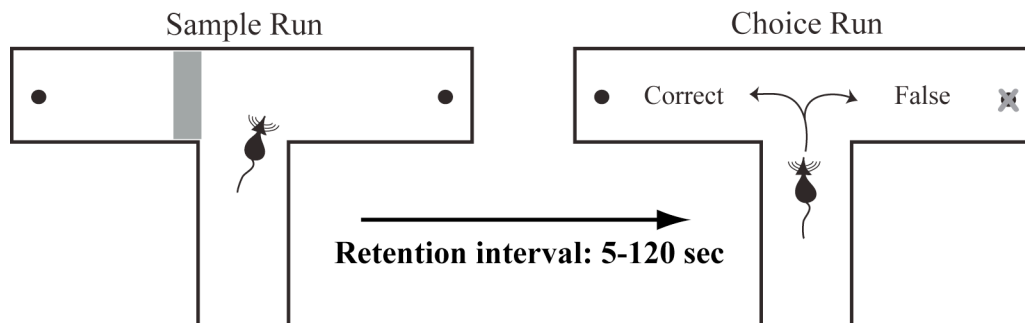
Figure 7: Illustration of rewarded alternation studied on the T-maze. This test was composed of two runs, a sample run (with one arm being blocked) and a choice run (with both arms accessible). Choosing the previously unvisited arm was considered a correct response (successful alternation) and was therefore rewarded.

2.5.3.2 Novel arm exploration on the Y-maze

Novel arm exploration was studied on an elevated Y-maze with several extra maze cues like described in Sanderson et al. (2009). Two arms of the Y-maze were assigned to each mouse (start arm and other arm) to which it was exposed during the exposure phase. The remaining third arm, which was blocked during the exposure phase, represented the novel arm during the test phase. Allocation of arms (start, other, and

novel) to specific spatial locations was counterbalanced within each experimental group. During the five exposure trials, mice were placed at the end of the start arm and were allowed to both the start and other arm for 2 min before being removed and returned to their home cage. Timing of the 2-min period began once the mouse had left the start arm.

Exposure trials were separated by a 1 min ITI. An entry into an arm was defined by a mouse placing all four paws inside an arm. Similarly, a mouse was considered to have left an arm if all four paws were placed outside the arm. Therefore, if a mouse had entered an arm but subsequently placed fewer than four paws outside the arm, it was still classed as remaining in the arm.

The test phase began 1 min after the last exposure trial. During the test phase, mice were allowed free access to all three arms. Mice were placed at the end of the start arm and were allowed to explore all three arms for 2 min once they had left the start arm. The amounts of time that mice spent in each of the three arms and the number of arm entries were recorded.

The three identical arms (50x9 cm, 0.5 cm beading) of the black wooden maze were connected to each other with a triangle. The arms of the maze were placed at an angle of 120° between two neighboring arms, and equipped with a feeder placed 3 cm from the distal end. The location and orientation of the maze relative to distal cues stayed the same throughout the training (Figure 8).
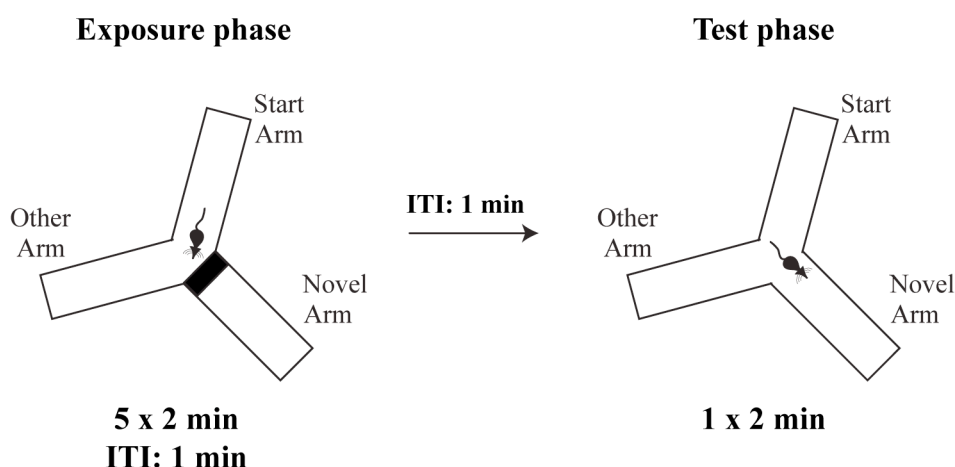
Figure 8: Novel arm exploration on the Y-maze. This test was separated into an exposure and a test phase. During the exposure phase mice were exposed five times for 2 min to two arms (start and other arm) of a Y-maze while the third arm (novel arm) was blocked. The ITI between each trial was 1 min. 1 min after the last trial of the exposure phase, the test phase was started. During this phase the block was removed and the mouse was allowed to explore all three arms.

2.5.4 Tests for emotionally motivated learning

2.5.4.1 Pavlovian fear conditioning

The conditioning system (commercially available from TSE, Bad Homburg, Germany) consisted of a soundproof box (58x30x27 cm) with a gray interior and a black Plexiglas chamber (35x20x20 cm) that was placed on a shock grid made of stainless steel rods (0.4 cm diameter, spaced 0.9 cm apart). The grid was connected to a shocker/scrambler unit delivering electrical shocks of defined duration and intensity. The chamber received ambient illumination from a 12 V house light. A speaker emitted a computer-generated tone/noise (set to 50 dB white noise or 7.5 kHz 200 dB sine tone). A fan supplied the chamber with fresh air. The chamber was surrounded by infrared detectors measuring locomotor activity of the mice (Figure 9a).

For Pavlovian fear conditioning, mice were transferred to the operant chamber and, after an initial acclimation period of 6 min, were presented with three pairings of the auditory conditioning stimulus with foot shock (0.4 mA; 2 sec). The cue was presented for 30 sec, and the shock was administered for the last 2 sec, co-terminating with the auditory cue. Pairings were separated by 2 min, and mice were removed from the chamber 2 min after the last shock presentation. 24 hours after training, mice were tested for the conditioned stimulus (CS)-induced conditioned responses. The black Plexiglas chamber was replaced by a transparent Plexiglas chamber and patterns were attached to the walls of the sound attenuation chamber. Additionally, the shock-grid was covered with a grey Plexiglas plate. After an initial acclimation period of 6 min, the CS was presented for 8 min (CS test). 24 hours later, an additional test was performed for context conditioning. The chambers were altered to the original configuration used during conditioning. Subjects were placed in the chamber for 8 min (context test). The mice of the *knock-out approach* were tested for contextual fear before they were tested for cued fear (Figure 9b).

During each stage of fear conditioning, freezing duration and activity were analyzed using the TSE analysis program.
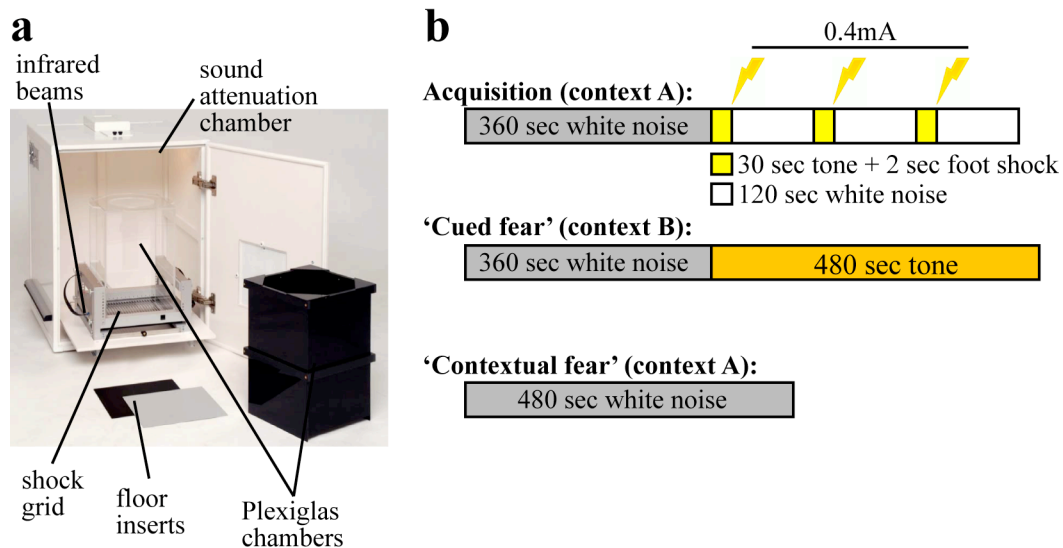
Figure 9: Schematic representation of the fear conditioning paradigm. In **(a)** the fear conditioning apparatus is shown. **(b)** The fear conditioning paradigm was separated into an acquisition phase (in context A) followed by a test for 'cued fear' (in context B) and a test for 'contextual fear' (in context A). During the acquisition phase mice were subjected three times to a 30 sec tone that was co-terminated with a 2 sec foot shock. After 24 hours mice were subjected to the tone that was previously associated with the foot-shock, in a different context. Another 24 hours later mice were placed into the original context and behavior was observed.

2.5.4.2 FST

The FST included two sessions of forced swimming administered at a 24 hours interval in a white plastic chamber (Ø 30 cm) filled with warm water (25±1°C) to a height of 10 cm. Both sessions were conducted similarly with the exception of the duration of sessions (Session 1: 15 min; Session 2: 10 min). At the start of each session, mice (all females) were individually placed at the centre of the pool and left alone to swim. After the session ended, mice were placed under a red light heating lamp and dried before returning it to their home cage.

A camera (COHU; Pieper GmbH, Schwerte, Germany) placed 140 cm above the chamber surface registered sessions at 25 Hz with a spatial resolution of ~0.6 mm/pixel. Software written by Dr. Tansu Celikel (USC, Los Angeles, California, USA) running in MATLAB (MathWorks, Natick, Massachusetts, USA) acquired a copy of each frame on-line and located the mouse in the chamber using center of mass calculation. Vector analysis on the location of the mouse across frames was performed to calculate the latency to immobility and time of immobility. Latency to immobility was described as the onset of the three consecutive bins (1 sec/bin) when

the speed of mouse movement was <3 cm/sec. This threshold was empirically quantified in pilot experiments and incorporates the passive mobility of the mouse due to water movements in the enclosed chamber even after mice start floating (Marx, 2007; Freudenberg et al., 2009). Rate of immobility is represented in percentile scale and was calculated as a ratio between the amount of time mice spent below threshold (speed of movement <3 cm/sec) and the duration of the session. This normalization on the duration of immobility was necessary to ensure that immobility measurements are comparable across the two sessions with different durations (Figure 10).
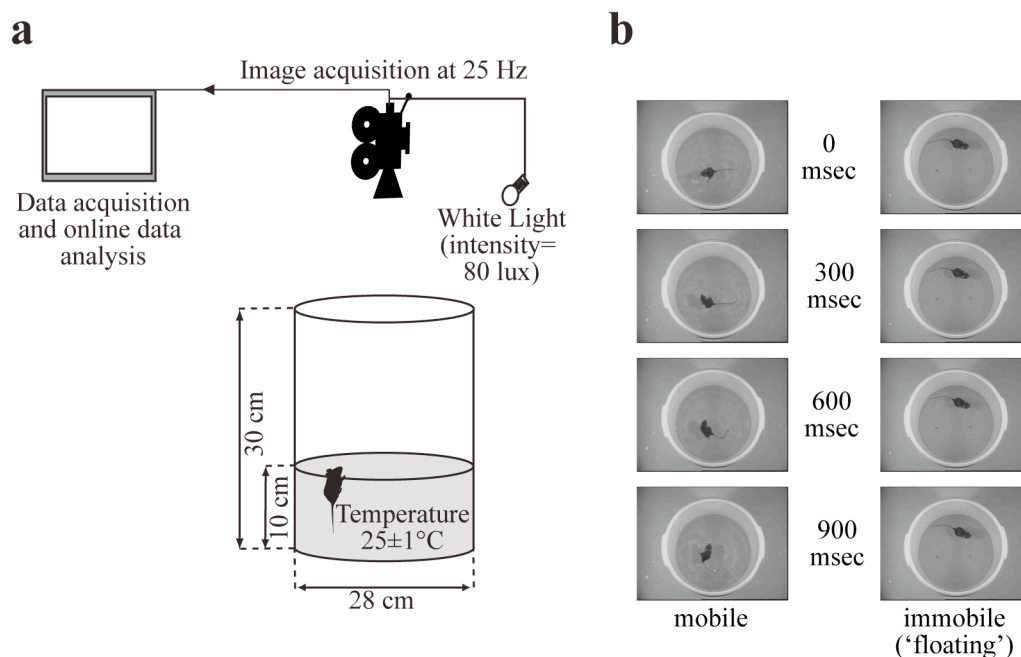
Figure 10: Behavioral despair measured with the FST. **(a)** The FST was composed of two sessions, separated by 24 hours, of forced swimming. Mice were put into a swimming pool and a computer, connected to a camera, analyzed their swimming behavior on-line. The time until mice started floating (Latency to immobility) and overall immobility were analyzed. **(b)** An exemplary movie frame series of a mouse when it is mobile (*i.e.* active; left image series) and when it is immobile (*i.e.* floating; right image series) is shown.

2.6 Statistical analysis

The analysis of variance (ANOVA) was used as the principal method for group comparisons after testing the data for normality and equal variance. When testing for one factor a One Way ANOVA was performed. If normality or equal variance test failed, non-parametric ANOVA on Ranks test was used for comparison. When testing for two factors a Two Way repeated measures (RM) ANOVA was performed. If

normality or equal variance tests failed data were transformed using a square root or rank transform before analysis. When ANOVA revealed a statistically significant difference pairwise multiple comparison procedures were used for post hoc testing. Regardless of the type of the test chosen, uncorrected alpha (desired significance level) was set to 0.05 (two-tailed). Data are displayed as the mean and standard error of the mean (SEM).

All statistical analysis was performed using SigmaStat (Systat, San José, California, USA).

3 Results

3.1 Viruses and virus infection

Before mice were injected for behavioral testing, the quality of the different viruses was determined. The tests for virus quality are presented for the GluA1- and Cre-expressing rAAVs. Additionally, the efficiency of injections of mice that were used for behavioral testing is shown.

3.1.1 GluA1 expressing viruses

3.1.1.1 Quality of virus purification and virus titers

To test for quality of heparin column purification, two different concentrations of GluA1-expressing rAAVs were loaded on an SDS-protein gel. These gels were stained with GelCode to visualize protein content. Gels loaded with GluA1(Q) and GluA1(R)-expressing viruses showed only bands for viral capsid proteins (VP1-3). Contamination by other proteins was not observed (Figure 11a).
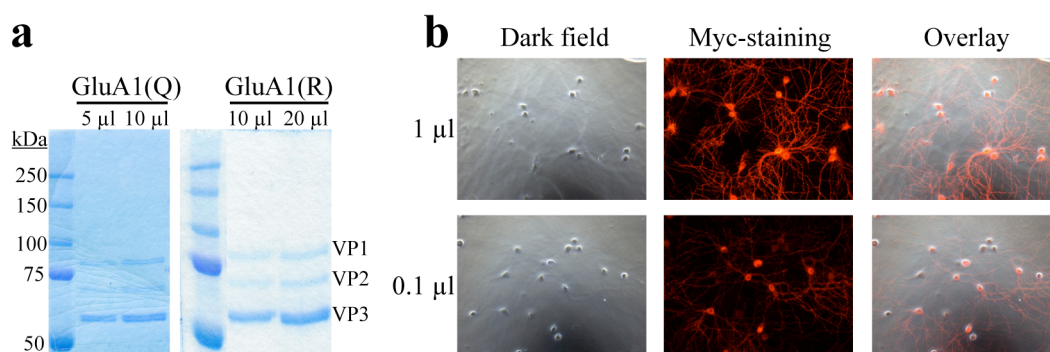
Figure 11: Quality controls of GluA1-expressing viruses. **(a)** GelCode stained SDS-gels loaded with GluA1(Q)- (left) and GluA1(R)-expressing rAAVs. **(b)** Hippocampal primary neurons infected with GluA1(Q)-expressing virus. Dark field images (left), myc-positive fluorescence and the overlay (right) are shown. Top images show neurons infected with 1 µl, bottom images with 0.1 µl of virus containing solution.

To test the infectious titer, hippocampal primary neurons were infected with 1 and 0.1 µl of GluA1(Q)-expressing virus-containing solution. The neurons were stained for the myc-tag and myc-positive neurons were counted. Five images for each virus dilution were evaluated. About 77 % of the neurons infected with 1 µl of virus were myc-positive and 0.1 µl of virus still infected about 56 % of the neurons. Since there are 50,000 neurons that can possibly infected, 1 µl of virus is potentially able to infect

approximately 160,000 neurons. However, variation between the two virus dilutions was very high (Figure 11b; Table 2).

Quantification of the genomic titer with real-time PCR resulted in 4.5 x 10^8 genomes/µl (data not shown). This is almost 3,000-times higher than the infectious titer. This is in relatively good agreement with the infectious titer, which, according to our observations, is usually 1,000-times lower than the genomic titer.

Table 2: Determination of infectious titer of Synapsin GluA1(Q)-expressing virus. For two different virus concentrations five dark field and fluorescent images were obtained and analyzed.

Image #	1µl virus		0.1 µl virus	
	Myc-positive neurons	Total number of neurons	Myc-positive neurons	Total number of neurons
1	18	23	12	19
2	18	24	11	19
3	12	15	16	29
4	17	22	14	28
5	20	26	8	14
Sum	**85**	**110**	**61**	**109**
	77.3 %		56.0 %	
	Amount of neurons infected by 1 µl (overall amount of neurons: 50,000)			
	38,650		**280,000**	
	Average: ~160,000			

3.1.1.2 Immunoblotting of virus infected HPCs

Efficiency of the GluA1(Q)-expressing virus was further assessed by immunoblotting. *GluA1*^{-/-} mice were unilaterally injected into the dorsal HPC with 2 µl of this virus. After three weeks, synaptoneurosomes were prepared from dorsal HPCs of the injected mice (injected and uninjected HPCs) and WT control mice. Immunoblots of the synaptoneurosomes were stained for GluA1 (Figure 12a) and the amount of protein was quantified by measuring the intensity of stained bands using the ImageJ software (Figure 12b,c). Quantification revealed that the amount of GluA1 in the injected HPCs was about 35 % of that in WT mice. Background from uninjected HPCs from *GluA1*^{-/-} mice resulted in approximately 7 % of WT GluA1-levels.

Taken together, purity, titer and efficiency of the GluA1-expressing viruses seemed to be sufficient for re-expression of GluA1 in the HPC of *GluA1⁻/⁻* mice.
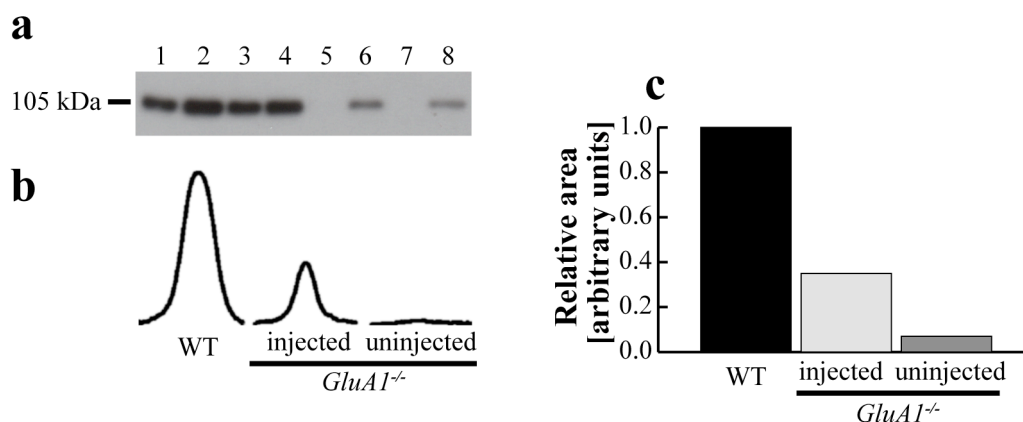

Figure 12: Quantification of the amount of GluA1 expressed by the GluA1(Q)-expressing rAAV. In (**a**) GluA1 the immunoblot from synaptoneurosomes of dorsal HPCs of WT mice (1-4) uninjected (5, 7) and GluA1(Q)-expressing virus injected (6, 8) *GluA1⁻/⁻* mice are shown. In (**b**) exemplary protein quantification is shown for WT and *GluA1⁻/⁻* (injected and uninjected HPCs) mice. The traces are profile plots from top (left) to bottom (right). The areas of these profile plots were quantified relative to those of WT mice using ImageJ (**c**).

3.1.1.3 Efficiency of virus injections

After virus quality was determined, *GluA1⁻/⁻* mice were stereotaxically injected and tested for behavioral performance (see 3.2). Subsequently, efficiency of virus injections with respect to the infected areas was assessed by staining coronal brain sections for GluA1.

Knock-in approach cohort 1: While any GluA1-signal was absent in uninjected *GluA1⁻/⁻* mice (Figure 13a), all *GluA1⁻/⁻* mice injected with a GluA1-expressing virus showed a GluA1-positive immunosignal (Figure 13b,c). Therefore, none of the mice was excluded from analysis of behavioral results. Visual inspection of these stainings revealed a strong expression in dorsal HPC for both GluA1-expressing viruses (*i.e.* GluA1(Q) and GluA1(R)) used. The immunosignal in ventral HPC was restricted to the DG and parts of CA1. Expression levels in dorsal HPC seemed to be comparable to those in *GluA1⁺/⁻* mice. Sections from dHPC A1(Q) mice were predominantly stained in the dendrites (*i.e.* stratum radiatum, stratum oriens of CA1-3 and molecular layer of DG) and only sparsely in the somata (*i.e.* pyramidal and granule cell layers)

(Figure 13b). In contrast, brain slices of dHPC A1(R) mice showed weaker staining in dendrites and a strong signal in somatic layers (Figure 13c).
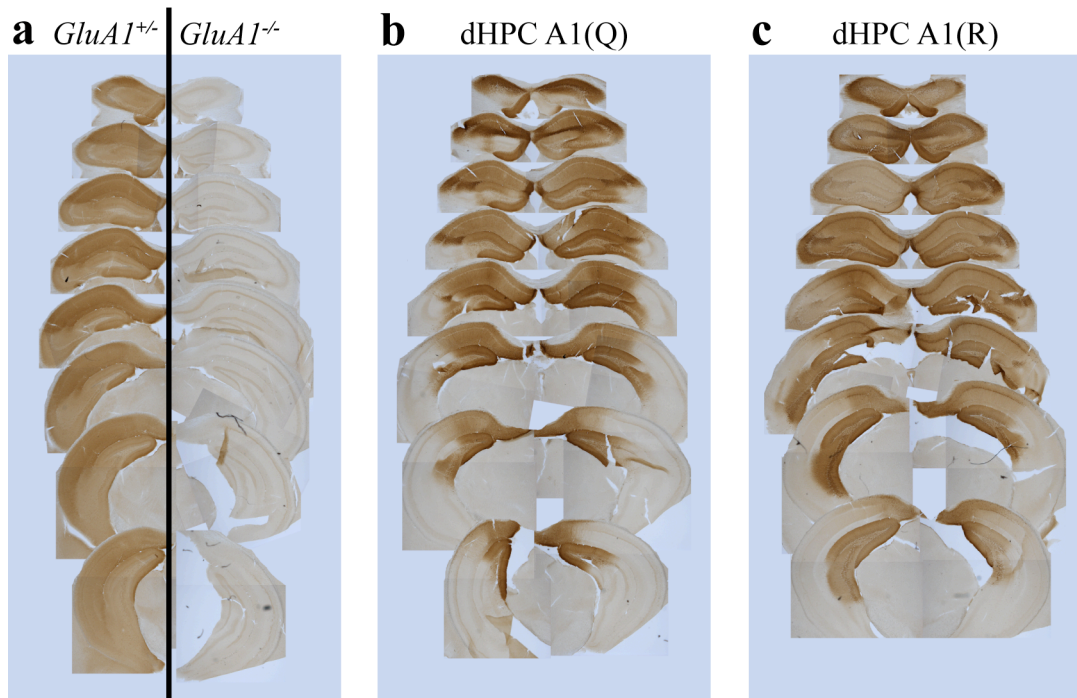
Figure 13: Representative images of stainings for GluA1 in *GluA1$^{+/-}$*, *GluA1$^{-/-}$* (**a**), dHPC A1(Q) (**b**) and dHPC A1(R) mice (**c**) from the first cohort of the *knock-in approach*. The distance between slices is 300 μm.

Knock-in approach cohort 2: One of the mice injected with a GluA1-expressing virus in complete HPC did not show any GluA1-positive signal and was therefore excluded from analysis of behavioral results. Three of the mice were not analyzed for expression yet, because they will be further tested in place cell recordings. All other mice showed a GluA1-positive signal after staining. Qualitative analysis of the slices showed a strong immunosignal for GluA1 in the whole HPC. Only in parts of the ventral HPC staining intensity decreased slightly, particularly in CA1. In all mice, the strongest signal was seen in the dendritic layers. In some slices expression levels were comparable to those observed in WT mice (Figure 14).
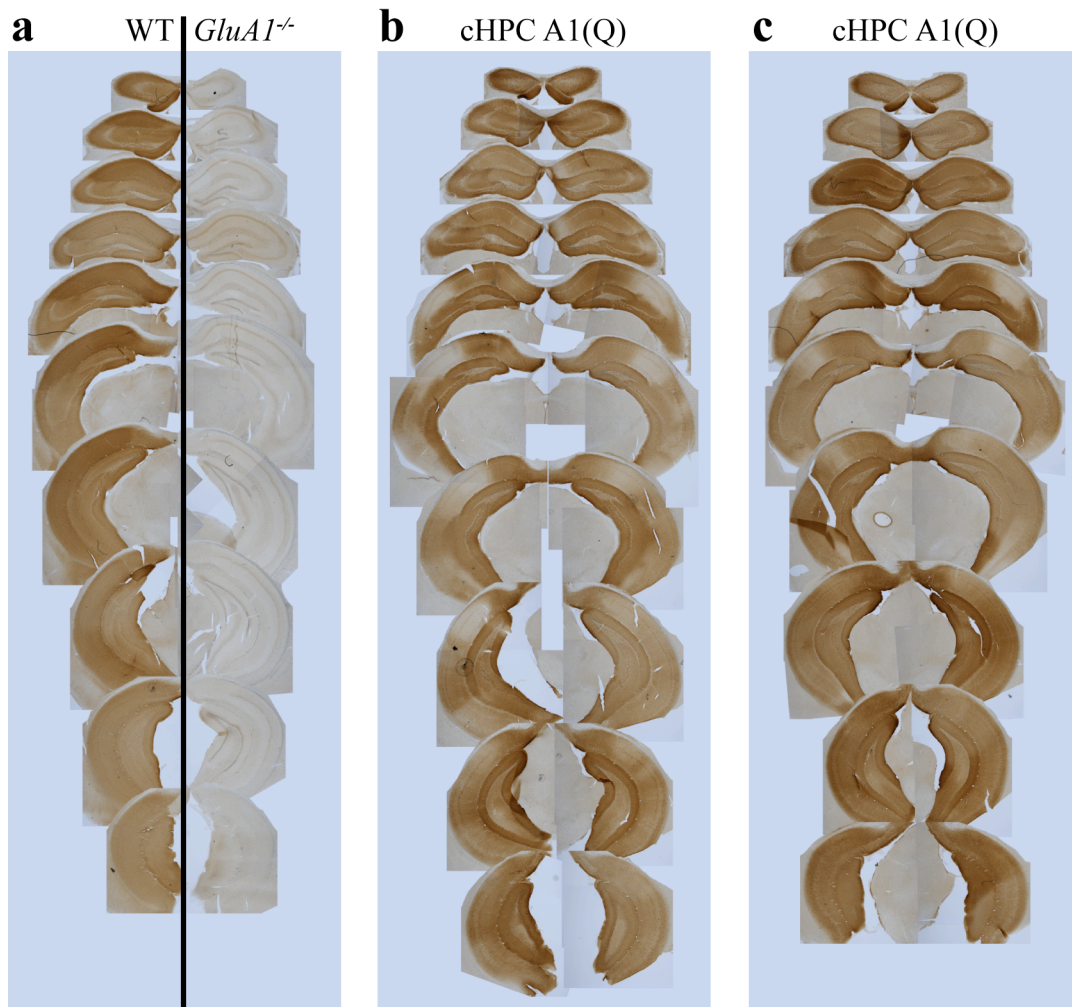
Figure 14: Representative images of GluA1-stainings in WT, *GluA1^{-/-}* (**a**) and cHPC A1(Q) mice (**b, c**) from the second cohort of the *knock-in approach*. The distance between slices is 300 μm.

One immunohistochemical finding in *GluA1^{-/-}* mice was a redistribution of the GluA2 subunit from dendritic to somatic sites, most likely because unassembled GluA2 stays trapped in the ER (Zamanillo et al., 1999). In fact, in GluA2-stainings of *GluA1^{-/-}* mice, we found a predominant immunosignal in the pyramidal and granule cell layers of HPC, while in WT mice mainly dendritic sites were GluA2-positive (Figure 15a,b). Both, dHPC A1(Q) and dHPC A1(R) mice still had a strong GluA2 signal in the somatic layers of hippocampal CA1 and CA3. Notably, the staining of granule cell bodies in DG was mostly gone in mice from both groups. Brain sections of both groups showed a substantial GluA2 positive staining in the dendrites. This was particularly pronounced in dHPC A1(Q) mice. These results suggest that the virally introduced GluA1-subunits are able to form functional receptor assemblies with endogenous GluA2 (Figure 15c,d).

Taken together, the immunohistological findings showed that strong expression of targeted areas was achieved and that the introduced GluA1-subunit seemed to form functional AMPA receptor channel assemblies.
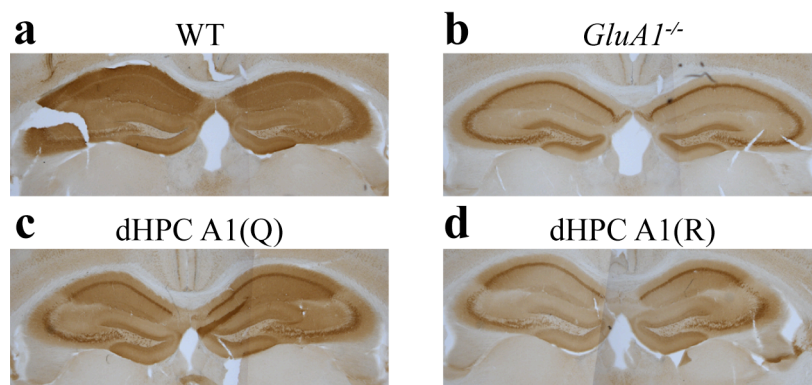
Figure 15: Images of stainings for GluA2 in dorsal HPC sections of a WT mouse (**a**), an uninjected *GluA1$^{-/-}$* mouse (**b**), and dHPC A1(Q) (**c**) and dHPC A1(R) (**d**) mice from the first cohort of the *knock-in approach*.

3.1.2 Cre-expressing virus

3.1.2.1 Quality of virus purification and virus titers

Equal to the GluA1-expressing viruses, a GelCode stained SDS-protein gel of the HA.Cre-expressing virus showed exclusively bands for VP1-3. Contamination by other proteins was not observed (Figure 16a).
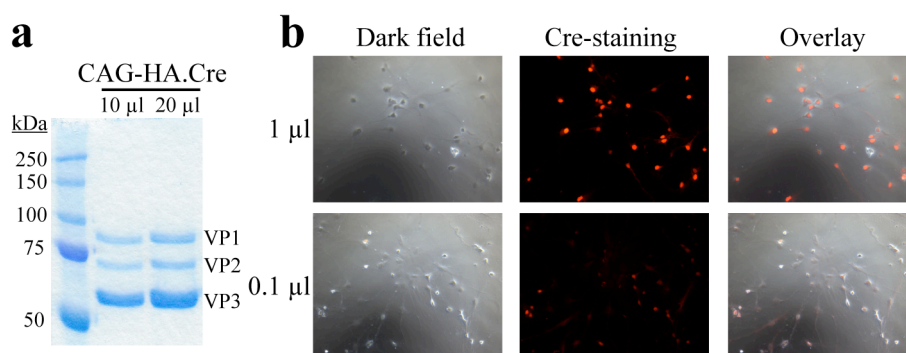
Figure 16: Quality of virus expressing HA-tagged Cre-recombinase under CAG promoter **(a)** A GelCode stained SDS-protein gel loaded with two different amounts of virus containing solution. **(b)** Hippocampal primary neurons infected with CAG-HA.Cre virus. Dark field images (left), Cre-staining fluorescence (middle) and the overlay of them (right) are shown. The top images show neurons infected with 1 µl, the bottom images with 0.1 µl of virus containing solution.

Like for the GluA1(Q) virus, infectious titer of the HA.Cre virus was determined by infection of hippocampal primary neurons, followed by a fluorescent staining for Cre-recombinase (Figure 16b). Infection of primary neurons with either 1 or 0.1 µl of virus containing solution showed about 77 % or 12 % of Cre-positive neurons respectively, resulting in an infectious titer of about 50,000 infectious units/µl. The variation between the two dilutions was relatively low (Table 3).

The genomic titer for the HA.Cre virus was 1×10^9 genomes/µl (data not shown). This is about 20,000 fold higher than the infectious titer and therefore much higher than the commonly observed 1,000 fold higher genomic titer.

Although the infectious titer suggested a relatively low infectivity of the Cre-expressing virus, the genomic titer was very high. Therefore, we assumed that this virus is able to give sufficient infection upon injection in mice.

Table 3: Determination of infectious titer of Synapsin GluA1(Q) virus. For two different virus concentrations four to five dark field and fluorescent images were obtained and analyzed.

Image #	1 µl		0.1 µl virus	
	Cre-positive neurons	Total number of neurons	Cre-positive neurons	Total number of neurons
1	26	33	4	40
2	22	24	5	32
3	19	29	4	47
4	22	29	7	54
5	22	30		
Sum	**111**	**145**	**20**	**173**
	76.6 %		11.6 %	
	Amount of neurons infected by 1 µl (overall amount of neurons: 50,000)			
	38,300		**58,000**	
	Average: ~48,000			

3.1.2.2 Efficiency of virus injections

Following determination of virus quality, we injected WT and *GluA1²ˡᵒˣ/²ˡᵒˣ* mice into HPC with the Cre-expressing virus and tested mice for behavioral performance (see 3.3).

Coronal brain slices from all injected mice were double-stained for Cre-recombinase and NeuN, as a neuronal marker. Slices of all injected mice showed a

Cre-positive signal and therefore none of the mice was excluded from behavioral analysis. However, two mice were excluded from image analysis (one ΔdHPC mouse because of unspecific NeuN staining and one ΔvHPC mouse because no dorsal section was available). Visual inspection of Cre/NeuN-stainings showed expression of Cre-recombinase mainly restricted to the targeted areas (*i.e.* dorsal and ventral HPC). However, sparse expression was observed in non-targeted areas. Mice injected in dorsal HPC (*i.e.* ΔdHPC) expressed Cre recombinase in CA1, DG and most of CA3 (Figure 17a,b). Mice injected in ventral HPC (*i.e.* ΔvHPC and WT-Cre) showed strong expression of Cre-recombinase in CA3 and DG and weaker expression in CA1 (Figure 17c,d).

Quantification of the percentage of neurons that were both Cre- and NeuN-positive showed symmetrical expression of Cre-recombinase. Dorsal HPC-injected mice had 30±2% Cre/NeuN overlay in dorsal HPC. In ventral HPC this rate significantly dropped down to 14±3% (paired t-test, $P<0.05$). For mice injected in the ventral HPC the opposite was observed. While in these mice 13±1% or 12±1% (ΔvHPC and WT-Cre respectively) of neurons in dorsal HPC were Cre- and NeuN-positive, the rate increased significantly to 32±3% or 33±2% (ΔvHPC and WT-Cre respectively) in ventral HPC (paired t-test, $P<0.05$; Figure 17e).

In summary, virus injection of mice from the *knock-out approach* resulted in high levels of expression and relatively high targeting-specificity.
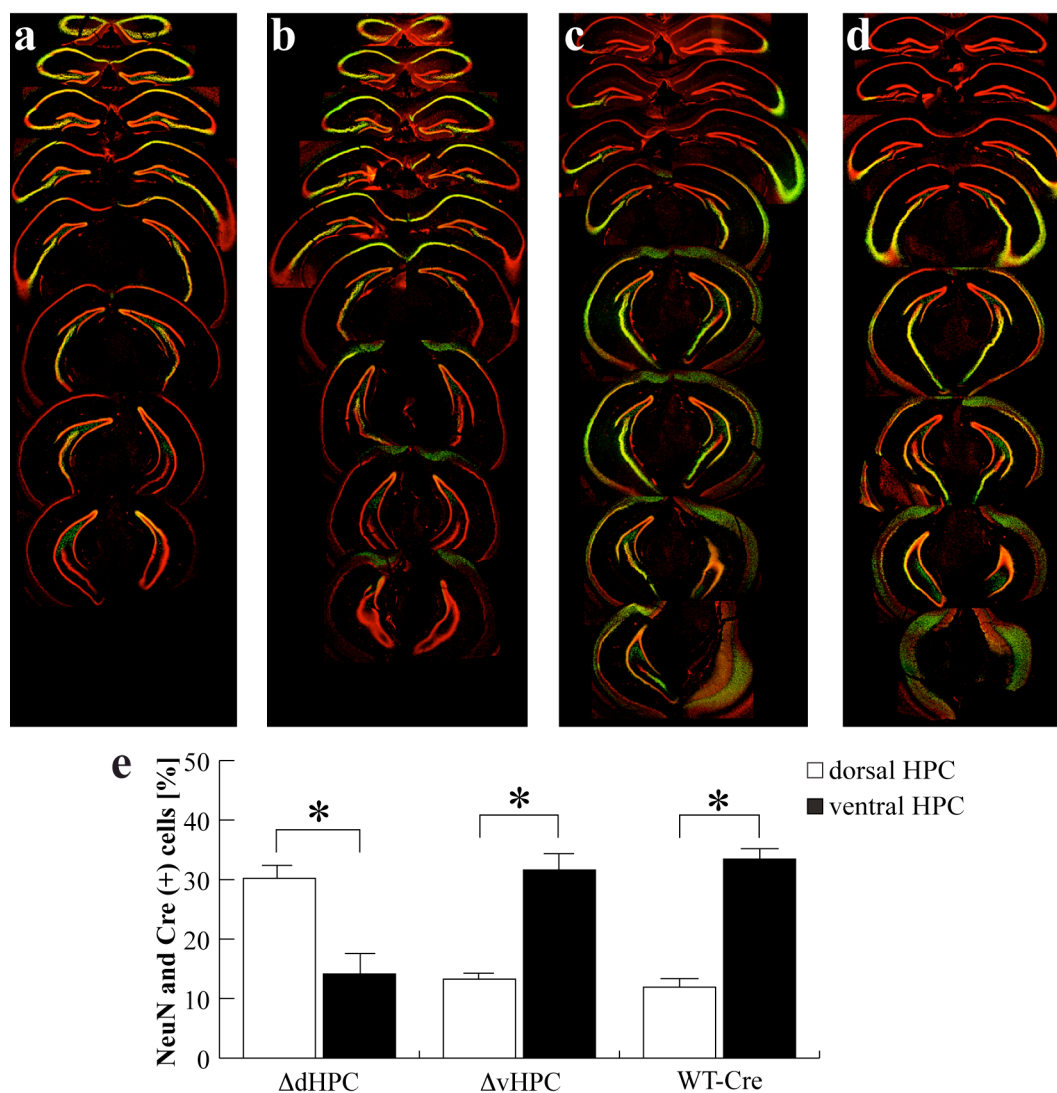
Figure 17: Representative images of Cre-expression in *GluA1*^{*2lox/2lox*} mice injected with Cre-expressing rAAV. Overlay of Cre- (green) and NeuN-staining (red) from hippocampal sections of ΔdHPC (**a, b**) and ΔvHPC (**c, d**) mice. Areas that are Cre-/NeuN-double-positive are illustrated in yellow. (**e**) Quantification of Cre- and NeuN-positive neurons in dorsal and ventral HPC of injected mice (WT-Cre, N=7; ΔdHPC, N=6; ΔvHPC, N=12) (Significant differences in the Cre-/NeuN-overlay of dorsal and ventral HPC are shown by an asterisk (*), paired t-test P<0.05).

3.2 Behavior of mice from the *knock-in approach*

For the *knock-in approach GluA1*^{*-/-*} mice were injected with GluA1 expressing virus in dorsal or complete HPC. For this approach two cohorts were injected. In the first cohort *GluA1*^{*-/-*} mice were injected with GluA1(Q)- (*i.e.* dHPC A1(Q) mice) or GluA1(R)-expressing virus (*i.e.* dHPC GluA1(R) mice) in dorsal HPC. Uninjected *GluA1*^{*+/-*} littermates were used as controls. For the second cohort, *GluA1*^{*-/-*} mice were injected with GluA1(Q)-expressing virus in complete HPC (*i.e.* cHPC A1(Q) mice).

In this cohort uninjected $GluA1^{-/-}$ and WT mice served as controls. In both cohorts behavioral testing started four weeks after virus injection.

3.2.1 Rescue of hyperactivity in the open field

$GluA1^{-/-}$ mice show hyperactivity in an open field (Bannerman et al., 2004; Wiedholz et al., 2008). Therefore, *knock-in approach* mice were tested for locomotion in the open field over a period of 5 min. Distance traveled in bins of 1 min (a measure for locomotor activity) and the overall time spent in the center (a measure for anxiety) were analyzed.

All activity traces from the first cohort were analyzable and therefore included in the analysis. In the second cohort, one of the $GluA1^{-/-}$ mice was excluded from analysis because of a tracking error.

Knock-in approach cohort 1: dHPC A1(R) mice were slightly more active than $GluA1^{+/-}$ and dHPC A1(Q) mice during the last three minutes of open field exploration. However, a Two Way RM ANOVA on square root-transformed data found no significant difference for the factors 'group' ($F_{2,114}=0.85$, $P>0.4$) and '1 min bin' ($F_{4,114}=1.016$, $P>0.4$) but for the interaction of these factors ($F_{8,114}=2.229$, $P<0.04$). Post hoc analysis revealed a significant decrease in locomotion for dHPC A1(Q) mice during the last two minutes compared to the first minute (Tukey test, $P<0.03$). In $GluA1^{+/-}$ and dHPC A1(R) mice however, locomotion did not change significantly over time (Tukey test, $P>0.2$). dHPC A1(R) mice only showed a trend towards increased locomotion during the last minute compared to $GluA1^{+/-}$ (Tukey test, $P=0.087$) and dHPC A1(Q) mice (Tukey test, $P=0.057$) (Figure 18a).

dHPC A1(R) mice spent slightly more time in the center of the open field than $GluA1^{+/-}$ and dHPC A1(Q) mice (One Way ANOVA, $F_{2,22}=1.481$, $P>0.25$) (Figure 18b).

The differences in locomotion found in the first cohort did not reach statistical significance. One reason might be that these mice underwent three other behavioral tests before being subjected to the open field and thus were used to exposure to novel environments. Therefore, mice from the second cohort were tested in the open field before they were subjected to any other task.

Knock-in approach cohort 2: As published (Bannerman et al., 2004; Wiedholz et al., 2008), $GluA1^{-/-}$ mice were more active than WT mice. This hyperactivity was

rescued in cHPC A1(Q) mice. A Two Way RM ANOVA on traveling distance data revealed a statistically significant effect for the factors 'group' ($F_{2,154}$=34.171, P<0.001), '1 min bin' ($F_{4,154}$=17.436, P<0.001) and the interaction of these factors ($F_{8,154}$=7.822, P<0.001). Post hoc comparison revealed comparable locomotion in all three groups during the first minute (Tukey test, P>0.3), but a significantly increased locomotion during the last four minutes for *GluA1*$^{-/-}$ mice compared to WT and cHPC A1(Q) mice (Tukey test, second bin: P<0.025, third to fifth bin: P<0.001). Compared to WT mice cHPC A1(Q) mice traveled a significantly shorter distance during the second minute (Tukey test, P<0.05) but not during any other times (Tukey test, P>0.08) (Figure 18c).

Analysis of time spent in the center of the open field revealed a significant difference between groups (Kruskal-Wallis One Way ANOVA on Ranks, H_2=15.498, P<0.001). Post hoc testing showed that WT and *GluA1*$^{-/-}$ mice spent a similar amount of time in the center of the open field (Dunn's Method, P>0.05), while cHPC A1(Q) mice spent a significantly decreased amount of time in the center compared to the other two groups (Dunn's Method, P<0.05) (Figure 18d).

Taken together, results from open field suggest that expression of GluA1 confined to the dorsal or complete HPC is sufficient to rescue the hyperactive phenotype of *GluA1*$^{-/-}$ mice. However, expression GluA1 in complete HPC in *GluA1*$^{-/-}$ mice also increased anxiety related behaviors in the open field.
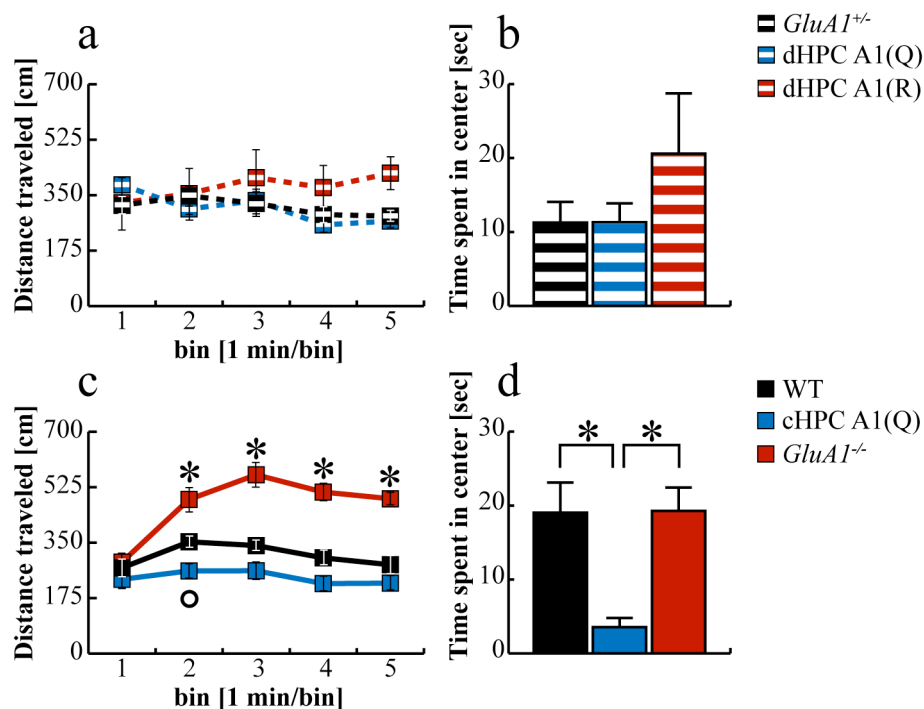
Figure 18: Open field behavior of *knock-in approach* mice. Distance traveled (in cm ±SEM) in 1 min bins (**a, c**) and time spent in the center (in sec +SEM) of the open field (**b, d**) are shown for both cohorts of the *knock-in approach* (first cohort (**a, b**): *GluA1*$^{+/-}$, N=10; dHPC A1(Q), N=8; dHPC A1(R), N=5; second cohort (**c, d**): WT, N=10; *GluA1*$^{-/-}$, N=10; cHPC A1(Q), N=11) (in (**c**) the asterisks (*) indicate statistically significant differences between *GluA1*$^{-/-}$ mice and both WT and cHPC A1(Q) mice and the circle (°) indicates a statistical difference between WT and cHPC A1(Q) mice, Tukey test P<0.05; in (**d**) the asterisks (*) indicate significant differences between groups, Dunn's Method (**d**) P<0.05)

3.2.2 Hippocampal GluA1-expression does not change general cognitive abilities in the puzzle box

In the puzzle box paradigm mice are exposed to an anxiogenic (white walls, bright illumination) start compartment. To escape from this compartment they have to shuttle to a more pleasant (black walls, dark) goal compartment through barriers of different features (*i.e.* a door barrier, an underpass, a sawdust-filled underpass and a plug-covered underpass). Reductions in the escape latency reflect impairments in general cognitive abilities (Galsworthy et al., 2005).

GluA1$^{-/-}$ mice were tested in preliminary experiments in our department for behavior in the puzzle box. In these experiments, *GluA1*$^{-/-}$ mice were only comparable to WT mice when using the door barrier. For all other barriers, *i.e.* underpass, sawdust-filled underpass and plug-covered underpass, *GluA1*$^{-/-}$ mice were impaired in shuttling to the dark goal compartment.

When mice from the first cohort of the *knock-in approach* were tested in the puzzle box, most of them managed to shuttle to the dark goal compartment for most of the barriers used. When using the sawdust-covered underpass, about half of the *GluA1*$^{+/-}$ and A1(Q) mice and only one of the A1(R) mice managed to shuttle to the dark goal compartment.

Mice from all groups needed a similar time to shuttle to the dark goal compartment when the door barrier was used (One Way ANOVA, $F_{2,22}=0.256$, $P>0.75$) (Figure 19a). A comparable time to shuttle to the dark goal compartment was also seen when the open underpass and the plug-covered underpass were used (Figure 19b,d). When using the sawdust-covered underpass A1(R) mice needed a longer time than *GluA1*$^{+/-}$ and A1(Q) mice (Figure 19c). However, statistical analysis for these three test phases was not possible because data never passed normality test, even after transformation. When a Two Way RM ANOVA was performed regardless of non-normal distribution, no group effects were found in any of the tests (Figure 19).

Since dHPC A1(R) mice were not as impaired as preliminary data suggested, this test was only performed with the first cohort of the *knock-in approach* mice.
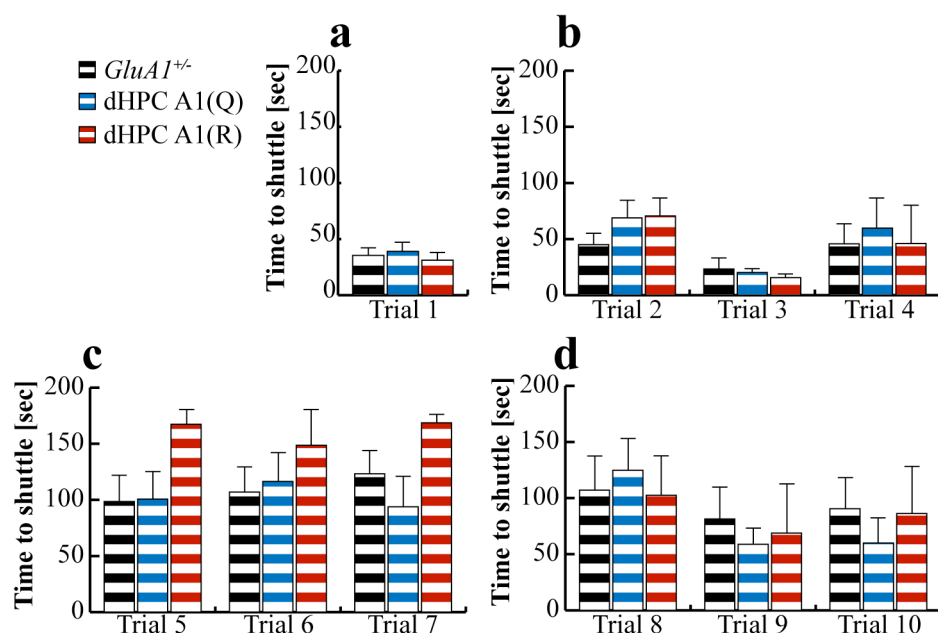
**Figure 19:** Puzzle box test for the first cohort of the *knock-in approach (GluA1*$^{+/-}$, N=10; dHPC A1(Q), N=8; dHPC A1(R), N=5). The average time to shuttle to the dark goal compartment (+SEM) is shown for the four different barriers that were used: (**a**) door barrier (Trial 1), (**b**) open underpass (Trials 2-4), (**c**) sawdust-covered underpass (Trials 5-7) and (**d**) plug-covered underpass (Trials 8-10).

3.2.3 SWM is not rescued by hippocampal expression of GluA1

GluA1$^{-/-}$ mice show a complete loss in SWM on different tasks including rewarded alternation on the T-maze (Reisel et al., 2002) and novel arm preference on the Y-maze (Sanderson et al., 2007; Sanderson et al., 2009). Notably, the SWM deficit on the T-maze was partially rescued by expression of GFP-tagged GluA1 in principal forebrain neurons (Schmitt et al., 2005). To see if expression of GluA1 restricted to principal neurons and interneurons of the HPC is equally sufficient to reinstate SWM in *GluA1$^{-/-}$* mice, *knock-in approach* mice were tested for rewarded alternation on the T-maze. A minimal retention interval (*i.e.* the time between forced and choice run) of about 5 sec was used at all times for both cohorts.

Knock-in approach cohort 1: All mice habituated normally to the T-maze and learned to consume the milk reward. Each mouse was tested for rewarded alternation for 48 trials. When a mouse did not move for more than 2 min it was removed from the T-maze and had to repeat a trial. Over all trials this happened for one *GluA1$^{+/-}$* mouse (twice) and two dHPC A1(Q) mice (once each). None of the dHPC A1(R) mice had to repeat a trial. There was no statistical difference in the number of repetitions between groups (Kruskal-Wallis One Way ANOVA on Ranks, $H_2=1.548$ $P>0.45$).

GluA1$^{+/-}$ mice had a success rate of ~70 % at the beginning of training. This performance slightly increased with successive training to almost 80 %. Both, dHPC A1(Q) and dHPC A1(R) mice alternated at chance (50 %) and did not increase their performance. A Two Way RM ANOVA on rank-transformed data showed a statistically significant effect for the factor 'group' ($F_{2,91}=19.236$, $P<0.001$) but not for the factor 'block' ($F_{3,91}=1.547$, $P>0.2$) or the interaction of these factors ($F_{6,91}=1.033$, $P>0.4$). Post hoc comparison revealed a significantly increased performance for *GluA1$^{+/-}$* mice compared to dHPC A1(Q) and dHPC A1(R) mice (Tukey test, $P<0.001$). However, dHPC A1(Q) and dHPC A1(R) mice did not differ from each other (Tukey test, $P>0.95$) (Figure 20a).

Knock-in approach cohort 2: The mice from all three groups habituated to the T-maze and learned to drink the milk reward. Each mouse experienced 48 trials over six days. Two of the WT mice had to repeat a trial once because they did not move for more than 2 min. In the *GluA1$^{-/-}$* group, four mice had to repeat a trial twice and in the cHPC A1(Q) group overall three mice had to repeat trials five or more times

(5 times=one mouse, 6 times=two mice). However, there was no statistically significant difference between groups in the number of repetitions (Kruskal-Wallis One Way ANOVA on Ranks, H_2=1.075 P>0.55).

WT mice started with a success rate of ~70 % and gradually increased their performance up to almost 85 %. In contrast, $GluA1^{-/-}$ mice performed at chance level at all times. This was not rescued in cHPC A1(Q) mice. Statistical analysis on rank-transformed data with a Two Way RM ANOVA revealed a significant effect for the factor 'group' ($F_{2,127}$=38.585, P<0.001) but not for the factor 'block' ($F_{3,127}$=0.687, P>0.55) or the interaction ($F_{6,127}$=0.87, P>0.5). Post hoc analysis showed a significantly higher performance for WT mice compared to $GluA1^{-/-}$ and cHPC A1(Q) mice (Tukey test, P<0.001). Performance of $GluA1^{-/-}$ and cHPC A1(Q) mice was statistically comparable (Tukey test, P>0.95) (Figure 20b).
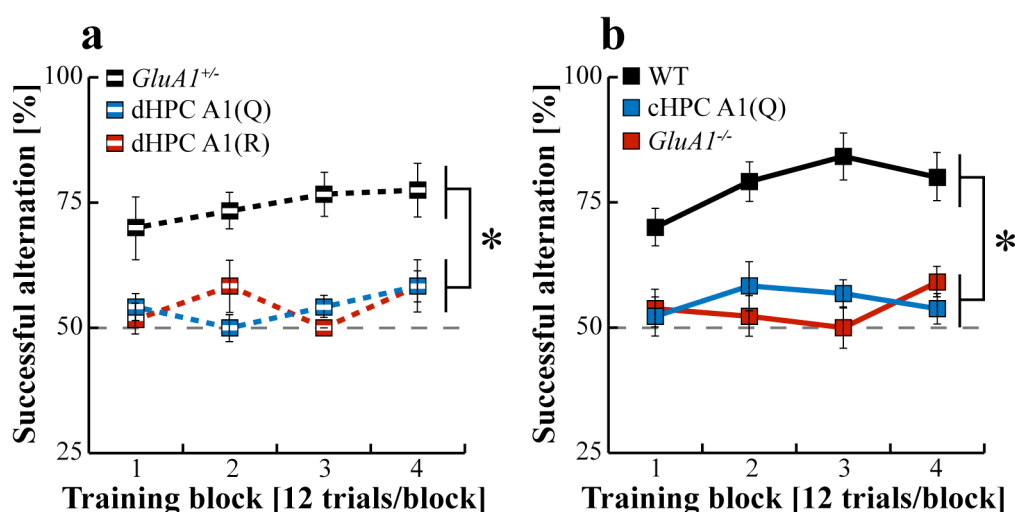
Figure 20: Rewarded alternation on the T-maze for *knock-in approach* mice. Successful alternation (in % ±SEM) over four training blocks (12 trials/block) is shown for (**a**) the first cohort of mice from the *knock-in approach* ($GluA1^{+/-}$, N=10; dHPC A1(Q), N=8; dHPC A1(R), N=5) and (**b**) the second cohort of mice from the *Knock-in approach* (WT, N=10; $GluA1^{-/-}$, N=11; cHPC A1(Q), N=11) (the dashed gray line indicates chance level (50 %); the asterisks (*) indicate statistically significant differences between groups independent of the training block, Tukey test P<0.05).

Another test for SWM is the novel arm exploration on the Y-maze. In this test mice are exposed five times to two arms of a Y-maze followed by a test trial where all three arms are accessible and novel arm preference (tested by an increased time spent in the novel arm) is measured. As with rewarded alternation on the T-maze, $GluA1^{-/-}$

mice also showed a complete loss of SWM in this test (Sanderson et al., 2007; Sanderson et al., 2009).

Mice from both cohorts readily explored the Y-maze during the exposure phase. Therefore, none of the mice was excluded from behavioral analysis.

Knock-in approach cohort 1: *GluA1$^{+/-}$* mice spent a pronounced amount of time in the novel arm, while dHPC A1(Q) and dHPC A1(R) mice spent similar amounts of time in all three arms of the Y-maze. A One Way RM ANOVA was performed for each group and showed a significant effect for *GluA1$^{+/-}$* mice (Friedman RM ANOVA on Ranks, Chi-square(2)=9.8, P<0.01) but not for dHPC A1(Q) ($F_{2,23}$=0.621, P>0.55) or dHPC A1(R) mice ($F_{2,14}$=1.213, P>0.3). Post hoc comparison for *GluA1$^{+/-}$* mice showed that these mice spent significantly more time in the novel than in the start arm (Tukey test, P<0.05). However, the difference in dwell time on novel and other arm did not reach significance (Tukey test, P>0.05) (Figure 21a).

Another parameter that can be analyzed during novel arm exploration is the total number of arm entries over all phases. This reflects activity of the mice on the Y-maze. Analysis of activity showed similar results to those from the open field. During all phases dHPC A1(R) mice performed more arm entries than *GluA1$^{+/-}$* and dHPC A1(Q) mice. A Two Way RM ANOVA on rank-transformed data found a statistical difference for the factors 'group' ($F_{2,137}$=5.602, P<0.015) and 'trial' ($F_{5,137}$=4.775, P<0.001) but not for the interaction of those factors ($F_{10,137}$=0.675, P>0.7). Post hoc comparison revealed a statistically higher amount of arm entries for dHPC A1(R) compared to *GluA1$^{+/-}$* mice (Tukey test, P<0.01) and a trend for more arm entries in dHPC A1(R) compared to dHPC A1(Q) mice (Tukey test, P=0.086). The number of arm entries was comparable between *GluA1$^{+/-}$* and dHPC A1(Q) mice (Tukey test, P>0.45) (Figure 21b).

Knock-in approach cohort 2: WT mice spent more time in the novel arm compared to the other two arms during the test phase, while *GluA1$^{-/-}$* mice spent a comparable amount of time in all three arms. This was only partially rescued in cHPC A1(Q) mice. Statistical analysis with One Way ANOVA for each group revealed a significant effect for WT mice ($F_{2,29}$=32.383, P<0.001), but not for cHPC A1(Q) ($F_{2,32}$=2.285, P>0.12) or *GluA1$^{-/-}$* mice ($F_{2,32}$=0.468, P>0.6). Post hoc comparison showed that WT mice spent significantly more time in the novel arm than in the other two arms (Tukey test, P<0.001) (Figure 21c).

Equal to the first cohort, analysis of arm entries showed similar results to those from the open field. *GluA1*$^{-/-}$ mice were hyperactive compared to WT mice (*i.e.* had more arm entries), and this hyperactivity was abolished in cHPC A1(Q) mice. Even after transformation, the data did not pass normality test. However, since visual inspection of the data showed clear differences, a Two Way RM ANOVA was performed to test for statistical differences. This analysis revealed a significant effect for the factors 'group' ($F_{2,191}$=30.08, P<0.001), 'trial' ($F_{5,191}$=4.068, P<0.005) and the interaction of those factors ($F_{10,191}$=6.699, P<0.001). Post hoc testing showed a significantly increased number of arms entries for *GluA1*$^{-/-}$ mice in comparison to WT from second to fifth trial (Tukey test, P<0.001). During the first and test trial, WT and *GluA1*$^{-/-}$ mice had a comparable number of arm entries (Tukey test, P>0.2). In comparison to cHPC A1(Q) mice, *GluA1*$^{-/-}$ mice were more active during all trials (Tukey test, first trial: P<0.03, all other trials: P<0.001). WT mice showed significantly more arm entries during the first and test trial (Tukey test, P<0.05) than cHPC A1(Q) mice. During all other trials the number of arm entries between WT and cHPC A1(Q) was comparable (Tukey test, P>0.2) (Figure 21d).

Taken together, the results from rewarded alternation on the T-maze and novel arm exploration on the Y-maze suggest that expression of GluA1 restricted to the HPC is not sufficient to reinstate defective SWM in *GluA1*$^{-/-}$ mice. In agreement with the results from open field, analysis of activity on the Y-maze showed that hyperactivity can be rescued by both dorsal and complete hippocampal expression of GluA1 in *GluA1*$^{-/-}$ mice.
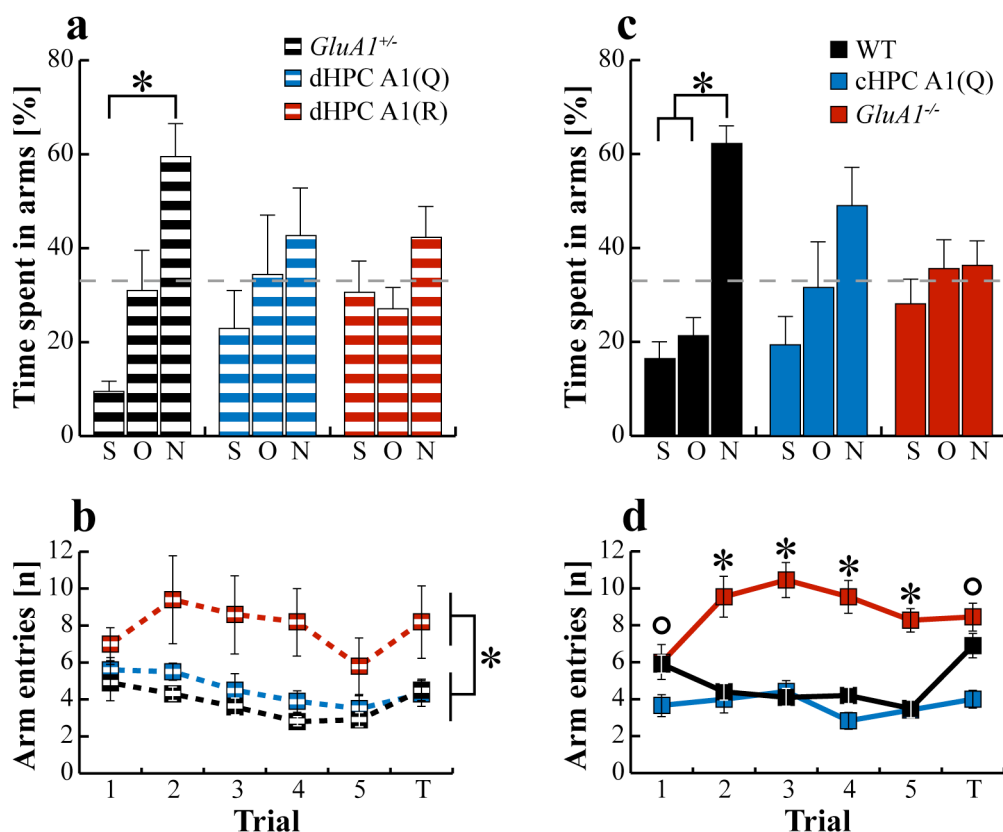
Figure 21: Novel arm exploration on the Y-maze for mice from the *knock-in approach*. The time spent in each arm (start (S), other (O) and novel (N) arm) during the test trial (T) in sec (+SEM) (**a, c**) and the number of arm entries (±SEM) during all trials (**b, d**) is shown for (**a, b**) the first (*GluA1*^{+/-}, N=10; dHPC A1(Q), N=8; dHPC A1(R), N=5) and (**c, d**) second cohort of the *knock-in approach* (WT, N=10; *GluA1*^{-/-}, N=11; cHPC A1(Q), N=11) (in (**a**) and (**c**) the asterisks (*) represent statistically significant differences in the time spent in the arms, the dashed gray lines show chance level performance (33 %); in (**b**) the asterisk (*) represents statistical significance between *GluA1*^{+/-} and dHPC A1(R) mice (independent of the trial); in (**d**) statistical significance between WT and *GluA1*^{-/-} compared to cHPC A1(Q) is represented by a circle (°) and between *GluA1*^{-/-} and both WT and cHPC A1(Q) mice by an asterisk (*), Tukey test P<0.05).

3.2.4 Pavlovian fear conditioning is not rescued by hippocampal expression of GluA1

Pavlovian fear conditioning is strongly impaired in *GluA1*^{-/-} mice during the acquisition phase. However, results on the ability of *GluA1*^{-/-} to express 'cued' or 'contextual fear' have been somewhat contradictory (Feyder et al., 2007; Humeau et al., 2007; Bosch, 2008).

Pavlovian fear conditioning was only assessed in mice from the first cohort of the *knock-in approach*. The percentage of freezing duration and activity were analyzed as measures of fear (a high amount of freezing and low amount of activity reflect high

states of fear). In contrast to Feyder et al. (2007) and Humeau et al. (2007), but as shown by Bosch (2008), the only obvious difference among groups was found during the acquisition phase. In this phase dHPC A1(Q) and dHPC A1(R) showed reduced freezing and higher activity after tone-shock pairing than $GluA1^{+/-}$ mice. When testing for 'cued' and 'contextual fear' no differences were found between groups. A Two Way RM ANOVA was performed for each testing phase to test for statistical differences.

During the acquisition phase a statistically significant difference was found for the factors 'group' (freezing duration: $F_{2,45}$=9.881, P<0.001; activity: $F_{2,45}$=9.773, P<0.002), 'phase' (freezing duration: $F_{1,45}$=38.212, P<0.001; activity: $F_{1,45}$=83.752, P<0.001) and the interaction of those factors (freezing duration: $F_{2,45}$=8.23, P<0.003; activity: $F_{2,45}$=20.719, P<0.001) for both, freezing duration (this data was square root-transformed for analysis) and activity. Post hoc analysis showed a comparable freezing duration and activity in all groups in the 120 sec before the first shock (Tukey test, P>0.25). In the 120 sec after the third shock, $GluA1^{+/-}$ and dHPC A1(Q) mice showed a significant increase in freezing (Tukey test, P<0.005) and reduction in activity (Tukey test, P<0.001). During this second phase, $GluA1^{+/-}$ mice froze for a significantly longer duration and had a significantly reduced activity compared to dHPC A1(Q) and dHPC A1(R) mice (Tukey test, P<0.001). dHPC A1(Q) and dHPC A1(R) showed a comparable freezing duration (Tukey test, P>0.15), whereas dHPC A1(Q) mice showed slightly but significantly reduced activity compared to dHPC A1(R) mice during this phase (Tukey test, P<0.03) (Figure 22a,d).

When testing 'cued fear' data for statistical significance, Two Way RM ANOVAs found a significant effect for the factor 'phase' (freezing duration: $F_{1,45}$=86.142, P<0.001; activity: $F_{1,45}$=73.679, P<0.001) but not for the factor 'group' (freezing duration: $F_{2,45}$=1.5, P>0.2; activity: $F_{2,45}$=1.104, P>0.35) or for the interaction of those factors (freezing duration: $F_{2,45}$=1.066, P>0.35; activity: $F_{2,45}$=0.989, P>0.35) for both, freezing duration and activity (for statistical analysis the freezing duration data was rank-transformed and the activity data was square root-transformed). Post hoc comparison showed a significantly increased freezing duration and significantly reduced activity in the 120 sec after tone onset compared to the 120 sec before tone onset (Tukey test, P<0.001) (Figure 22b,e).

A Two Way RM ANOVA on the data from 'contextual freezing' showed no significant change for the factors 'group' (freezing duration: $F_{2,45}$=3.025, P>0.07;

activity: $F_{2,45}$=2.038, P>0.15), 'phase' (freezing duration: $F_{1,45}$=0.00797, P>0.9; activity: $F_{1,45}$=0.197, P>0.65) and the interaction of those factors (freezing duration: $F_{2,45}$=0.462, P>0.6; activity: $F_{2,45}$=1, P>0.35) for both, freezing duration (this data was square root-transformed for statistical analysis) and activity (Figure 22c,f).

In summary, similar to results from Bosch (2008), *GluA1^{-/-}* mice (*i.e.* dHPC A1(R)) were only impaired during the acquisition of Pavlovian fear. This was partially, but not strongly rescued by expression of GluA1 in the dorsal HPC of *GluA1^{-/-}* mice. Because there was no pronounced rescue in the first cohort of the *knock-in approach*, Pavlovian fear conditioning was not further assessed in the second cohort.
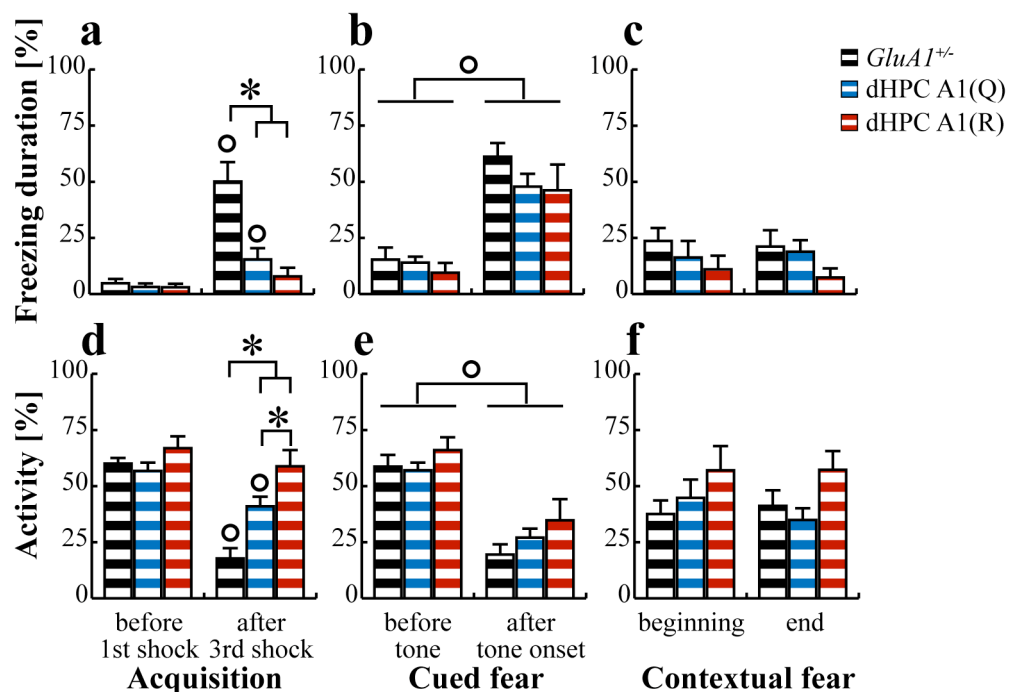
Figure 22: Pavlovian fear conditioning of mice from the first cohort of the *knock-in approach* (*GluA1^{+/-}*, N=10; dHPC A1(Q), N=8; dHPC A1(R), N=5). Freezing duration (+SEM) (**a-c**) and activity (+SEM) (**d-e**) both in percentages are shown (statistical significance between groups is shown by an asterisk (*), and statistically significant changes across phases are shown by circles (°), Tukey test P<0.05).

3.3 Behavior of mice from the *knock-out approach*

For the *knock-out approach GluA1^{2lox/2lox}* mice were injected with Cre-expressing virus in dorsal (*i.e.* ΔdHPC) or ventral (*i.e.* ΔvHPC) HPC. WT controls were injected

with a Cre-expressing virus in ventral HPC (*i.e.* WT-Cre). For these groups, behavioral testing started twelve weeks after virus injection.

3.3.1 Lack of GluA1 in HPC partially impairs SWM

SWM that is impaired in *GluA1$^{-/-}$* mice (Reisel et al., 2002) was also tested in mice from the *knock-out approach*. All mice habituated normally to the T-maze and learned to take the milk reward. Each mouse was tested for rewarded alternation for 96 trials. None of the mice ever failed to move within the first 2 min and therefore none of them had to repeat a trial.

The mice were first subjected to rewarded alternation on the T-maze with a minimal retention interval of approximately 5 sec. WT-Cre mice started with a performance of about 70 % and increased their performance to more than 90 % with successive training. Both ΔdHPC and ΔvHPC mice started with a performance of about 75 % and 65 % respectively, but failed to increase their performance above 80 %. However statistical analysis of the data with a Two Way RM ANOVA only showed a significant effect for the factor 'block' ($F_{3,75}=5.372$, $P<0.005$), but not for the factor 'group' ($F_{2,75}=2.808$, $P>0.08$) or the interaction of those factors ($F_{6,75}=1.664$, $P>0.1$). Post hoc comparison for the factor 'block' revealed a significant increase in overall performance for the last compared to the first block, independent of the group (Tukey test, $P<0.005$) (Figure 23a).

After mice reached asymptotic performance levels with a minimal retention interval, mice were subjected to rewarded alternation with four different retention intervals (5, 30, 60 and 120 sec) for eight trials per interval. Again, both ΔdHPC and ΔvHPC mice showed lower performance than WT-Cre mice. This difference was particularly pronounced during the 30 sec retention interval. Statistical analysis with a Two Way RM ANOVA showed a significant effect for the factor 'group' ($F_{2,71}=5.871$, $P<0.015$) and 'retention interval' ($F_{3,71}=8.802$, $P<0.001$) but not for the interaction of those factors ($F_{6,71}=0.578$, $P>0.746$). Post hoc analysis showed a significantly lower performance for ΔdHPC mice in comparison to WT-Cre mice (Tukey test, $P<0.015$). Although performance of ΔvHPC mice was impaired, data did not reach statistical significance compared to those from WT-Cre mice (Tukey test, $P>0.13$). However, the performance between ΔdHPC and ΔvHPC mice was comparable (Tukey test, $P>0.5$) (Figure 23b).

In summary, data suggest that GluA1 is required in ventral and particularly dorsal HPC for intact SWM. However, deletion of GluA1 from dorsal or ventral HPC was not sufficient to completely abolish SWM on the T-maze, suggesting that non-targeted parts of the HPC or other parts of the brain partially compensate for the lack of GluA1 in dorsal or ventral HPC.
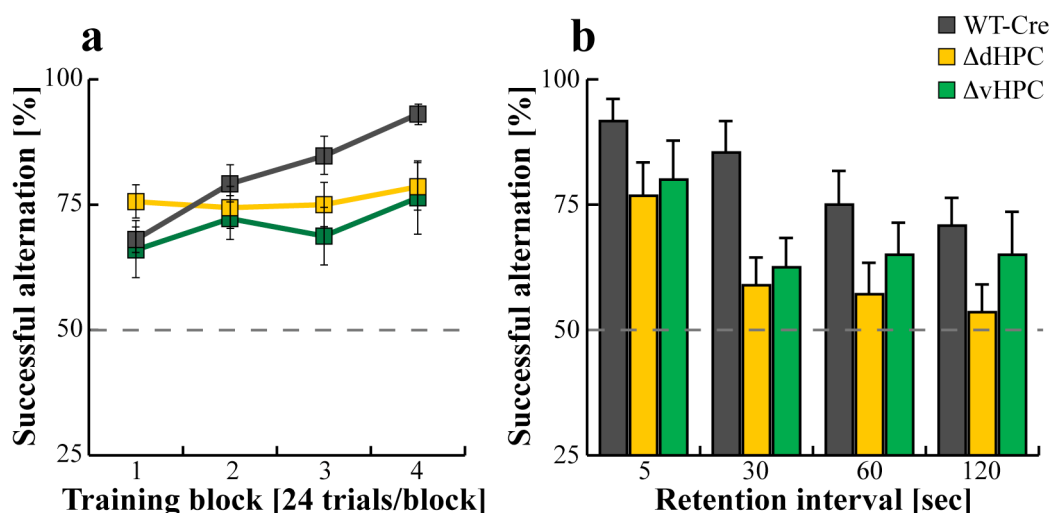
Figure 23: T-maze rewarded alternation of the *knock-out approach* mice (WT-Cre, N=6; ΔdHPC, N=7; ΔvHPC, (**a**) N=6 or (**b**) N=5). Mice were first tested with a minimal retention interval (~5 sec) until they reached asymptotic performance levels (**a**). Subsequently, mice were subjected to training with four different retention intervals (5, 30, 60 and 120 sec) (**b**).

3.3.2 Pavlovian fear conditioning is not dependent on GluA1 in dorsal or ventral HPC

When testing the mice from the *knock-out approach* in Pavlovian fear conditioning essentially no differences between groups were found in both freezing duration and activity during acquisition, 'cued' and 'contextual fear'.

A Two Way RM ANOVA showed a significant increase in freezing and decrease in activity (activity data were square root-transformed for statistical analysis) in the 120 sec after tone foot-shock pairing in comparison to the 120 sec before foot-shocks (freezing duration: $F_{1,35}=118.926$, P<0.001; activity: $F_{1,35}=100.783$, P<0.001). The factor 'group' (freezing duration: $F_{2,35}=0.463$, P>0.6; activity: $F_{2,35}=0.744$, P>0.45) or the interaction of 'group' and 'phase' (freezing duration: $F_{2,35}=0.189$, P>0.8; activity: $F_{2,35}=0.22$, P>0.8) showed no significant effect in both freezing duration and activity (Figure 24a,d).

When testing for 'cued fear' a Two Way RM ANOVA revealed a significant increase in freezing and decrease in activity after tone onset (freezing duration: $F_{1,35}=122.133$, $P<0.001$; activity: $F_{1,35}=183.562$, $P<0.001$), independent of the group. For the freezing duration there were no differences for the factor 'group' ($F_{2,35}=2.421$, $P>0.12$) or the interaction of the factors 'group' and 'phase' ($F_{2,35}=0.879$, $P>0.4$), however, for activity ANOVA revealed a significant effect for the interaction of the factors 'group' and 'phase' ($F_{2,35}=3.768$, $P<0.05$) but not for the factor 'group' ($F_{2,35}=2.743$, $P>0.09$). Post hoc comparison only revealed a significantly higher activity for ΔdHPC mice compared to WT-Cre mice during the 120 sec before tone onset (Tukey test, $P<0.015$) but not after tone onset ($P>0.3$) (Figure 24b,e).

When testing for 'contextual fear' a Two Way RM ANOVA revealed no statistical differences for square root-transformed freezing duration data for the factors 'phase' ($F_{1,35}=2.694$, $P>0.12$), 'group' ($F_{2,35}=1.081$, $P>0.35$) and the interaction of those factors ($F_{2,35}=0.134$, $P>0.85$). For activity data the Two Way RM ANOVA revealed a significant effect for the factor 'phase' ($F_{1,35}=4.557$, $P<0.05$) (*i.e.* activity was significantly lower in the last 120 sec compared to the first 120 sec independent of the group) but not for the factor 'group' ($F_{2,35}=0.966$, $P>0.4$) or the interaction of those factors ($F_{2,35}=0.458$, $P>0.6$) (Figure 24c,f).

In summary, data from Pavlovian fear conditioning revealed no pronounced effect of deletion of GluA1 from dorsal or ventral HPC. This suggests, that GluA1 in dorsal or ventral HPC does not contribute to the expression of Pavlovian fear.
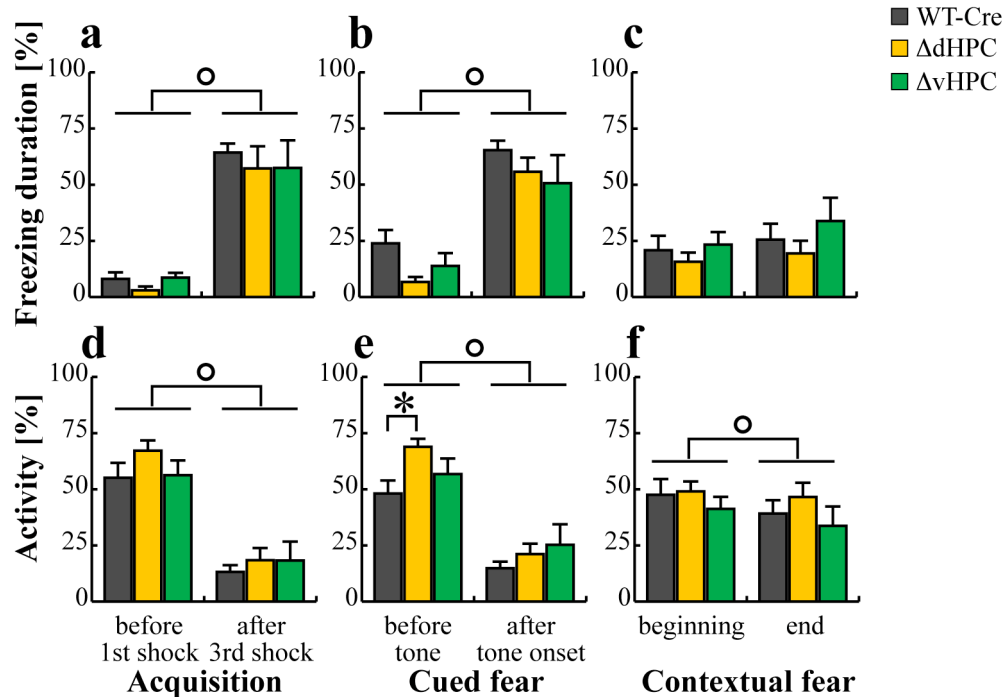
Figure 24: Pavlovian fear conditioning of the *knock-out approach* mice (WT-Cre, N=6; ΔdHPC, N=7; ΔvHPC, N=5). The freezing duration (**a-c**) and activity (**d-e**), both in percentage (+SEM) are illustrated (statistical significance between groups is shown by an asterisk (*), and statistical changes across phases is shown by a circle (°), Tukey test P<0.05).

3.3.3 GluA1 in dorsal and ventral HPC is required for the expression of behavioral despair in FST

The FST comprises two sessions, 24 hr apart, of forced swimming in an enclosed chamber. Mice normally show a decreased latency to immobility and an increase in immobility during the second compared to the first session, reflecting experience-dependent expression of behavioral despair in the FST. *GluA1⁻ᐟ⁻* mice are impaired in the expression of behavioral despair since they do not exhibit a decrease in latency to, and increase in immobility after repeated exposure to the FST. This impairment was rescued by expression of GFP-tagged GluA1 in principal forebrain neurons (Marx, 2007; Freudenberg et al., 2009). To elucidate the contribution of the HPC to the impairment in experience-dependent expression of behavioral despair, mice from the *knock-out approach* were tested in the FST.

All tested mice were able to swim and all activity traces were analyzable. However, one of the ΔdHPC mice never stopped swimming during the first session and was therefore excluded from analysis.

Only WT-Cre mice showed normal experience-dependent expression of behavioral despair. During the second FST session these mice showed a significant decrease in latency to immobility and a significant increase in overall immobility (pared t-test, P<0.05). However, ΔdHPC and ΔvHPC mice showed impaired experience dependent expression of behavioral despair. These mice showed comparable latency to, and overall immobility in both sessions of the FST (paired t-test, P>0.25) (Figure 25).

Taken together the results demonstrate that experience-dependent expression of behavioral despair in the FST requires GluA1 in dorsal and ventral HPC.
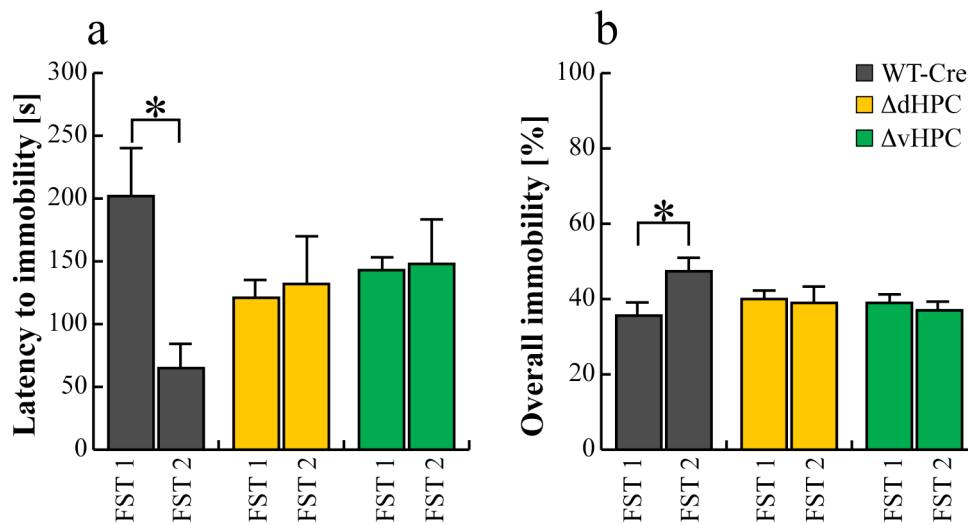
**Figure 25:** Performance in the FST for *knock-out approach* mice (WT-Cre, N=6; ΔdHPC, N=6; ΔvHPC, N=13). The latency to immobility in sec (+SEM) (**a**) and overall immobility in percentage (+SEM) (**b**) are shown for the first (FST 1) and second (FST 2) session of the FST (statistical significance within groups is shown by an asterisk (*), paired t-test P<0.05).

4 Discussion

AMPA receptors containing the GluA1-subunit are critical for mediating synaptic plasticity in brain areas important for learning and memory, like the HPC (Zamanillo et al., 1999; Shi et al., 2001). In *GluA1*$^{-/-}$ mice, globally lacking functional GluA1-alleles, hippocampal principal neurons show normal strength of excitatory synaptic transmission, but lack somatic AMPA receptor-mediated currents and CA3$\rightarrow$CA1 LTP. In *GluA1*$^{-/-}$ mice the GluA2 subunit (the major GluA1 partner in hippocampal principal neurons) is redistributed from dendrites to the soma (Zamanillo et al., 1999; Jensen et al., 2003). Moreover, *GluA1*$^{-/-}$ mice show distinct HPC-dependent behavioral phenotypes. These mice are hyperactive (Bannerman et al., 2004; Wiedholz et al., 2007), have no SWM while SRM stays intact (Reisel et al., 2002) and are impaired in Pavlovian fear conditioning (Feyder et al., 2007; Humeau et al., 2007; Bosch, 2008) and in the expression of experience-dependent behavioral despair (Marx, 2007; Freudenberg et al., 2009). Notably, some of these phenotypes were partially rescued by transgenic expression of a GFP-tagged GluA1 subunit in forebrain principal neurons of *GluA1*$^{-/-}$ mice (Mack et al., 2001; Schmitt et al., 2005; Marx, 2007; Freudenberg et al., 2009).

Results from hippocampal lesion and pharmacological studies suggest a basic involvement of the HPC in the behavioral phenotypes found in *GluA1*$^{-/-}$ mice (*e.g.* Bannerman et al., 1999; Anagnostaras et al., 2001; Daenen et al., 2001; Padovan & Guimarães, 2004). However, the specific contribution of hippocampal GluA1 to these behaviors could not be investigated in global *GluA1*$^{-/-}$ mice. Therefore, my work aimed at separating the specific contribution of GluA1-containing AMPA receptors in HPC to the behavioral impairments found in *GluA1*$^{-/-}$ mice. To achieve this, two approaches were used. To elucidate the contribution of confined GluA1-expresion in the HPC to learning behavior, *GluA1*$^{-/-}$ mice were stereotaxically injected into the HPC with an rAAV expressing GluA1 (*knock-in approach*). Vice versa, to show the requirement of GluA1 in the HPC for learning behavior, GluA1 was deleted from the HPC by stereotaxically injecting a Cre-expressing rAAV into the HPCs of *GluA1*$^{2lox/2lox}$ mice (*knock-out approach*).

The results show that hyperactivity in *GluA1*$^{-/-}$ mice is due to the lack of GluA1 in HPC, since hyperactivity was rescinded in mice only expressing GluA1 in HPC (*knock-in approach* mice). Surprisingly, intact SWM is not solely dependent on the

HPC, since mice expressing GluA1 in HPC (*knock-in approach* mice) still were impaired in two different tests for SWM (*i.e.* rewarded alternation on the T-maze and novel arm exploration on the Y-maze), and mice lacking GluA1 in HPC (*knock-out approach* mice) were only partially impaired during rewarded alternation on the T-maze. Interestingly, GluA1 in the HPC does not contribute to the expression of Pavlovian fear, since mice from both approaches were unaffected in Pavlovian fear conditioning. However, GluA1-containing AMPA receptors in the HPC are required for experience-dependent expression of behavioral despair, because mice lacking GluA1 in HPC (*knock-out approach* mice) showed a behavior similar to *GluA1$^{-/-}$* mice in the FST (*i.e.* they did not show an increased immobility after repeated testing).

4.1 Stereotaxic injections of rAAVs induce efficient transduction of hippocampal neurons

In this work I used rAAV to express transgenes in hippocampal principal neurons and interneurons. Transduction of hippocampal neurons with rAAVs was highly efficient, since staining for the virally expressed proteins was prominent in most of hippocampal subfields. Only few subfields (*e.g.* CA3 in dorsal HPC injected mice and CA1 in ventral HPC injected mice) showed sparse expression, most likely due to a lack of virus diffusion to these areas.

Quantification of transduction efficiency by immunoblotting revealed that the GluA1(Q) virus expressed GluA1 at 30 % of WT GluA1-levels in the targeted areas. Since no electrophysiological tests were performed with these mice, it is uncertain if this amount of protein is sufficient to rescue GluA1-dependent signaling. However, transgenic expression of less than 10 % of endogenous GluA1-levels was sufficient to partially rescue LTP and behavioral impairments in the *GluA1$^{-/-}$* background (Mack et al., 2001; Schmitt et al., 2005; Marx, 2007; Freudenberg et al., 2009), suggesting that in fact 30 % of endogenous GluA1-levels should be sufficient to rescue GluA1-dependent physiology in HPC.

To see, if the virally introduced GluA1-subunits formed functional receptor assemblies, distribution of the GluA2-subunit was tested by immunostaining. Mice expressing a functional GluA1-subunit showed a stronger GluA2-staining in the dendrites than *GluA1$^{-/-}$* mice. However, GluA2-staining of somata was still strong, indicating a high amount of unassembled GluA2. One reason for that might be that

the virally introduced GluA1 mostly forms homomeric receptors. This can be particularly the case, when GluA1 is expressed at high levels (Shi et al., 2001). Homomeric GluA1 AMPA receptors show rectification at positive potentials (Shi et al., 2001). Therefore, the rescue of the virally introduced GluA1-subunit might not ultimately reflect endogenous GluA1-dependent signaling. However, the somatic GluA2-staining is mostly gone at sites of highest viral infection (*i.e.* DG and the lateral parts of CA1). Therefore, the most likely reason for the strong somatic GluA2-staining is that 30 % of endogenous GluA1-levels still leave large amounts of unassembled GluA2 in the ER.

Cre-positive neurons were quantified by immunostaining to test for transduction efficiency of the Cre-expressing virus. More than 30 % of the neurons in the targeted areas expressed Cre-recombinase. This might be an underestimate, since staining properties of the antibodies for Cre-recombinase and NeuN (as a neuronal marker) are different. In fact, visual inspection of stainings suggests an even higher amount of transduced neurons in the targeted areas.

Since less than 10 % of endogenous GluA1-levels are sufficient to partially rescue LTP and behavioral impairments (Mack et al., 2001; Schmitt et al., 2005; Marx, 2007; Freudenberg et al., 2009), it is not clear whether the lack of GluA1 in about 30 % of hippocampal neurons is sufficient to induce the behavioral impairments found in *GluA1$^{-/-}$* mice. However, while in my study mice lacked all GluA1 in at least 30 % of the neurons in the targeted areas, in the case of the *GluA1$^{-/-}$* mice expressing a GFP-tagged GluA1-subunit (Mack et al., 2001) less than 10 % of endogenous GluA1-levels were expressed in all principal forebrain neurons. Therefore, the complete lack of GluA1 in only a part of hippocampal neurons might be sufficient to find behavioral phenotypes dependent on GluA1-containing AMPA receptors. Of note, it was reported that impaired GluA1-dependent signaling in about 20 % of neurons in the amygdala was sufficient to induce behavioral impairments (Rumpel et al., 2005).

4.2 Hyperactivity of *GluA1$^{-/-}$* mice is abolished by hippocampal expression of GluA1

To test for locomotor activity, *GluA1$^{-/-}$* mice expressing GluA1 in HPC (*i.e. knock-in approach* mice) were tested in the open field. Expression of GluA1 in the dorsal or complete HPC was sufficient to abolish hyperactivity of *GluA1$^{-/-}$* mice. An annulment

of hyperactivity in *knock-in approach* mice is also supported by analysis of activity on the Y-maze during novel arm exploration.

This annulment is in contrast to results from $GluA1^{-/-}$ mice expressing a GFP-tagged GluA1-subunit in forebrain neurons, which remain hyperactive (Marx, 2007; Freudenberg et al., 2009). One reason for this difference might be that in the viral approach used in this thesis-work, GluA1 is expressed in both principal neurons and interneurons, while in other studies (Marx, 2007; Freudenberg et al., 2009) GluA1 is only expressed in principal neurons. However, this explanation is unlikely, since mice lacking GluA1 only in principal neurons of the HPC showed hyperactivity (Bus, 2009), while mice lacking GluA1 in forebrain interneurons showed WT-like locomotor activity in the open field (Fuchs et al., 2007), suggesting that locomotor activity is mainly modulated by principal neurons of the HPC.

An alternative explanation for the discrepancy in the annulment of hyperactivity concerns differences in the expression levels. In this thesis neurons of *knock-in approach* mice expressed 30 % of endogenous hippocampal GluA1, which abolished hyperactivity. In contrast, hippocampal neurons of $GluA1^{-/-}$ mice expressing a GFP-tagged GluA1-subunit (Marx, 2007; Freudenberg et al., 2009) expressed less than 10 % of endogenous GluA1 levels, which might not suffice to abolish hyperactivity.

Notably, the abolishment of hyperactivity in the open field was not as pronounced in $GluA1^{-/-}$ mice expressing GluA1 in dorsal HPC (*i.e.* dHPC A1(Q)). This is mostly due to the fact that $GluA1^{-/-}$ mice expressing a mutant GluA1-subunit (*i.e.* dHPC A1(R) mice) only showed a trend towards significantly higher activity. This cannot be explained by an abolishment of hyperactivity by the mutant GluA1 subunit, since mice globally expressing this subunit ($GluA1^{R/R}$ mice), show hyperactivity similar to $GluA1^{-/-}$ mice (Vekovischeva et al., 2001). The hyperactivity in dHPC A1(R) mice was most likely reduced, since they were subjected to three other tasks before open field-testing, and probably were used to novel environments.

It is unclear by which mechanism expression of GluA1 in dorsal or complete HPC abolishes hyperactivity in the open field. The HPC sends modulatory glutamatergic projections to the nucleus accumbens (Kelley & Domesick, 1982; Totterdell & Smith, 1989), inducing dopamine release in this brain area (Legault & Wise; 1999; Legault et al., 2000) and thereby modulates locomotor activity (Sharp et al., 1987). Therefore, it is possible that glutamatergic modulation of the nucleus accumbens is disturbed in

GluA1⁻ᐟ⁻ mice, thereby leading to hyperactivity, and this modulation is rescued by viral expression of GluA1 in *knock-in approach* mice.

Interestingly, it was shown that dopamine-clearance in the striatum, which includes the nucleus accumbens, is retarded in *GluA1⁻ᐟ⁻* mice (Wiedholz et al., 2008). Possibly, activity of the dopamine transporter in these mice is downregulated by homeostatic mechanisms, because of the disturbed glutamatergic modulation of the nucleus accumbens. Since glutamatergic modulation of the nucleus accumbens by the HPC might be restored in *knock-in approach* mice, striatal dopamine clearance is likely to be intact in these mice, explaining the abolished hyperactivity. This is also supported by the fact that hyperactivity in rats induced by dopamine receptor activation in the nucleus accumbens is facilitated by inhibition of the dorsal HPC by lidocain (Rouillon et al., 2007; Degoulet et al., 2008). Moreover, hyperactivity induced by hippocampal lesions can be increased by amphetamine (Whishaw & Mittleman, 1991; Bannerman et a., 1999; Bannerman et al., 2002).

An alternative explanation for the hyperactivity in *GluA1⁻ᐟ⁻* mice, suggested by Sanderson et al. (2007), is a reduction or lack of habituation to novel environments in *GluA1⁻ᐟ⁻* mice. This offers a common trait for the hyperactivity and SWM-deficit of *GluA1⁻ᐟ⁻* mice in the sense that these mice show no short-term habituation to environments and therefore consistently experience environments previously exposed to as novel. However, it is very unlikely that this is an explanation for the hyperactivity of *GluA1⁻ᐟ⁻* mice, since *knock-in approach* mice did not show any rescue in SWM (see 4.4).

4.3 Anxiety-related behaviors in the open field are increased by expression of GluA1 in complete HPC of *GluA1⁻ᐟ⁻* mice

Anxiety-related behaviors were evaluated by analysis of the time spent in the center of the open field (Walsh & Cummins, 1976; Prut & Belzung, 2003). *GluA1⁻ᐟ⁻* mice expressing GluA1 in complete HPC (*i.e.* cHPC A1(Q) mice) barely explored the center of the open field, implying enhanced anxiety in these mice.

One factor confounding the analysis of anxiety-related behaviors in the open-field is hyperactivity. Therefore, *GluA1⁻ᐟ⁻* mice might be generally increased in anxiety, which cannot be observed in the open field due to hyperactivity of these mice (Bannerman et al., 2004; Wiedholz et al., 2007). Although we (Marx, 2007;

Freudenberg et al., 2009) and others (Vekovischeva et al., 2004) did not find any changes in anxiety, Bannerman et al. (2004) showed an increase in anxiety-related behaviors of *GluA1*$^{-/-}$ mice. In fact, Bannerman et al. (2004) used a test that was mostly independent of locomotor activity, while studies that found no differences in anxiety (Vekovischeva et al., 2004; Marx, 2007; Freudenberg et al., 2009) employed tests that use locomotor activity for the assessment of anxiety-related behaviors.

Since results about anxiety levels in *GluA1*$^{-/-}$ mice are controversial it is possible that the increased anxiety-related behavior of cHPC A1(Q) mice in the open-field is specific to GluA1-expression restricted to the HPC. In fact, a contribution of hippocampal GluA1-containing AMPA receptors in anxiety has already been shown. Withdrawal from benzodiazepines, typical anxiolytic compounds, increases anxiety in rats (Van Sickle et al., 2004; Das et al., 2008), which is accompanied by an increased synaptic incorporation of GluA1-containing AMPA receptors in HPC (Van Sickle & Tietz, 2002; Das et al., 2008). Therefore, it might be that *GluA1*$^{-/-}$ mice expressing GluA1 in the entire HPC have an exaggerated synaptic incorporation of GluA1-containing AMPA receptors, thereby inducing enhanced anxiety in these mice.

4.4 General cognitive abilities are not altered in *GluA1*$^{-/-}$ mice

To test for general cognitive abilities the puzzle box paradigm was used. No differences in the latency to shuttle to the dark goal compartment were found between groups of the first cohort of the *knock-in approach*. These data are in strong contrast to a preliminary study from our department, where *GluA1*$^{-/-}$ mice were only comparable to WT mice when the door barrier was used. For all other barriers *GluA1*$^{-/-}$ mice were severely impaired to shuttle to the dark goal compartment (unpublished data).

There are essentially two large differences between these two studies. First, in the preliminary study the floor and one of the walls of the start compartment of the puzzle box were black, which mostly abolished the anxiogenic properties of this compartment. Therefore, mice with higher anxiety (as might be the case for *GluA1*$^{-/-}$ mice) (Bannerman et al., 2004; Vekovischeva et al., 2004; Freudenberg et al., 2009) might have already felt safe enough in the start compartment and were more anxious of shuttling to the unknown goal compartment.

Another reason for the differences found in these two studies might be the groups used. While in the preliminary study performance of WT and *GluA1*$^{-/-}$ mice was compared, in this thesis-work *GluA1*$^{+/-}$ mice were used instead of WT mice. Although *GluA1*$^{+/-}$ mice usually show behaviors comparable to WT mice, these mice were never directly compared to *GluA1*$^{-/-}$ or WT mice in the puzzle box paradigm. It cannot be ruled out that the lack of only one GluA1 allele in *GluA1*$^{+/-}$ mice is already sufficient to induce impairment in the puzzle box. Therefore, differences between *GluA1*$^{+/-}$ mice and *GluA1*$^{-/-}$ mice expressing the mutant GluA1 subunit in dorsal HPC (*i.e.* dHPC A1(R)) might not have been strong enough to reach statistically significant levels.

Another factor that is affecting both, the preliminary study and this thesis-work is the size of the start compartment, which was much smaller than the one in the study that originally established the puzzle box paradigm (Galsworthy et al., 2005). The use of a bigger start compartment increases the anxiogenic properties and therefore makes it more likely to find impaired general cognitive abilities in the puzzle box.

The puzzle box paradigm was developed by Galsworthy et al. (2005) to test for general cognitive abilities in mice. However, since the puzzle box paradigm was never used in any other study, it is relatively uncertain which factors might confound results obtained in this paradigm. Impairment in the puzzle box to shuttle to the dark goal compartment can probably be induced by several independent factors (*e.g.* hyperactivity, impaired SWM, impaired short-term habituation, increased anxiety, lack of motivation) most of which have been shown for *GluA1*$^{-/-}$ mice (*e.g.* Bannerman et al., 2004; Reisel et al., 2002; Wiedholz et al., 2008). Therefore, it is questionable whether impairments found in *GluA1*$^{-/-}$ mice can be attributed to impaired general cognitive abilities or to a single factor contributing to impairment in the puzzle box.

4.5 SWM is not solely dependent on GluA1-containing AMPA receptors in HPC

Rewarded alternation on the T-maze and novel arm exploration on the Y-maze was used to test for SWM. In these tests *GluA1*$^{-/-}$ mice expressing GluA1 in dorsal or complete HPC (*i.e. knock-in approach* mice) still had impaired SWM. This is in contrast to *GluA1*$^{-/-}$ mice expressing a GFP-tagged GluA1 subunit in principal

forebrain neurons, which were at least partially rescued in SWM (Schmitt et al., 2005). This discrepancy cannot be attributed to differences in expression levels, since neurons in mice from Schmitt et al. (2005) expressed less than 10 % of endogenous GluA1, while neurons in *knock-in approach* mice expressed about 30 % of endogenous GluA1 in targeted areas. However, the fraction of neurons expressing the GluA1-subunit was not quantified. Quantification from the Cre-expressing virus however suggests that with the viral approach used in this study at least 30 % of the neurons in the injected area were transduced. Therefore, the amount of hippocampal neurons in *knock-in approach* mice expressing the GluA1 subunit could have been too low to reinstate SWM.

Another possible explanation for the lack of rescued SWM might be that expression of GluA1 in the HPC alone is not sufficient to mediate SWM. One brain area that seems to be equally necessary for intact SWM is the entorhinal cortex (Ramirez & Stein, 1984; Good & Honey, 1997; Bannerman et al., 2001; Steffenach et al., 2005). Potentially, input from the entorhinal cortex to the HPC is required for intact SWM. This might be mediated by tuning of hippocampal place cells by grid cells from entorhinal cortex (Fyhn et al., 2008; Moser et al., 2008). In fact, place specific firing of CA1 pyramidal neurons was shown to be impaired in *GluA1$^{-/-}$* mice (Resnik, 2007). However, it is not known if grid cell firing in the entorhinal cortex of *GluA1$^{-/-}$* mice is intact. Since in *knock-in approach* mice the entorhinal cortex is not expressing GluA1, impaired formation of grid cells might explain the lack of rescued SWM by expression of GluA1 restricted to the dorsal or complete HPC.

Mice lacking GluA1 in dorsal or ventral HPC (*i.e. knock-out approach* mice) had partially impaired SWM in rewarded alternation when using a minimal retention interval and strongly impaired SWM when using longer retention intervals. These results support the requirement of GluA1-containing AMPA receptors for intact SWM.

One consideration when using Cre-recombinase for specific gene targeting is toxicity of Cre-recombinase at high expression levels (Schmidt-Supprian & Rajewsky, 2007). WT controls used in this study were also injected with Cre-recombinase. Therefore, if Cre-toxicity is the reason for the SWM-deficit, these mice should have been affected to an equal extent, which was not the case.

The SWM impairment found in *knock-out approach* mice is in contrast to findings from mice lacking GluA1 in principal neurons of the HPC, which are not impaired in

rewarded alternation and only slightly impaired in spontaneous alternation (both tested on the T-maze) (Bus, 2009). This discrepancy might be attributed to the fact that in the study from Bus (2009) mice only lacked GluA1 in principal neurons, while in *knock-out approach* mice GluA1 was additionally lacking in interneurons. In fact, expression of GluA1 in interneurons was shown to be important for the mediation of SWM (Fuchs et al., 2007).

Of note is the finding in mice from the *knock-out approach* that showed impairment in SWM when GluA1 was lacking in dorsal HPC (*i.e.* ΔdHPC mice) or ventral HPC (*i.e.* ΔvHPC). This is in contrast to lesion studies, which only show involvement of the dorsal HPC to SWM (Bannerman et al., 1999; Bannerman et al., 2002; Bannerman et al., 2003). One possible explanation for this might be that unspecific deletion of GluA1 in dorsal HPC of ΔvHPC mice induced the SWM deficit. In fact, quantification of immunostainings showed that about 15 % of the neurons in dorsal HPC of ΔvHPC mice were expressing Cre-recombinase. Therefore, it is possible that this deletion was sufficient to partially impair SWM. This is also supported by the fact that ΔvHPC mice were not as strongly impaired as ΔdHPC mice, suggesting that in fact GluA1 in dorsal HPC mainly contributes to impaired SWM.

4.6 The acquisition of Pavlovian fear conditioning does not depend on GluA1-containing AMPA receptors in HPC

To test for fear-related behaviors mice were tested in the Pavlovian fear conditioning paradigm. Expression of GluA1 in the dorsal HPC of *GluA1$^{-/-}$* mice (*i.e.* dHPC A1(Q) mice) only slightly rescued the impaired expression of fear related behaviors (*i.e.* less freezing/higher activity). One confounding factor for assessing fear-conditioned responses can be hyperactivity (Good & Honey, 1997). Therefore, the increased freezing and decreased activity of dHPC A1(Q) mice is probably due to the abolished hyperactivity rather than to an increased fear response.

Interestingly, when testing for 'cued' or 'contextual fear' *GluA1$^{-/-}$* mice (independent of the injected virus) were indistinguishable from *GluA1$^{+/-}$* controls. This in a agreement with data from Bosch (2008), but in great contrast to two other studies (Feyder et al., 2007; Humeau et al., 2007), which found decreased fear related behaviors when testing for 'cued' or 'contextual fear'. One explanation for this

discrepancy might be that the hyperactivity of *GluA1^{-/-}* mice confounded the results from Feyder et al. (2007) and Humeau et al. (2007). However, hyperactivity should have equally affected results from this thesis.

A more likely explanation concerns differences in the protocols used. While the protocol in Humeau et al. (2007) was very similar to the one used here, Feyder et al. (2007) used a different protocol with higher shock intensity and four instead of three tone-foot shock pairings. Additionally, both studies (*i.e.* Feyder et al. (2007) and Humeau et al. (2007)) assessed the freezing rate by an experimenter observing the behavior of the mice via a video camera, while in our department freezing was analyzed by the software controlling the fear conditioning-chamber. Differences in freezing rates found in these studies might therefore be due to the different ways of analysis.

For assessing 'cued fear' Feyder et al. (2007) used a different conditioning chamber in a different room. In contrast, in our department the configuration of the very same conditioning-chamber is changed by covering the shock-grid with a Plexiglas plate and exchanging the black walls of the chamber with transparent walls. The conditioning-chamber stays the same and conditioning takes place in the same room. Therefore, it is possible that the configuration of the set-up was not different enough, and *GluA1^{-/-}* mice might have received sufficient stimuli to recognize the conditioning chamber as a fearful environment. In fact, in this thesis-work, the freezing duration in all groups of the *knock-in* and *knock-out approach* was slightly higher before tone onset during the 'cued fear' test compared to the freezing before the first shock during acquisition, suggesting that mice at least partially recognized the conditioning chamber and/or room.

Another factor influencing the assessment of conditioned fear is anxiety (Bannerman et al., 2003; Ponder et al., 2007; Muigg et al., 2008). Since a different level of anxiety in *GluA1^{-/-}* mice cannot be ruled out (Bannerman et al., 2004; Vekovischeva et al., 2004; Marx, 2007; Freudenberg et al., 2009), any differences found in Pavlovian fear conditioning in these mice need to be interpreted carefully.

Mice lacking GluA1 in dorsal or ventral HPC (*i.e. knock-out approach* mice) did not manifest any impaired expression of fear-related behavior during the acquisition or when tested for 'cued' or 'contextual fear'. This, together with the impaired fear behavior of dHPC A1(Q) mice during acquisition, suggests that GluA1 in HPC is not involved in the acquisition of Pavlovian fear. To which extent the HPC is involved in

the expression of 'cued' or 'contextual fear' cannot be clarified with the data at hand. Since no differences in 'cued' or 'contextual fear' were found for mice globally lacking GluA1, it is unlikely that a potential deficit is found in mice lacking GluA1 in HPC with the set-up or protocol used in this study.

4.7 Experience-dependent expression of behavioral despair requires GluA1-containing AMPA receptors in HPC

To test for experience-dependent expression of behavioral despair, mice were tested on two consecutive days in the FST. An increase in immobility after repeated testing in the FST is a commonly used measure for experience-dependent behavioral despair (Porsolt et al., 1977; DePablo et al., 1989; West, 1990). Mice lacking GluA1 in dorsal (*i.e.* ΔdHPC) or ventral (*i.e.* ΔvHPC) HPC showed a comparable latency to immobility and overall immobility in both sessions of the FST, resembling results for *GluA1$^{-/-}$* mice (Marx, 2007; Freudenberg et al., 2009). This impairment in the expression of behavioral despair cannot be attributed to Cre-toxicity, since WT controls were also expressing Cre in ventral HPC. Therefore, the results suggest that the lack of GluA1-containing AMPA receptors in at least 30 % of principal and interneurons of the dorsal or ventral HPC is sufficient to disturb the experience-dependent expression of behavioral despair.

The FST is a test commonly used to find antidepressants (Porsolt et al., 1977). However, it is very unlikely that the deficit in the expression of behavioral despair in mice lacking GluA1 in HPC is reflecting a 'depressive' phenotype. In fact, several studies have shown a 'non-depressive' phenotype for *GluA1$^{-/-}$* mice. For example, glucose consumption in female *GluA1$^{-/-}$* mice (Bannerman et al., 2004) and learned helplessness (Chourbaji et al., 2008), both commonly used tests for modeling depression in rodents, were reduced. More likely is a generally disturbed learning or memory of the inescapable nature of the FST in *knock-in approach* mice.

Several studies showed that increases in hippocampal AMPA receptor activation induce impairment in behavioral despair in the FST (Bai et al., 2001; Li et al., 2001; Li et al., 2003; Gould et al., 2008). This is in strong contrast to the lack of increase in immobility found *knock-out approach* mice, since these mice supposedly have a lowered AMPA receptor activation. Therefore, it is possible that a generally disturbed

AMPA receptor activation in HPC induces a disturbed experience-dependent expression of behavioral despair.

4.8 Conclusions

The *knock-in* and *knock-out approaches* used in this study provide complementary models to study the contribution of hippocampal GluA1-containing AMPA receptors to several behavioral impairments found in *GluA1$^{-/-}$* mice. Taken together, results from this study reveal a critical role for hippocampal GluA1-containing AMPA receptors in hyperactivity, SWM and behavioral despair. In contrast, GluA1 in HPC is not required for mediating general cognitive abilities or Pavlovian fear conditioning.

Further studies should be helpful to support the results from this study. First, functionality of the virally introduced GluA1 subunit could be tested using electrophysiological methods. Second, the contribution of GluA1 in principal and interneurons might be investigated by using cell-type specific promoters for the expression of GluA1 or Cre-recombinase (*e.g.* Ca^{2+}/calmodulin-dependent protein kinase II (CaMKII)-promoter for expression in principal neurons and glutamate decarboxylase 67 (GAD67)-promoter for expression in interneurons). Third, the changes in anxiety in the open field might be investigated in more detail, using protocols that are more independent of locomotor activity. Moreover, the fear conditioning protocol might be improved to be able to test for the contribution of hippocampal GluA1 to 'cued' or 'contextual fear'. Also, it might be interesting to investigate the role of hippocampal GluA1-containing AMPA receptors to experience-dependent behavioral despair by making use of the *knock-in approach*.

Further studies using the approaches used here might help to find the contribution of GluA1-containing AMPA receptors in different behavioral paradigms that are impaired in *GluA1$^{-/-}$* mice. For example the contribution of the entorhinal cortex to the SWM impairment and the contribution of the amygdala to impairments in Pavlovian fear conditioning could be investigated using these approaches.

Finally, the complementary nature of the approaches used here might be a model for future studies on the necessity and sufficiency of specific genes on certain phenotypes in targeted brain areas.

5 Abbreviations

AAV = adeno-associated virus

AMPA = α-amino-3-hydroxy-5-methyl-4-isoxazolepropionic acid

ANOVA = analysis of variance

ATD = amino-terminal domain

bGH pA = bovine growth hormone poly-adenylation sequence

BSA = bovine serum albumin

CA = cornu ammonis

CAG = cytomegalovirus enhanced chicken beta actin

CaMKII = Ca^{2+}/calmodulin-dependent protein kinase II

CS = conditioned stimulus

CTD = carboxy-terminal domain

DAB = diaminobenzidine

DG = dentate gyrus

ER = endoplasmatic reticulum

FST = (Porsolt) forced swim test

GABA = γ-amino butyric acid

GAD67 = glutamate decarboxylase 67

g factor = factor underlying general cognitive abilities

GFP = green fluorescent protein

GluA1$^{-/-}$ = mice lacking functional GluA1 alleles

GluA1$^{+/-}$ = mice lacking one functional GluA1 allele

GluA1$^{2lox/2lox}$ = mice with floxed GluA1 alleles

GluA1$^{R/R}$ = mice expressing a mutant (non-functional) GluA1-subunit

HA = hemaglutinin

HPC = hippocampus

HRP = horseradish-peroxidase

HSPG = heparan sulfate proteoglycan

hSynapsin = human synapsin

iGluR = ionotropic glutamate receptor

ITI = inter-trial interval

ITR = inverted terminal repeat

LTD = long-term depression

LTP = long-term potentiation

MAGUK = membrane associated guanylate kinase

NGS = normal goat serum

NMDA = *N*-methyl-*D*-aspartate

ON = overnight

PBS = phosphate-buffered saline

PCR = polymerase chain reaction

PDZ = PSD-95/Discs large/zona occludens-1

PFA = paraformaldehyde

PFC = prefrontal cortex

PSD = post-synaptic density

PSD-93/-95 = PSD protein of 93/95 kDa

Q/R-editing = mRNA editing from glutamine to arginine

rAAV = recombinant AAV

R/G-editing = mRNA editing from arginine to glycine

RM = repeated measures

RT = room temperature

SAP = synapse-associated protein

SDS = sodium dodecyl sulfate

SEM = standard error of the mean

SH3 = Src-homology 3

SRM = spatial reference memory

SWM = spatial working memory

TARP = transmembrane AMPA receptor regulatory protein

TBS = tris-buffered saline

VP = viral capsid protein

WPRE = woodchuck hepatitis virus posttranscriptional regulatory element

WT = wild type

6 References

Airan RD, Meltzer LA, Roy M, Gong Y, Chen H & Deisseroth K (2007) High-speed imaging reveals neurophysiological links to behavior in an animal model of depression. Science 317:819-823

Alger BE & Teyler TJ (1976) Long-term and short-term plasticity in the CA1, CA3, and dentate regions of the rat hippocampal slice. Brain Res 110:463-480

Amaral DG & Dent JA (1981) Development of the mossy fibers of the dentate gyrus: I. A light and electron microscopic study of the mossy fibers and their expansions. J Comp Neurol 195:51-86

Amaral DG & Lavenex P (2007) Hippocampal neuroanatomy. In The Hippocampus Book (eds Andersen P, Morris RGM, Amaral DG, Bliss TVP & O'Keefe J) 37-114 (Oxford Univ. Press, New York)

Amaral DG & Witter MP (1989) The three-dimensional organization of the hippocampal formation: a review of anatomical data. Neuroscience 31:571-591

Anagnostaras SG, Gale GD & Fanselow MS (2001) Hippocampus and contextual fear conditioning: recent controversies and advances. Hippocampus 11:8-17

Andrásfalvy BK, Smith MA, Borchardt T, Sprengel R & Magee JC (2003) Impaired regulation of synaptic strength in hippocampal neurons from GluR1-deficient mice. J Physiol 552:35-45

Babinet C (2000) Transgenic mice: an irreplaceable tool for the study of mammalian development and biology. J Am Soc Nephrol 11:88-94

Bai F, Li X, Clay M, Lindstrom T & Skolnick P (2001) Intra- and interstrain differences in models of "behavioral despair". Pharmacol Biochem Behav 70:187-192

Bannerman DM, Deacon RM, Brady S, Bruce A, Sprengel R, Seeburg PH & Rawlins JN (2004) A comparison of GluR-A-deficient and wild-type mice on a test battery assessing sensorimotor, affective, and cognitive behaviors. Behav Neurosci 118:643-7

Bannerman DM, Deacon RM, Offen S, Friswell J, Grubb M & Rawlins JN (2002) Double dissociation of function within the hippocampus: spatial memory and hyponeophagia. Behav Neurosci 116:884-901

Bannerman DM, Grubb M, Deacon RM, Yee BK, Feldon J & Rawlins JN (2003) Ventral hippocampal lesions affect anxiety but not spatial learning. Behav Brain Res 139:197-213

Bannerman DM, Yee BK, Good MA, Heupel MJ, Iversen SD & Rawlins JN (1999) Double dissociation of function within the hippocampus: a comparison of dorsal, ventral, and complete hippocampal cytotoxic lesions. Behav Neurosci 113:1170-1188

Bannerman DM, Yee BK, Lemaire M, Wilbrecht L, Jarrard L, Iversen SD, Rawlins JN & Good MA (2001) The role of the entorhinal cortex in two forms of spatial learning and memory. Exp Brain Res 141:281-303

Bliss TV & Lømo T (1973) Long-lasting potentiation of synaptic transmission in the dentate area of the anaesthetized rabbit following stimulation of the perforant path. J Physiol 232:331-356

Bosch V (2008) Genetic interference to study amygdala function in mice. Inaugural Dissertation, Ruprecht Karl University of Heidelberg

Burger C, Nash K & Mandel RJ (2005) Recombinant adeno-associated viral vectors in the nervous system. Hum Gene Ther 16:781-791

Bus T (2009) Genetic investigations into the role of ionotropic glutamate receptors in hippocampal learning. Inaugural Dissertation, Ruprecht Karl University of Heidelberg

Celikel T, Marx V, Freudenberg F, Zivkovic A, Resnik E, Hasan MT, Licznerski P, Osten P, Rozov A, Seeburg PH & Schwarz MK (2007) Select overexpression of homer1a in dorsal hippocampus impairs spatial working memory. Front Neurosci 1:97-110

Chourbaji S, Vogt MA, Fumagalli F, Sohr R, Frasca A, Brandwein C, Hörtnagl H, Riva MA, Sprengel R & Gass P (2008) AMPA receptor subunit 1 (GluR-A) knockout mice model the glutamate hypothesis of depression. FASEB J 22:3129-3134

Collingridge GL, Kehl SJ & McLennan H (1983) Excitatory amino acids in synaptic transmission in the Schaffer collateral-commissural pathway of the rat hippocampus. J Physiol 334:33-46

Collingridge GL, Olsen RW, Peters J & Spedding M (2009) A nomenclature for ligand-gated ion channels. Neuropharmacology 56:2-5

Coura Rdos S, & Nardi NB (2007) The state of the art of adeno-associated virus-based vectors in gene therapy. Virol J 4:1-7

Daenen EW, Van der Heyden JA, Kruse CG, Wolterink G & Van Ree JM (2001) Adaptation and habituation to an open field and responses to various stressful events in animals with neonatal lesions in the amygdala or ventral hippocampus. Brain Res 918:153-165

Das P, Lilly SM, Zerda R, Gunning WT 3rd, Alvarez FJ & Tietz EI (2003) Increased AMPA receptor GluR1 subunit incorporation in rat hippocampal CA1 synapses during benzodiazepine withdrawal. J Comp Neurol 511:832-846

Deacon RM & Rawlins JN (2006) T-maze alternation in the rodent. Nat Protoc 1:7-12

Degoulet M, Rouillon C, Rostain JC, David HN & Abraini JH (2008) Modulation by the dorsal, but not the ventral, hippocampus of the expression of behavioural sensitization to amphetamine. Int J Neuropsychopharmacol 11:497-508

De Pablo JM, Parra A, Segovia S & Guillamón A (1989) Learned immobility explains the behavior of rats in the forced swimming test. Physiol Behav 46:229-237

Dingledine R, Borges K, Bowie D & Traynelis SF (1999) The glutamate receptor ion channels. Pharmacol Rev 51:7-61

During MJ, Young D, Baer K, Lawlor P & Klugmann M (2003) Development and optimization of adeno-associated virus vector transfer into the central nervous system. Methods Mol Med 76:221-236

Ekstrom AD, Kahana MJ, Caplan JB, Fields TA, Isham EA, Newman EL & Fried I (2003) Cellular networks underlying human spatial navigation. Nature 425:184-148

Elias GM, Funke L, Stein V, Grant SG, Bredt DS & Nicoll RA (2006) Synapse-specific and developmentally regulated targeting of AMPA receptors by a family of MAGUK scaffolding proteins. Neuron 52:307-320

Elias GM & Nicoll RA (2007) Synaptic trafficking of glutamate receptors by MAGUK scaffolding proteins. Trends Cell Biol 17:343-352

Fanselow MS (1984) What is conditioned fear? Trends Neurosci 7:460-462

Fendt M & Fanselow MS (1999) The neuroanatomical and neurochemical basis of conditioned fear. Neurosci Biobehav Rev 23:743-760

Feyder M, Wiedholz L, Sprengel R & Holmes A (2007) Impaired Associative Fear Learning in Mice with Complete Loss or Haploinsufficiency of AMPA GluR1 Receptors. Front Behav Neurosci 1:1-5

Freudenberg F, Marx V, Mack V, Layer LE, Holmes A, Schwarz MK, Sprengel R, Seeburg PH & Celikel T (2009) GluA1 PDZ domain binding is required for experience-dependent behavioral plasticity. in preparation

Freund TF & Buzsáki G (1996) Interneurons of the hippocampus. Hippocampus 6:347-470

Fuchs EC, Zivkovic AR, Cunningham MO, Middleton S, Lebeau FE, Bannerman DM, Rozov A, Whittington MA, Traub RD, Rawlins JN & Monyer H (2007) Recruitment of parvalbumin-positive interneurons determines hippocampal function and associated behavior. Neuron 53:591-604

Fyhn M, Hafting T, Witter MP, Moser EI & Moser MB (2008). Grid cells in mice. Hippocampus 18:1230-1238

Fyhn M, Molden S, Witter MP, Moser EI & Moser MB (2004). Spatial representation in the entorhinal cortex. Science 305:1258-1264

Galsworthy MJ, Paya-Cano JL, Liu L, Monleón S, Gregoryan G, Fernandes C, Schalkwyk LC & Plomin R (2005) Assessing reliability, heritability and general cognitive ability in a battery of cognitive tasks for laboratory mice. Behav Genet 35:675-692

Good M & Honey RC (1997) Dissociable effects of selective lesions to hippocampal subsystems on exploratory behavior, contextual learning, and spatial learning. Behav Neurosci 111:487-493

Gould TD, O'Donnell KC, Dow ER, Du J, Chen G & Manji HK (2008) Involvement of AMPA receptors in the antidepressant-like effects of lithium in the mouse tail suspension test and forced swim test. Neuropharmacology 54:577-587

Gruart A, Muñoz MD & Delgado-García JM (2006) Involvement of the CA3-CA1 synapse in the acquisition of associative learning in behaving mice. J Neurosci 26:1077-1087

Hafting T, Fyhn M, Molden S, Moser MB & Moser EI (2005) Microstructure of a spatial map in the entorhinal cortex. Nature 436:801-806

Hauck B, Chen L & Xiao W (2003) Generation and characterization of chimeric recombinant AAV vectors. Mol Ther 7:419-425

Hebb DO (1949) The organization of behavior: a neuropsychological theory (Wiley, New York).

Hickman-Davis JM & Davis IC (2006) Transgenic mice. Paediatr Respir Rev 7:49-53

Hock BJ Jr & Bunsey MD (1998) Differential effects of dorsal and ventral hippocampal lesions. J Neurosci 18:7027-7032

Hoffman DA, Sprengel R & Sakmann B (2002) Molecular dissection of hippocampal theta-burst pairing potentiation. Proc Natl Acad Sci U S A 99:7740-7745

Hoshaw BA, Hill TI, Crowley JJ, Malberg JE, Khawaja X, Rosenzweig-Lipson S, Schechter LE & Lucki I (2008) Antidepressant-like behavioral effects of IGF-I produced by enhanced serotonin transmission. Eur J Pharmacol 594:109-116

Hughes KR (1965) Dorsal and ventral hippocampus lesions and maze learning: influence of preoperative environment. Can J Psychol 19:325-332

Humeau Y, Reisel D, Johnson AW, Borchardt T, Jensen V, Gebhardt C, Bosch V, Gass P, Bannerman DM, Good MA, Hvalby Ø, Sprengel R & Lüthi A (2007) A pathway-specific function for different AMPA receptor subunits in amygdala long-term potentiation and fear conditioning. J Neurosci 27:10947-10956

Insausti R, Herrero MT & Witter MP (1997) Entorhinal cortex of the rat: cytoarchitectonic subdivisions and the origin and distribution of cortical efferents. Hippocampus 7:146-183

Ishizuka N, Cowan WM & Amaral DG (1995) A quantitative analysis of the dendritic organization of pyramidal cells in the rat hippocampus. J Comp Neurol 362:17-45

Izaki Y, Takita M & Akema T (2008) Specific role of the posterior dorsal hippocampus-prefrontal cortex in short-term working memory. Eur J Neurosci 27:3029-3034

Jensen V, Kaiser KM, Borchardt T, Adelmann G, Rozov A, Burnashev N, Brix C, Frotscher M, Andersen P, Hvalby Ø, Sakmann B, Seeburg PH & Sprengel R (2003) A juvenile form of postsynaptic hippocampal long-term potentiation in mice deficient for the AMPA receptor subunit GluR-A. J Physiol 553:843-856

Joca SR & Guimarães FS (2006) Inhibition of neuronal nitric oxide synthase in the rat hippocampus induces antidepressant-like effects. Psychopharmacology (Berl) 185:298-305

Kato AS, Zhou W, Milstein AD, Knierman MD, Siuda ER, Dotzlaf JE, Yu H, Hale JE, Nisenbaum ES, Nicoll RA & Bredt DS (2007) New transmembrane AMPA receptor regulatory protein isoform, gamma-7, differentially regulates AMPA receptors. J Neurosci 27:4969-4977

Kato AS, Siuda ER, Nisenbaum ES & Bredt DS (2008) AMPA receptor subunit-specific regulation by a distinct family of type II TARPs. Neuron 59:986-996

Kelley AE & Domesick VB (1982) The distribution of the projection from the hippocampal formation to the nucleus accumbens in the rat: an anterograde- and retrograde-horseradish peroxidase study. Neuroscience 7:2321-2335

Kiss J, Csáki A, Bokor H, Shanabrough M & Leranth C (2000) The supramammillo-hippocampal and supramammillo-septal glutamatergic/aspartatergic

projections in the rat: a combined [3H]D-aspartate autoradiographic and immunohistochemical study. Neuroscience 97:657-669

Kjelstrup KG, Tuvnes FA, Steffenach HA, Murison R, Moser EI & Moser MB (2002) Reduced fear expression after lesions of the ventral hippocampus. Proc Natl Acad Sci U S A 99:10825-10830

Klugmann M, Symes CW, Leichtlein CB, Klaussner BK, Dunning J, Fong D, Young D & During MJ (2005) AAV-mediated hippocampal expression of short and long Homer 1 proteins differentially affect cognition and seizure activity in adult rats. Mol Cell Neurosci 28:347-360

Köhler C (1985) Intrinsic projections of the retrohippocampal region in the rat brain. I. The subicular complex. J Comp Neurol 236:504-522

Lee HK (2006) Synaptic plasticity and phosphorylation. Pharmacol Ther 112:810-832

Legault M, Rompré PP & Wise RA (2000) Chemical stimulation of the ventral hippocampus elevates nucleus accumbens dopamine by activating dopaminergic neurons of the ventral tegmental area. J Neurosci 20:1635-1642

Legault M & Wise RA (1999) Injections of N-methyl-D-aspartate into the ventral hippocampus increase extracellular dopamine in the ventral tegmental area and nucleus accumbens. Synapse 31:241-249

Li XG, Somogyi P, Ylinen A & Buzsáki G (1994). The hippocampal CA3 network: an in vivo intracellular labeling study. J Comp Neurol 339:181-208

Li X, Tizzano JP, Griffey K, Clay M, Lindstrom T & Skolnick P (2001) Antidepressant-like actions of an AMPA receptor potentiator (LY392098). Neuropharmacology 40:1028-1033

Li X, Witkin JM, Need AB & Skolnick P (2003) Enhancement of antidepressant potency by a potentiator of AMPA receptors. Cell Mol Neurobiol 23:419-430

Lorente de Nó R (1933) Studies on the structure of the cerebral cortex. I. The area entorhinalis. J Psychol Neurol 45:381-438

Lorente de Nó R (1933) Studies on the structure of the cerebral cortex. II. Continuation of the study of the ammonic system. J Psychol Neurol 46:113-177

Lynch G & Baudry M (1984) The biochemistry of memory: a new and specific hypothesis. Science 224:1057-1063

Lynch G, Larson J, Kelso S, Barrionuevo G & Schottler F (1983). Intracellular injections of EGTA block induction of hippocampal long-term potentiation. Nature 305:719-721

Mack V, Burnashev N, Kaiser KM, Rozov A, Jensen V, Hvalby O, Seeburg PH, Sakmann B & Sprengel R (2001) Conditional restoration of hippocampal synaptic potentiation in Glur-A-deficient mice. Science 292:2501-2504

Maglóczky Z, Acsády L & Freund TF (1994) Principal cells are the postsynaptic targets of supramammillary afferents in the hippocampus of the rat. Hippocampus 4:322-334

Malinow R & Malenka RC (2002) AMPA receptor trafficking and synaptic plasticity. Annu Rev Neurosci 25:103-126

Marx V (2006) Molecular alterations of AMPA receptors and their effects on hippocampus dependent tasks. Inaugural Dissertation, Ruprecht Karl University of Heidelberg

Mayer ML & Armstrong N (2004) Structure and function of glutamate receptor ion channels. Annu Rev Physiol 66:161-181

McCown TJ (2005) Adeno-associated virus (AAV) vectors in the CNS. Curr Gene Ther 5:333-338

McHugh TJ, Blum KI, Tsien JZ, Tonegawa S & Wilson MA (1996) Impaired hippocampal representation of space in CA1-specific NMDAR1 knockout mice. Cell 87:1339-13349

Milner B (1962) Les troubles de la mémoire accompagnent des lesions hippocampique bilatérales. In: P. Passouant, Editor, Physiologie de l'Hippocampe, Editions de Centre Nationale de la Recherche Scientifique, Paris 257–272

Mogensen J, Hjortkjaer J, Ibervang KL, Stedal K & Malá H (2007) Prefrontal cortex and hippocampus in posttraumatic functional recovery: spatial delayed

alternation by rats subjected to transection of the fimbria-fornix and/or ablation of the prefrontal cortex. Brain Res Bull 73:86-95

Moser EI, Kropff E & Moser MB (2008) Place cells, grid cells, and the brain's spatial representation system. Annu Rev Neurosci 31:69-89

Moser E, Moser MB & Andersen P (1993) Spatial learning impairment parallels the magnitude of dorsal hippocampal lesions, but is hardly present following ventral lesions. J Neurosci 13:3916-3925

Moser MB, Moser EI, Forrest E, Andersen P & Morris RG (1995) Spatial learning with a minislab in the dorsal hippocampus. Proc Natl Acad Sci U S A 92:9697-9701

Muigg P, Hetzenauer A, Hauer G, Hauschild M, Gaburro S, Frank E, Landgraf R & Singewald N (2008) Impaired extinction of learned fear in rats selectively bred for high anxiety--evidence of altered neuronal processing in prefrontal-amygdala pathways. Eur J Neurosci 28:2299-2309

Naber PA, Lopes da Silva FH & Witter MP (2001) Reciprocal connections between the entorhinal cortex and hippocampal fields CA1 and the subiculum are in register with the projections from CA1 to the subiculum. Hippocampus 11:99-104

Neves G, Cooke SF & Bliss TV (2008) Synaptic plasticity, memory and the hippocampus: a neural network approach to causality. Nat Rev Neurosci 9:65-75

Nicoll RA, Tomita S & Bredt DS (2006) Auxiliary subunits assist AMPA-type glutamate receptors. Science 311:1253-1256

O'Keefe J & Dostrovsky J (1971) The hippocampus as a spatial map. Preliminary evidence from unit activity in the freely-moving rat. Brain Res 34:171-175

O'Keefe J (1976) Place units in the hippocampus of the freely moving rat. Exp Neurol 51:78-109

Ono T, Nakamura K, Fukuda M & Tamura R (1991) Place recognition responses of neurons in monkey hippocampus. Neurosci Lett 121:194-198.

Padovan CM & Guimarães FS (2004) Antidepressant-like effects of NMDA-receptor antagonist injected into the dorsal hippocampus of rats. Pharmacol Biochem Behav 77:15-19

Pastalkova E, Serrano P, Pinkhasova D, Wallace E, Fenton AA & Sacktor TC (2006) Storage of spatial information by the maintenance mechanism of LTP. Science 313:1141-1144

Phelps EA & LeDoux JE (2005) Contributions of the amygdala to emotion processing: from animal models to human behavior. Neuron 48:175-187

Pikkarainen M, Rönkkö S, Savander V, Insausti R & Pitkänen A (1999) Projections from the lateral, basal, and accessory basal nuclei of the amygdala to the hippocampal formation in rat. J Comp Neurol 403:229-260

Pitkänen A, Pikkarainen M, Nurminen N & Ylinen A (2000) Reciprocal connections between the amygdala and the hippocampal formation, perirhinal cortex, and postrhinal cortex in rat. A review. Ann N Y Acad Sci 911:369-391

Plomin R (2001) The genetics of g in human and mouse. Nat Rev Neurosci 2:136-141

Ponder CA, Kliethermes CL, Drew MR, Muller J, Das K, Risbrough VB, Crabbe JC, Gilliam TC & Palmer AA (2007) Selection for contextual fear conditioning affects anxiety-like behaviors and gene expression. Genes Brain Behav 6736-749

Porsolt RD, Le Pichon M & Jalfre M (1977) Depression: a new animal model sensitive to antidepressant treatments. Nature 266:730-732

Prut L & Belzung C (2003) The open field as a paradigm to measure the effects of drugs on anxiety-like behaviors: a review. Eur J Pharmacol 463:3-33

Racine R, Newberry F & Burnham WM (1975) Post-activation potentiation and the kindling phenomenon. Electroencephalogr Clin Neurophysiol 39:261-271

Ramirez JJ & Stein DG (1984) Sparing and recovery of spatial alternation performance after entorhinal cortex lesions in rats. Behav Brain Res 13:53-61

Ramón y Cajal S (1893) Estructura del asta de Ammon y fascia dentata. Ann Soc Esp Hist Nat 22

Reisel D, Bannerman DM, Schmitt WB, Deacon RM, Flint J, Borchardt T, Seeburg PH & Rawlins JN (2002) Spatial memory dissociations in mice lacking GluR1. Nat Neurosci 5:868-873

Resnik E (2008) Impaired representation of space in the hippocampus of GluR-A knockout mice. Inaugural Dissertation, Ruprecht Karl University of Heidelberg

Richmond MA, Yee BK, Pouzet B, Veenman L, Rawlins JN, Feldon J & Bannerman DM (1999) Dissociating context and space within the hippocampus: effects of complete, dorsal, and ventral excitotoxic hippocampal lesions on conditioned freezing and spatial learning. Behav Neurosci 113:1189-1203

Rotenberg A, Mayford M, Hawkins RD, Kandel ER & Muller RU (1996) Mice expressing activated CaMKII lack low frequency LTP and do not form stable place cells in the CA1 region of the hippocampus. Cell 87:1351-13561

Rouillon C, Abraini JH & David HN (2007) Hippocampal modulation of locomotor activity induced by focal activation of postsynaptic dopamine receptors in the core of the nucleus accumbens. Hippocampus 17:1028-1036

Rumpel S, LeDoux J, Zador A & Malinow R (2005) Postsynaptic receptor trafficking underlying a form of associative learning. Science 308:83-88

Sanderson DJ, Good MA, Skelton K, Sprengel R, Seeburg PH, Rawlins JNP & Bannerman DM (2009) Enhancement of hippocampus-dependent spatial learning in GluR-A AMPA receptor subunit knockout mice. submitted

Sanderson DJ, Gray A, Simon A, Taylor AM, Deacon RM, Seeburg PH, Sprengel R, Good MA, Rawlins JN & Bannerman DM (2007) Deletion of glutamate receptor-A (GluR-A) AMPA receptor subunits impairs one-trial spatial memory. Behav Neurosci 121:559-569

Schmidt-Supprian M & Rajewsky K (2007) Vagaries of conditional gene targeting. Nat Immunol 8:665-668

Schmitt WB, Deacon RM, Seeburg PH, Rawlins JN & Bannerman DM (2003) A within-subjects, within-task demonstration of intact spatial reference

memory and impaired spatial working memory in glutamate receptor-A-deficient mice. J Neurosci 23:3953-3959

Schmitt WB, Sprengel R, Mack V, Draft RW, Seeburg PH, Deacon RM, Rawlins JN & Bannerman DM (2005) Restoration of spatial working memory by genetic rescue of GluR-A-deficient mice. Nat Neurosci 8:270-272

Schwabe K, Enkel T, Klein S, Schütte M & Koch M (2004) Effects of neonatal lesions of the medial prefrontal cortex on adult rat behaviour. Behav Brain Res 153:21-34

Schwartzkroin PA & Wester K (1975) Long-lasting facilitation of a synaptic potential following tetanization in the in vitro hippocampal slice. Brain Res 89:107-119

Schwenk J, Harmel N, Zolles G, Bildl W, Kulik A, Heimrich B, Chisaka O, Jonas P, Schulte U, Fakler B & Klöcker N (2009) Functional proteomics identify cornichon proteins as auxiliary subunits of AMPA receptors. Science 323:1313-1319

Scoville WB & Milner B (1957) Loss of recent memory after bilateral hippocampal lesions. J Neurol Neurosurg Psychiatry 20:11-21

Seeburg PH, Single F, Kuner T, Higuchi M & Sprengel R (2001) Genetic manipulation of key determinants of ion flow in glutamate receptor channels in the mouse. Brain Res 907:233-243

Sesack SR & Pickel VM (1990) In the rat medial nucleus accumbens, hippocampal and catecholaminergic terminals converge on spiny neurons and are in apposition to each other. Brain Res 527:266-279

Sharp T, Zetterström T, Ljungberg T & Ungerstedt U (1987) A direct comparison of amphetamine-induced behaviours and regional brain dopamine release in the rat using intracerebral dialysis. Brain Res 401:322-330

Shaw C & Aggleton JP (1993) The effects of fornix and medial prefrontal lesions on delayed non-matching-to-sample by rats. Behav Brain Res 54:91-102

Shepherd JD & Huganir RL (2007) The cell biology of synaptic plasticity: AMPA receptor trafficking. Annu Rev Cell Dev Biol 23:613-643

Shi S, Hayashi Y, Esteban JA & Malinow R (2001) Subunit-specific rules governing AMPA receptor trafficking to synapses in hippocampal pyramidal neurons. Cell 105:331-343

Sinnamon HM, Freniere S & Kootz J (1978) Rat hippocampus and memory for places of changing significance. J Comp Physiol Psychol 92:142-155

Soto D, Coombs ID, Renzi M, Zonouzi M, Farrant M & Cull-Candy SG (2009). Selective regulation of long-form calcium-permeable AMPA receptors by an atypical TARP, gamma-5. Nat Neurosci 12:277-285

Spearman C (1904) 'General intelligence' objectively determined and measured. Am J Psychol 15:201-293

Sprengel R (2006) Role of AMPA receptors in synaptic plasticity. Cell Tissue Res 326:447-455

Squire LR (2009) The legacy of patient H.M. for neuroscience. Neuron. 61:6-9

Squire LR & Zola-Morgan S (1991) The medial temporal lobe memory system. Science 253:1380-1386

Steffenach HA, Witter M, Moser MB & Moser EI (2005) Spatial memory in the rat requires the dorsolateral band of the entorhinal cortex. Neuron 45:301-313

Stern-Bach Y (2004) AMPA receptor activation: not a square dance. Neuron 41:309-311

Stevens R & Cowey A (1973) Effects of dorsal and ventral hippocampal lesions on spontaneous alternation, learned alternation and probability learning in rats. Brain Res 52:203-224

Steward O & Scoville SA (1976) Cells of origin of entorhinal cortical afferents to the hippocampus and fascia dentata of the rat. J Comp Neurol 169:347-370

Teitelbaum H & Milner P (1963) Activity changes following partial hippocampal lesions in rats. J Comp Physiol Psychol 56:284-289

Totterdell S & Smith AD (1989) Convergence of hippocampal and dopaminergic input onto identified neurons in the nucleus accumbens of the rat. J Chem Neuroanat 2:285-298

Tukker JJ, Fuentealba P, Hartwich K, Somogyi P & Klausberger T (2007) Cell type-specific tuning of hippocampal interneuron firing during gamma oscillations in vivo. J Neurosci 27:8184-8189

van Haaren F, De Bruin JP, Heinsbroek RP & Van de Poll NE (1985) Delayed spatial response alternation: effects of delay-interval duration and lesions of the

medial prefrontal cortex on response accuracy of male and female Wistar rats. Behav Brain Res 18:41-49

Van Sickle BJ & Tietz EI (2002) Selective enhancement of AMPA receptor-mediated function in hippocampal CA1 neurons from chronic benzodiazepine-treated rats. Neuropharmacology 43:11-27

Van Sickle BJ, Xiang K & Tietz EI (2004) Transient plasticity of hippocampal CA1 neuron glutamate receptors contributes to benzodiazepine withdrawal-anxiety. Neuropsychopharmacology 29:1994-2006

van Strien NM, Cappaert NL & Witter MP (2009) The anatomy of memory: an interactive overview of the parahippocampal-hippocampal network. Nat Rev Neurosci 10:272-282

Vekovischeva OY, Zamanillo D, Echenko O, Seppälä T, Uusi-Oukari M, Honkanen A, Seeburg PH, Sprengel R & Korpi ER (2001) Morphine-induced dependence and sensitization are altered in mice deficient in AMPA-type glutamate receptor-A subunits. J Neurosci 21:4451-4459

Vekovischeva OY, Aitta-Aho T, Echenko O, Kankaanpää A, Seppälä T, Honkanen A, Sprengel R & Korpi ER (2004) Reduced aggression in AMPA-type glutamate receptor GluR-A subunit-deficient mice. Genes Brain Behav 3:253-265

Verwer RW, Meijer RJ, Van Uum HF & Witter MP (1997) Collateral projections from the rat hippocampal formation to the lateral and medial prefrontal cortex. Hippocampus 7:397-402

Walsh RN & Cummins RA (1976) The Open-Field Test: a critical review. Psychol Bull 83:482-504

West AP (1990) Neurobehavioral studies of forced swimming: the role of learning and memory in the forced swim test. Prog Neuropsychopharmacol Biol Psychiatry 14:863-877

Whishaw IQ & Mittleman G (1991) Hippocampal modulation of nucleus accumbens: behavioral evidence from amphetamine-induced activity profiles. Behav Neural Biol 55:289-306

Wiedholz LM, Owens WA, Horton RE, Feyder M, Karlsson RM, Hefner K, Sprengel R, Celikel T, Daws LC & Holmes A (2008) Mice lacking the AMPA GluR1 receptor exhibit striatal hyperdopaminergia and 'schizophrenia-related' behaviors. Mol Psychiatry 13:631-640

Witter MP & Moser EI (2006) Spatial representation and the architecture of the entorhinal cortex. Trends Neurosci 29:671-678

Whitlock JR, Heynen AJ, Shuler MG & Bear MF (2006) Learning induces long-term potentiation in the hippocampus. Science 313:1093-1097

Zamanillo D, Sprengel R, Hvalby O, Jensen V, Burnashev N, Rozov A, Kaiser KM, Köster HJ, Borchardt T, Worley P, Lübke J, Frotscher M, Kelly PH, Sommer B, Andersen P, Seeburg PH & Sakmann B (1999) Importance of AMPA receptors for hippocampal synaptic plasticity but not for spatial learning. Science 11:284:1805-1811

7 Scientific contributions

7.1 Diploma thesis

Freudenberg F (2005) Charakterisierung des Verhaltens beim selektiv
gezüchteten Endophänotypen "Defekte Reaktionsunterdrückung" in
Wistar Ratten, Diploma thesis, University of Bremen

7.2 Publications

Freudenberg F*, Marx V*, Mack V, Layer LE, Holmes A, Schwarz MK,
Sprengel R, Seeburg PH & Celikel T (2009) GluA1 PDZ domain binding
is required for experience-dependent behavioral plasticity. in preparation

Celikel T, Marx V*, **Freudenberg F***, Zivkovic A, Resnik E, Hasan MT,
Licznerski P, Osten P, Rozov A, Seeburg PH & Schwarz MK (2007)
Select overexpression of homer1a in dorsal hippocampus impairs spatial
working memory. Frontiers in Neuroscience 1:97-110

Schwabe K*, **Freudenberg F*** & Koch M (2007) Selective breeding of reduced
sensorimotor gating in Wistar rats. Behavior Genetics 37:706-712

Dieckmann M, **Freudenberg F**, Klein S, Koch M & Schwabe K (2007) Disturbed
social behavior and motivation in rats selectively bred for deficient
sensorimotor gating. Schizophrenia Research 97:250-253

Freudenberg F, Dieckmann M, Winter S, Koch M & Schwabe K (2007) Selective
breeding for deficient sensorimotor gating is accompanied by increased
perseveration in rats. Neuroscience 148:612-62

Cetin T, **Freudenberg F**, Füchtemeier M & Koch M (2004) Dopamine in the
orbitofrontal cortex regulates operant responding under a progressive ratio
of reinforcement in rats. Neuroscience Letters 370:114-117

* Equal contributors

7.3 Abstracts

Freudenberg F, Marx V, Mack V, Layer LE, Schwarz MK, Sprengel R, Seeburg PH & Celikel T (2008) Acquisition of behavioral despair is mediated by GluR-A containing AMPA receptors in the ventral hippocampus. Society for Neuroscience 38th annual meeting, Washington DC

Bonn S, Celikel T, **Freudenberg F**, Seeburg PH & Schwarz MK (2007) Tactile information transfer requires biallelic gamma-Protocadherin expression. Society for Neuroscience 37th annual meeting, San Diego

Schwabe K, **Freudenberg F** & Koch M (2007) Developmental and parametric characteristics of deficient prepulse inhibition induced by selective breeding of rats. Society for Neuroscience 37th annual meeting, San Diego

Schwarz MK, Celikel T, Zivkovic A, Marx V, **Freudenberg F**, Osten P, Rozov A & Seeburg PH (2007) Sustained Homer1a expression impairs AMPA-R mediated synaptic plasticity and spatial working memory. Society for Neuroscience 37th annual meeting, San Diego

Schwabe K, **Freudenberg F**, Hadamitzky M & Koch M (2006) Deficit of prepulse inhibition induced by selective breeding of rats: a possible animal model for psychiatric disorders? Society for Neuroscience 36th annual meeting, Atlanta

8 Acknowledgments

"At times our own light goes out and is rekindled by a spark from another person. Each of us has cause to think with deep gratitude of those who have lighted the flame within us."

--Albert Schweitzer--

I would like to thank all the people that helped throughout the course of this thesis-work and beyond for their advice, patience and friendship in many situations.

Prof. Dr. Peter H. Seeburg for providing me with a place to work and an interesting project. For your supervision, innumerable fruitful discussion, and your continuous support.

Prof. Dr. Hannah Monyer for reading and evaluating my thesis, and Prof. Dr. Michael Brunner and Prof. Dr. Christoph Schuster for being on my committee.

The Graduate College 791, particularly Catherine Munzig and the chairpersons Prof. Monyer and Prof. Seeburg, for giving me financial support and for a helpful PhD-program.

Dr. Tansu Celikel for all your support and help with the behavioral tests and the analysis and your professional advice. Thanks for giving me a place to work as a post-doc.

Dr. Miya Higuchi for your help with animal breeding, for your helpful advice and for being a friend and giving support on many occasions.

Dr. Martin Schwarz for help with the viruses and letting me work on some of your projects. Thanks for reading the first draft of this thesis and for your helpful advice.

Dr. Rolf Sprengel for help with the behavioral set-ups and for the mice.

Noam, Yair, and Sophie for your friendship. I couldn't have done it without you.

All the friends that I made in the lab in the GK and outside, Pawel, Evgeny, Sascha, Anne, Natalie, Valery, Verena, Lena, PG, and so many more.

The great technicians in the lab, namely Judith, Horst, Anette, Sabine, and Simone.

All my friends, particularly Tim and Carsten, for what you are.

Uschi for always being there and for raising an angel.

My brothers, Daniel and Christian, for your support and friendship.

My parents, for your love and support and helpful advice in all circumstances. I wouldn't be here without you.

My soon to-be wife Stephanie, for your love and affection. For always being there, for your trust and for the endless train trips. You make my life complete.